OAK RIDGE
NATIONAL LABORATORY
MANAGED BY UT-BATTELLE
FOR THE DEPARTMENT OF ENERGY

ORNL/TM-2004/257

Assessment of Hydrogen Detonation Loads in the Cold Source Beam Tube of the High Flux Isotope Reactor

Seokho H. Kim

UT-BATTELLE
ORNL-27 (4-00)

DOCUMENT AVAILABILITY

Reports produced after January 1, 1996, are generally available free via the U.S. Department of Energy (DOE) Information Bridge.

Web site http://www.osti.gov/bridge

Reports produced before January 1, 1996, may be purchased by members of the public from the following source.

National Technical Information Service
5285 Port Royal Road
Springfield, VA 22161
Telephone 703-605-6000 (1-800-553-6847)
TDD 703-487-4639
Fax 703-605-6900
E-mail info@ntis.fedworld.gov
Web site http://www.ntis.gov/support/ordernowabout.htm

Reports are available to DOE employees, DOE contractors, Energy Technology Data Exchange (ETDE) representatives, and International Nuclear Information System (INIS) representatives from the following source.

Office of Scientific and Technical Information
P.O. Box 62
Oak Ridge, TN 37831
Telephone 865-576-8401
Fax 865-576-5728
E-mail reports@adonis.osti.gov
Web site http://www.osti.gov/contact.html

This report was prepared as an account of work sponsored by an agency of the United States Government. Neither the United States government nor any agency thereof, nor any of their employees, makes any warranty, express or implied, or assumes any legal liability or responsibility for the accuracy, completeness, or usefulness of any information, apparatus, product, or process disclosed, or represents that its use would not infringe privately owned rights. Reference herein to any specific commercial product, process, or service by trade name, trademark, manufacturer, or otherwise, does not necessarily constitute or imply its endorsement, recommendation, or favoring by the United States Government or any agency thereof. The views and opinions of authors expressed herein do not necessarily state or reflect those of the United States Government or any agency thereof.

ORNL/TM-2004/257

Nuclear Science and Technology Division

ASSESSMENT OF HYDROGEN DETONATION LOADS IN THE COLD SOURCE BEAM TUBE OF THE HIGH FLUX ISOTOPE REACTOR

Seokho H. Kim

November 2004

Prepared by the
OAK RIDGE NATIONAL LABORATORY
Oak Ridge, TN 37831-6283
managed by
UT-BATTELLE, LLC
for the
U.S. DEPARTMENT OF ENERGY
under contract DE-AC05-00OR22725

CONTENTS

Page

LIST OF FIGURES

LIST OF TABLES

Table **Page**

ASSESSMENT OF HYDROGEN DETONATION LOADS IN THE COLD SOURCE BEAM TUBE OF THE HIGH FLUX ISOTOPE REACTOR

Seokho H. Kim

ABSTRACT

The High Flux Isotope Reactor (HFIR) at Oak Ridge National Laboratory (ORNL) is a versatile 85-MW isotope production and test reactor with the capabilities for performing a wide variety of irradiation experiments. Several beam tubes penetrate through the reflector, one of which is to include a cold source. The HFIR cold source is to utilize supercritical hydrogen as a moderator for production of cold neutrons. Significant efforts have been introduced in the design effort to keep the likelihood of hydrogen-air detonations within the vacuum tube region to an extremely low value ($<10^{-6}$/year). A study was initiated to evaluate the consequences of a hydrogen detonation and to demonstrate system robustness. This report presents a perspective overview of the modeling work as well as results of hydrogen detonation assessments for evaluating the safety margins associated with hydrogen detonation events in the proposed cold source of the HFIR. Four cases of different detonation locations in the front- and back-end portions of the beam tube were studied. Initial conditions were assumed for a stoichiometric air/hydrogen mixture at 92 K and 0.1 MPa for the detonations in the front-end tube and 300 K and 0.1 MPa in the back-end tube, respectively. A point detonation in the front-end tube yields the peak pressure (due to geometrical focusing) to be about 18 ~ 25 MPa along the centerline of the tube. An initial detonation wave propagates with about 5-MPa amplitude and is followed by pressure waves that show a significant dissipation to about 2 MPa. Detonations in the back-end tube yield initial pressure peaks of about 1.2 MPa that are amplified later to about 3 ~ 4 MPa. The pressure wave is substantially dissipated while traveling through the collimator and becomes about 1 MPa when it arrives at the bottom window. The gas mixture temperatures have been predicted to as high as about 3,000 K. However, to use the gas temperature for safety implications, it is suggested to multiply the safety factor (based on the difference between CET89 and CTH predictions) to the CTH-predicted temperature because the C-J temperature predicted using CTH turns out to be lower than the CET89 prediction.

---

1. INTRODUCTION

The High Flux Isotope Reactor (HFIR) at Oak Ridge National Laboratory (ORNL) is a versatile 85-MW isotope production and test reactor with the capabilities for performing a wide variety of irradiation experiments. The reactor core is surrounded with a beryllium reflector that several beam tubes penetrate through. As part of an effort to upgrade HFIR's capabilities, a cold source is being introduced into one of the beam tubes. The HFIR cold source will utilize supercritical hydrogen as a moderator for production of cold neutrons. Significant efforts have been introduced in the design effort to keep the likelihood of hydrogen-air detonations within the vacuum tube region to an extremely low value ($<10^{-6}$/year) to ensure that overall risk of such hypothetical events is acceptable. A defense-in-depth philosophy has been adopted by HFIR

management. Therefore, despite the low initiating event frequencies associated with detonation events, a study was initiated to evaluate the consequences of a hydrogen detonation and to demonstrate system robustness. This report presents a brief description of the modeling work as well as results of hydrogen detonation assessments for evaluating the safety margins associated with hydrogen detonation events in a vacuum / beam tube of the proposed cold source of the HFIR.

A schematic representation of the front section of the pertinent HFIR cold-source structures is depicted in Fig. 1. As seen, it consists of a moderator vessel enclosed in a vacuum tube, which is further surrounded by several other structural members (including a water gap, etc.). A study was performed previously with a series of conservative assumptions to attain a state wherein air in-leakage takes place within the vacuum tube volume located within the beryllium reflector.[1] The primary focus of the previous study was to evaluate the detonation pressure profile incident on the front beam window for its structural integrity evaluation. The current study extends the previous work by considering the rear portion of the beam tube outboard of the vacuum tube.

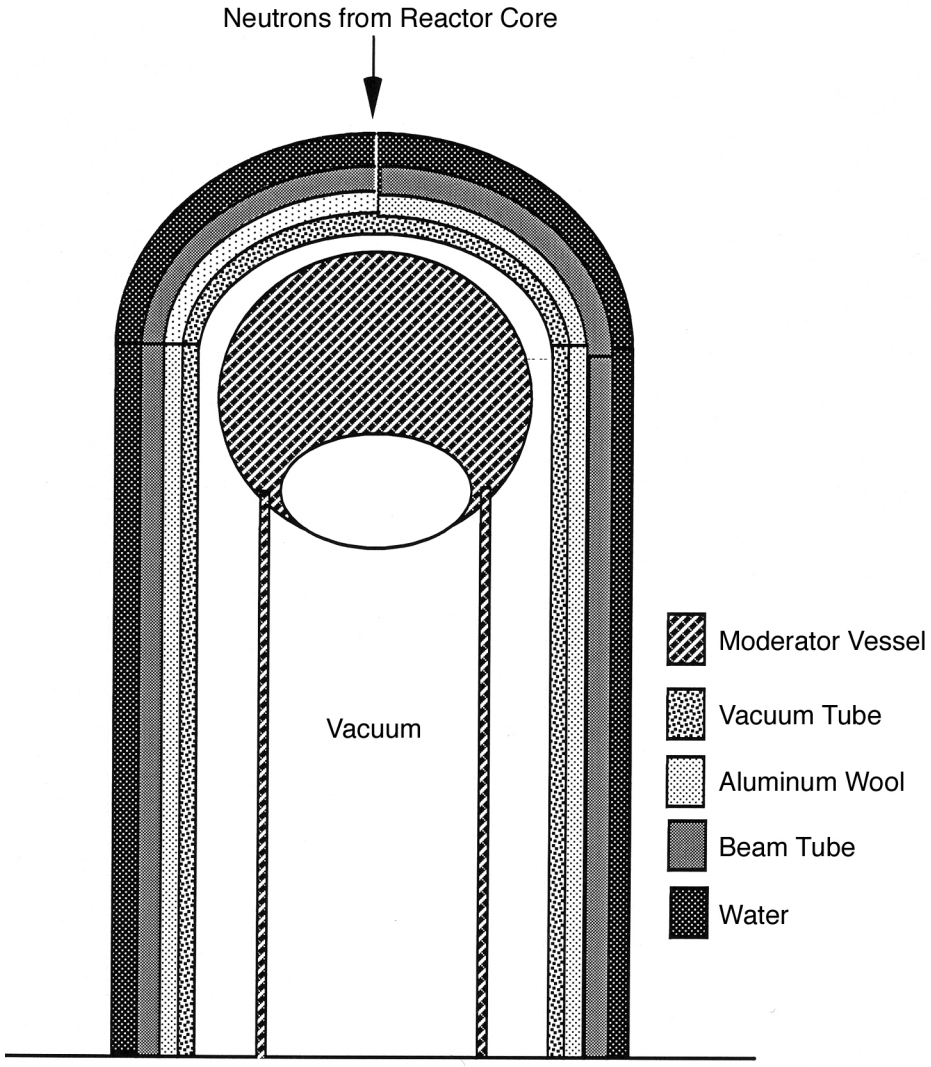

Fig. 1. Schematic representation of proposed HFIR cold source.[1] (Note: Aluminum wool layer does not exist in the current design.)

Included is the effect of the presence of the collimator. The detonation pressure profile along the inner surface of the outer neutron window is of primary importance.

Figures 2 and 3 show simplified geometry of the front- and back-ends of the beam tube, assumed for the current hydrogen detonation analyses. The front-end vacuum tube, as seen in the figure, is assumed to have a tight fit at the front portion of the tube with its surrounding beam tube of which the exterior contacts with water. The volume slightly expands at about one-third section down toward the back-end, and the helium gap exists between the vacuum tube and the beam tube from this point. Therefore, a thick aluminum layer (lumped a vacuum tube and beam tube walls) is modeled for the front part with water boundary (~1.8 cm, 0.72 in.). A thin vacuum tube layer at the remaining lower section (0.56 cm, 0.22 in.), however, can be easily expand due to pressure buildup inside, and such an expansion closes the gap that is very thin and filled with helium between beam and vacuum tubes. For the current study, therefore, the side-wall at the lower section was assumed as a single thick aluminum layer of 2.065 cm (0.813 in.) as seen in the figure. It is also seen in the same figure that the front-end vacuum/beam tube expands its volume [inner radius from 6.59 cm (2.59 in.) to 13.89 cm (5.47 in.)] at lower section. In the figures, numbers in parentheses represent x- and y-dimensions from the origin that is assumed to be at the bottom center. Other numeric numbers from 1 through 85 are history points at which pressures and temperatures are monitored from hydrogen detonation simulations. The history points, 85, 86, and 87 are for pressure monitoring in water surrounding the front hemispherical region.

A simplified sketch of the back-end vacuum tube is shown in Fig. 3. The section close to the bottom-end contains three collimators made of steel that substantially reduce open volume inside the vacuum tube. The collimator at the center has 56.8 cm^2 (8.8 $in.^2$) of cross-sectional opening that tapers down to 51 cm^2 (7.9 $in.^2$) toward the end. The other two collimators at each side of the one at the center have 56.8 cm^2 (8.8 $in.^2$) and 53.4 cm^2 (8.2 $in.^2$) of cross-sectional openings, respectively. These areas taper to 49.7 cm^2 (7.7 $in.^2$) and 45.2 cm^2 (7.0 $in.^2$), respectively. As seen in the figure, three openings of the collimators (total average opening area of ~156 cm^2) are lumped into one with 14.1-cm (5.6-in.) diameter. Slightly curved top- and bottom-end windows of this part of the beam tube are assumed to be flat, so that entire section is treated as a flat cylindrical geometry with about 0.955-cm (0.376-in.) thick aluminum wall containing steel collimator inside at its lower section. Aluminum wall is bounded with coolant water. Top and bottom of the cylinder are 0.51-cm (0.2-in.) thick aluminum windows, each bounded by vacuum at the top and air at the bottom.

The problem to be solved consists of determining the dynamic pressures as a result of a hydrogen detonation event within the vacuum/beam tube. The scenario to be resolved is one wherein it is assumed that a mixture of hydrogen and air fills the entire volume and then is conservatively assumed to spontaneously detonate. For the purpose of evaluating the structural response, a detonation wave model is initiated at set locations and then allowed to propagate outward spherically. In the previous detonation study,[1] pressure profiles were analyzed with the onset of detonation at various discrete locations as well as assuming volumetric detonation (viz., to model effects of distributed sparks). The case with the detonation onset at the center of the front hemisphere turned out to yield the highest pressure response. As in the previous study,[1] it was also assumed that a two-dimensional (2-D) axisymmetric simulation of the shock wave generation, transport, and interactions with surrounding structures is adequate for capturing the principal effects of a detonation event in the HFIR cold source beam tube.

In general, the same approach used in the previous study was also used in the current study; that is, the CET89 and CTH computer codes were used as primary tools. CET89 is a chemical equilibrium code developed to calculate thermodynamic and transport properties of complex chemical systems.[2] CTH is a highly sophisticated tool used to model shock wave physics,

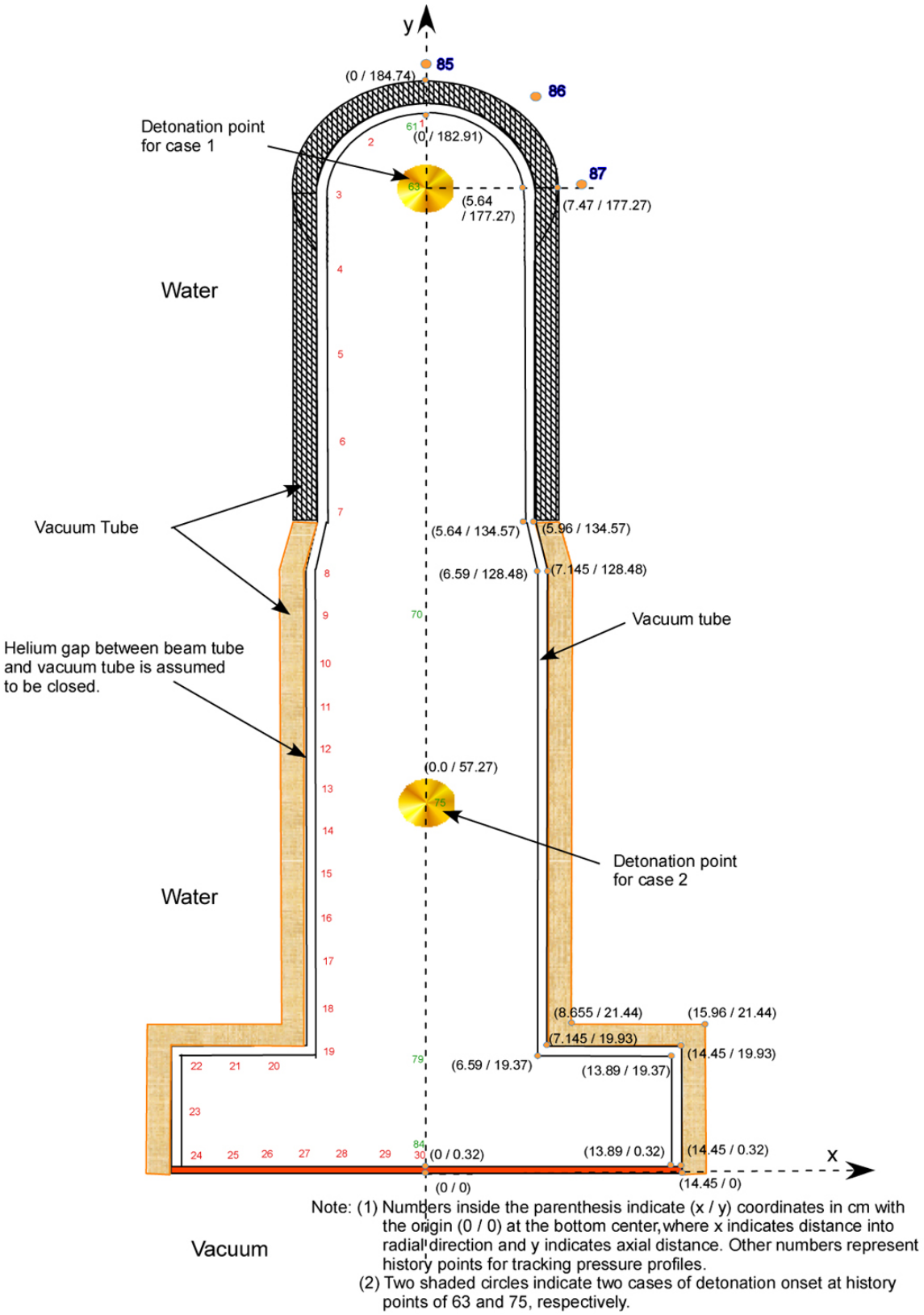

Fig. 2. A schematic geometry of the front end of the cold source vacuum tube assumed for hydrogen detonation analysis.

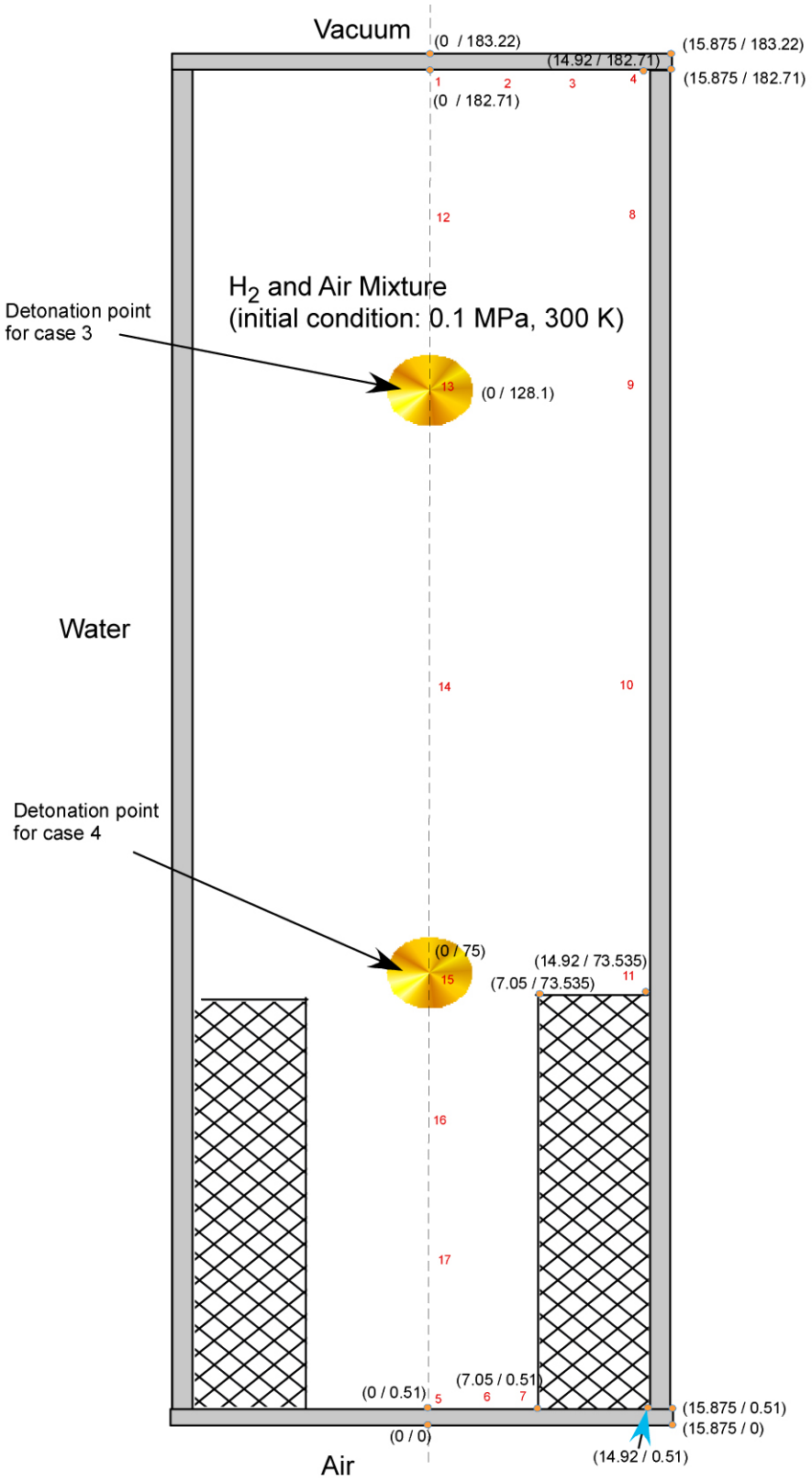

Fig. 3. A schematic geometry of the back end of the cold source beam tube assumed for hydrogen detonation analysis.

fluid-structure interactions, and penetration dynamics for one-, two-, and three-dimensional multimaterial motion and response problems.[3] For the best-estimate evaluation of hydrogen detonation studies, CET89 was first used to determine detonation parameters (for a Chapman-Jouguet or C-J detonation), such as postburn mixture density, specific heat ratio of preburn and postburn mixture, detonation velocity, etc. It also provides estimates of static pressure and temperature increase after the burn completes. These CET89 evaluations are used to obtain CTH model input for simulating a high-explosive burning process. Thereafter, CTH can be used for evaluating important effects related to fluid-structure interactions as well as to capture possible effects of wave focusing.

Gaseous detonation can be modeled in CTH by specifying the appropriate gas mixture as a "high explosive." The high-explosive detonation option in CTH uses a programmed burn model. In this model a burn is simulated by the release of internal energy in a small region (two or three computational cells), which moves through the mesh at a constant detonation velocity that is specified by the user as an input parameter along with some other detonation parameters. The energy release corresponds to the chemical energy released in a detonation. The location and time of ignition must also be specified by the user. In this report, we present front-end evaluations of the detonation process using the CET89 code, along with detonation wave propagation, its interaction with structures, and dissipation using the CTH code.

2. FRONT-END EVALUATION OF DETONATION PROCESS

An extensive parametric study using the CET89 code was conducted before in a lumped framework to evaluate levels of possible pressurization, detonation velocities, and temperatures of burn mixtures.[1] The study[1] was conducted for three different concentrations ranging from the lower detonation limit of 12 vol % to the upper limit of 58 vol % of hydrogen, including the stoichiometric value of ~29 vol %. The results of the study indicate that the values of pressure and temperature rise ratios are greatest, as might be expected, for stoichiometric mixtures of hydrogen and air. Therefore, the current study has been performed only for the stoichiometric mixture. Initial conditions and C-J conditions estimated using CET89 are summarized in Table 1. The initial pressures in the front-end vacuum tube and in the back-end tube are all 0.1 MPa while the initial temperatures are 92 K and 300 K, respectively. As seen in the Table 1, pressure magnitudes at the detonation front are expected to be ~5 MPa and ~1.5 MPa in the front- and the back-end beam tubes, respectively. Also it is seen that the detonation front moves at 2000 m/s and 1970 m/s of the velocity in the front- and the back-end beam tube, respectively. Behind the detonation front where the postburn gas mixture exists, the pressure waves are expected to travel at 1092 m/s as seen in the table.

Table 1. Initial conditions and detonation parameters estimated using CET89

	Initial condition		**C-J conditions estimated using CET89**								
	Temperature (K)	**Pressure (MPa)**	**v%**	**P_{CJ}/P_o**	**T/T_o**	**γ_{pre}**	**γ_{post}**	**u**	**M**	**c_{pre}**	**c_{post}**
Front-tube	92	0.1	29	50.69	31.93	1.40	1.18	2000	8.83	227	1092
Back-tube	300	0.1	29	15.50	9.82	1.40	1.16	1970	4.82	409	1092

Note: v% = hydrogen volume percent, P_{CJ}/P_O & T/T_O = C-J pressure and temperature ratio to initial values, $\gamma = c_p/c_v$, u = detonation velocity (m/s), M = mach number, c = sonic velocity, and subscripts “pre” and “post” denote preburn and postburn mixture conditions, respectively.

3. EVALUATION OF DYNAMIC DETONATION PROCESS

CET89 code calculations provide valuable information for first-cut assessments, but they do not account for energy losses, thermal stresses, or focusing effects of shock waves. CET89 results, however, provide the necessary detonation parameters (e.g., burn mixture properties, detonation velocity for flame-front, etc.) for initializing CTH shock wave calculations. A two-dimensional cylindrical vacuum tube is modeled for CTH calculations as shown in Figs. 2 and 3. The upper portion of the vacuum tube on the front-end has a tight-fit between the vacuum tube wall and beam tube structure during operation because of thermal expansion. The lower section of the front-end has a helium gap layer that separates the beam tube and the vacuum tube. The helium gap, however, is expected to be closed following detonation due to the beam tube wall expansion because of pressure buildup followed by the hydrogen detonation in the tube. In this study, therefore, it was assumed that the vacuum tube with uniform thickness (e.g., 1.8 cm at the upper section and 2.06 cm at the lower section) was directly surrounded by water as seen in Fig. 2. The back-end of the beam tube has an aluminum wall (0.955-cm thick) also directly bounded by water.

The front-end of the vacuum tube was assumed to be filled with a uniform stoichiometric mixture (e.g., 29 vol.%) of air and hydrogen at 92 K and 0.1 MPa before detonation started, while the back-end section was assumed to have the mixture initially at 300 K and 0.1 MPa. Transient pressures and temperatures of the gas mixture are monitored at various history tracer points depicted in Figs. 2 and 3.

The presence of internal structures inside the vacuum tube (as seen in Fig. 1) is not modeled in the CTH analysis. The role of such structures (such as the moderator vessel and the transfer lines) on delivered loads is not clear. They may act to absorb combustion energy to mitigate the loading delivered to the internal hemispherical surface of the vacuum tube. However, the timescale for energy transfer/absorption is usually much longer compared to that associated with shock transport and structural reaction. It is also possible, with the presence of these internal structures, that a shock can be amplified near the vacuum tube surface. The role of such internal structures to detonation propagation and pressure wave reflection is unclear without more detailed modeling. The presence of such internal structures in the path of the hydrogen burn front accelerates the deflagration burn front and possibly causes the deflagration-detonation-transition (DDT). In the current study, however, we conservatively assume that DDT already occurs, and the problem is assumed to start with detonation.

For all the CTH calculations, the water outside the vacuum/beam tubes is assumed at 0.1 MPa, the same as the gas mixture pressure inside the tubes. In reality, however, the water surrounding the front-end tube is under a high pressure of ~3.45 MPa (500 psia). The rationale for assuming 0.1 MPa of water pressure will be explained in the following section.

Four cases of CTH calculations were performed. Cases 1 and 2 involve detonation in the front-end structure, while cases 3 and 4 involve detonation in the back-end structure. For case 1, a detonation was initiated at the geometrical focal point (x = 0 cm, and y = 177.27 cm) of the hemispherical end (as seen in Fig. 2). Case 2 assumes detonation onset in the lower section of the front-end vacuum tube structure (y = 57.27 cm). The detonation point for case 1 was selected because the previous study indicated that the highest pressure focusing was predicted with the detonation initiated at the center of the hemispherical nose section of the tube.[1] The detonation point for case 2 was selected arbitrarily to represent detonation initiated in the middle section of the tube. For cases 3 and 4 (see Fig. 3) in the back-end structure, point detonations were initiated at the location of x = 0, with y = 128.1 cm, and y = 75 cm, respectively. The detonation point for case 4 was chosen to simulate detonation initiated around the collimator, and the case 3 location was chosen arbitrarily to represent detonation initiated in the upper portion of the beam tube.

3.1 CASE 1 RESULTS: POINT DETONATION AT (0, 177.27) IN FRONT-END VACUUM TUBE

3.1.1 Detonation Wave Propagation and Following Pressure Profiles

The results for case 1 are shown in Figs. 4–24. Figures 4–8 show transient pressure profiles at various history points. Figures 4 and 5 illustrate the transient pressure profile near the vacuum tube wall at various locations. It is shown that the initial detonation pressure amplitude upon arriving the wall varies around 6 ~ 8 MPa, followed by slow dissipation to a relatively steady pressure of about 2 MPa. Pressure profiles in the middle region of the hemispherical section of the tube are shown in Fig. 6. Initial amplitude of the detonation wave at time = 0 at the history point-63 is not illustrated well in the figure because of a limited number of time history data points captured and also immediate dispersion (or propagation) of the initial detonation wave at the point-63 as seen in Fig. 6. The C-J pressure is expected to be 5.069 MPa according to the CET89 code calculations as seen in Table 1. Using the data from the CET89 calculations (i.e., initial density and pressure of the gas mixture, specific heat capacity and c_p/c_v-value of the postburn mixture, and detonation velocity), CTH predicts 5.089 MPa (that is not seen in the figures) and 2,346 K for the C-J pressure and temperature, respectively. CTH's C-J pressure is in good agreement with that of CET89; however, it turns out that CTH (as in Table 1) underpredicts the C-J temperature (2,346 K from CTH vs 2,937 K from CET89 as seen in Table 1). It has been decided not to investigate further to find causes of such a discrepancy in the C-J detonation temperature.

Pressure profiles in the lower section of the tube are shown in Figs. 7 and 8. Specifically, Fig. 8 shows the detonation pressure magnitude impacting on the bottom window. As also seen in the same figure, the detonation wave touches the bottom window at ~0.9 ms; that is, the detonation event ends at around 0.9 ms. Detonation wave that is initiated at y = 177.27 cm and propagates at 2,000 m/s of velocity, is expected to take ~0.89 ms to reach the bottom window (y = 0 cm). The detonation propagation behavior predicted by CTH is in good agreement. The pressure wave is expected to propagate at the speed of sound in the postburn gas mixture once the detonation front moves away. The speed of sound in the postburn gas mixture is predicted to be 1,092 m/s by CET89 as seen in Table 1. The pressure wave focusing at the centerline (x = 0) upon being reflected at the tube side wall is expected to occur at every ~0.1 ms (i.e., the vacuum tube diameter, 11.28 cm, divided by the sound speed, 1,092 m/s). It is clearly seen in Figs. 4 and 6 that CTH correctly predicts wave focusing with ~0.1-ms interval (pressure profiles at the points-5 and -65 clearly indicate such focusing behavior). The pressure wave near the bottom window is seen to go up as high as about 25 MPa (Fig. 8).

The detonation wave propagation and following pressure wave profiles are further displayed in Figs. 9–14. In these figures, pressure profiles are plotted as a function of location, and thus each curve represents a snapshot of pressure at various time moments. Figure 9 shows the pressure profiles on the centerline (x = 0) along the y-axis from 0 to 0.97 ms, with each curve representing 0.02-ms interval. The y-locations are depicted in Fig. 2. It is seen that the pressure is amplified to be as high as ~17 MPa at the origin of the detonation (as also seen in Fig. 6) due to geometrical focusing. The previous study for a similar geometry indicated that the focused pressure went up as high as 40 MPa. (Ref. 1). The main difference between the previous and current studies is in the boundary conditions. The previous study assumed that a helium flowing gap existed between the vacuum tube and the beam tube. The current study assumes that a tight contact between these structures so that a part of wave energy can be directly transmitted to the water surrounding the beam tube wall. Another difference is in the detonation velocity; the previous study used 2,400 m/s, and the current study uses 2,000 m/s. In the previous study, gas

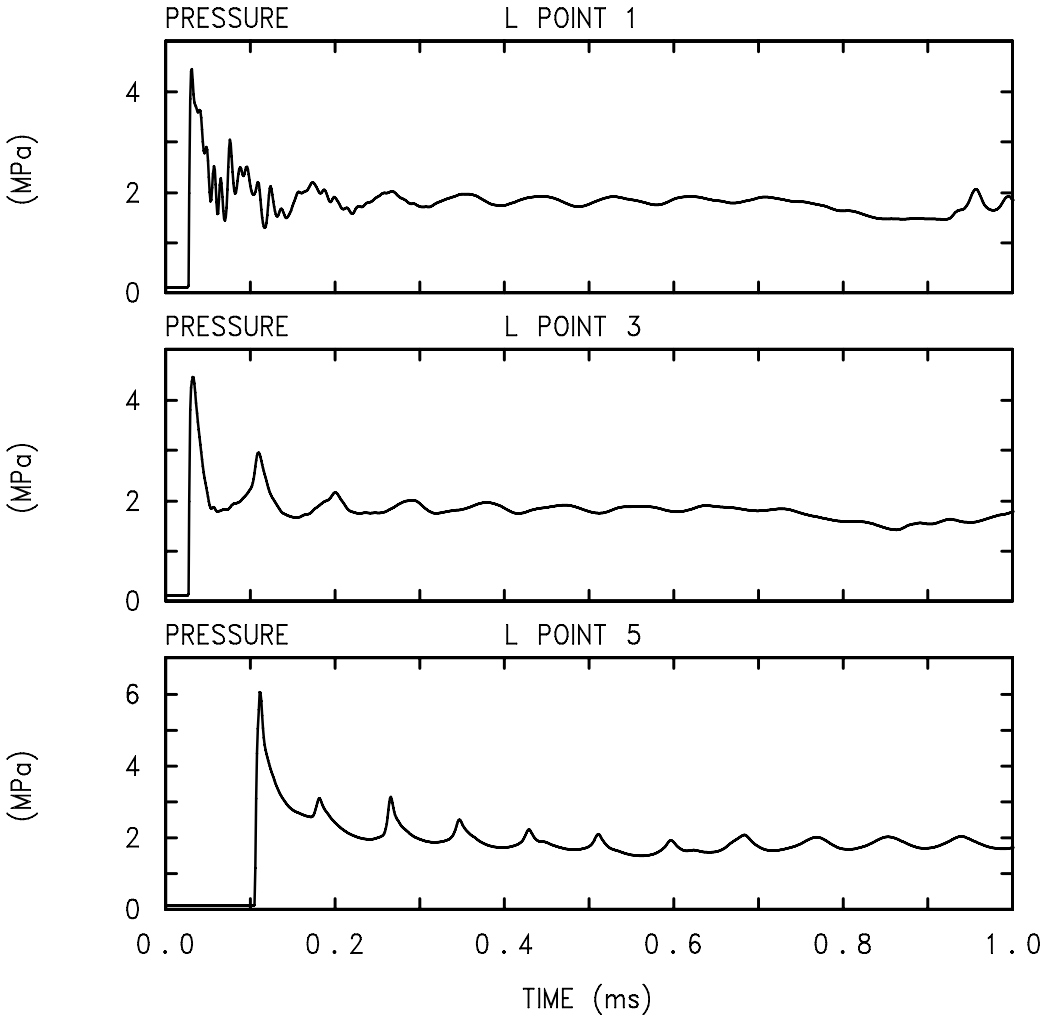

Fig. 4. Case 1 (detonation at upper region of the front-end tube)—pressure profile near the tube wall in the upper hemispherical section.

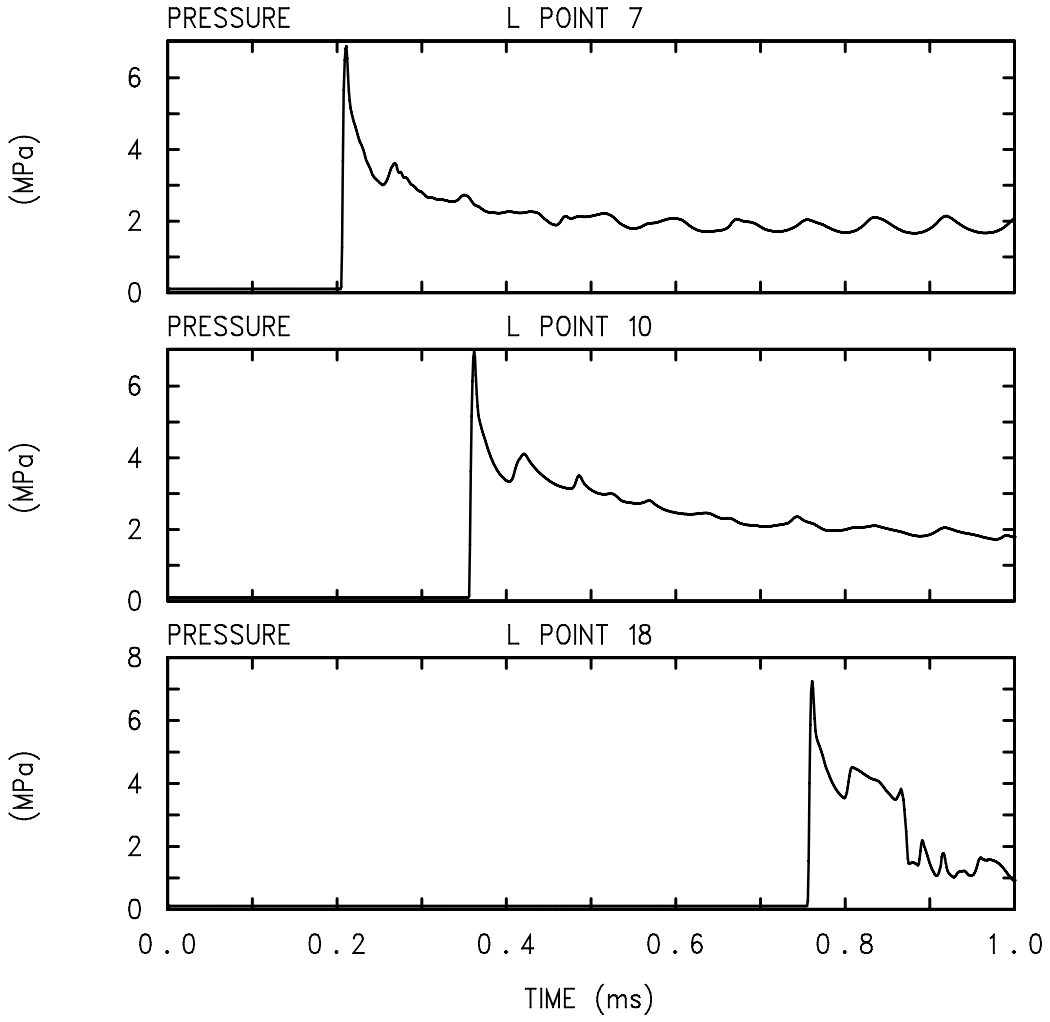

Fig. 5. Case 1 (detonation at upper region of the front-end tube)—pressure profile near the tube wall.

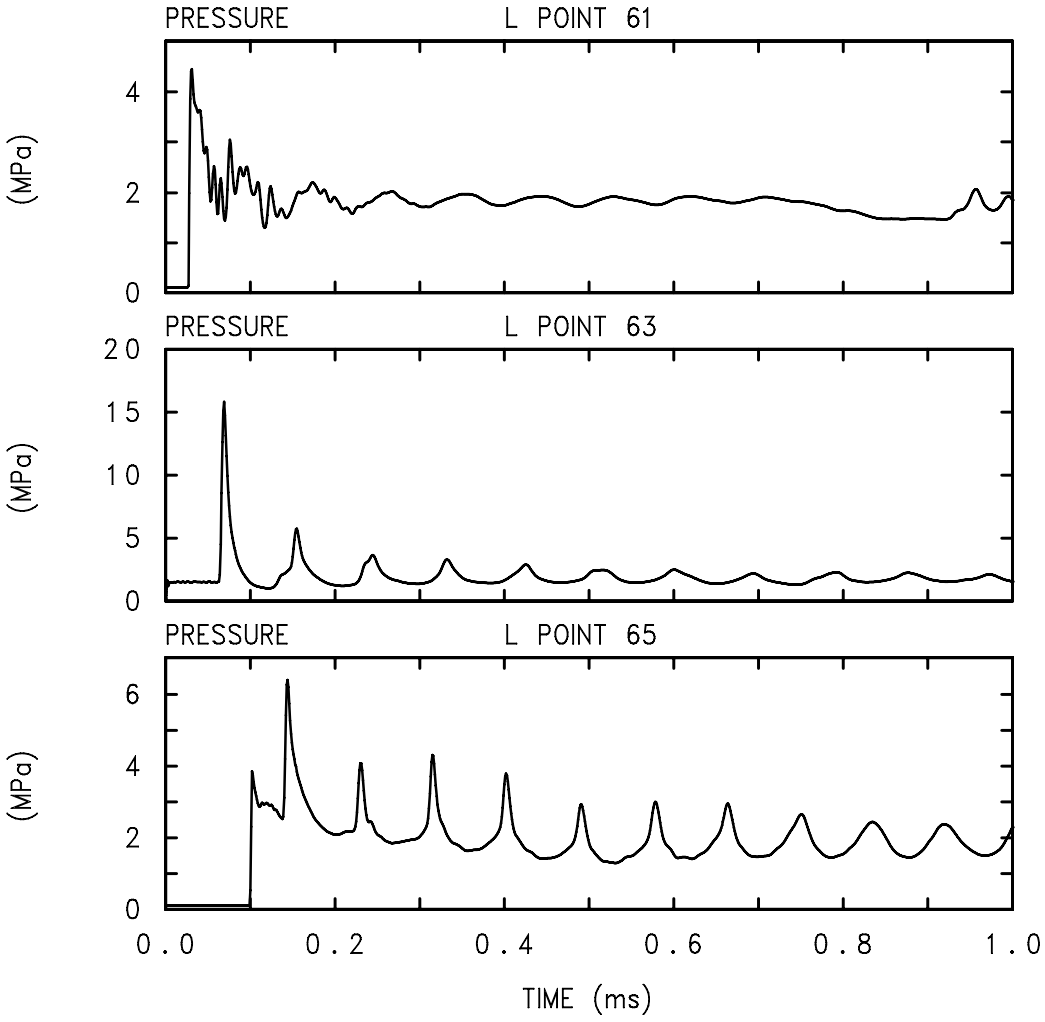

Fig. 6. Case 1 (detonation at upper region of the front-end tube)—pressure profile along the center line (x = 0) in the hemispherical section of the tube.

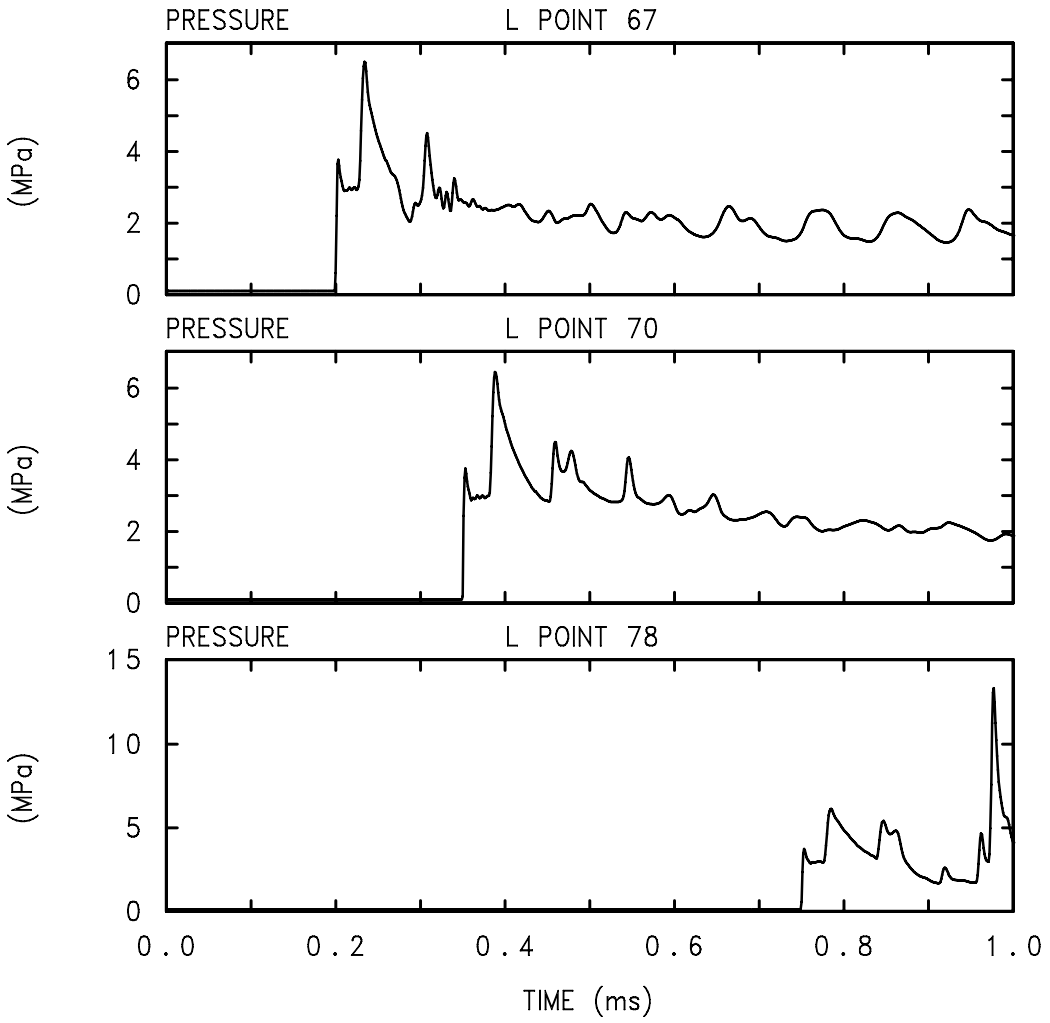

Fig. 7. Case 1 (detonation at upper region of the front-end tube)—pressure profile along the center line (x = 0).

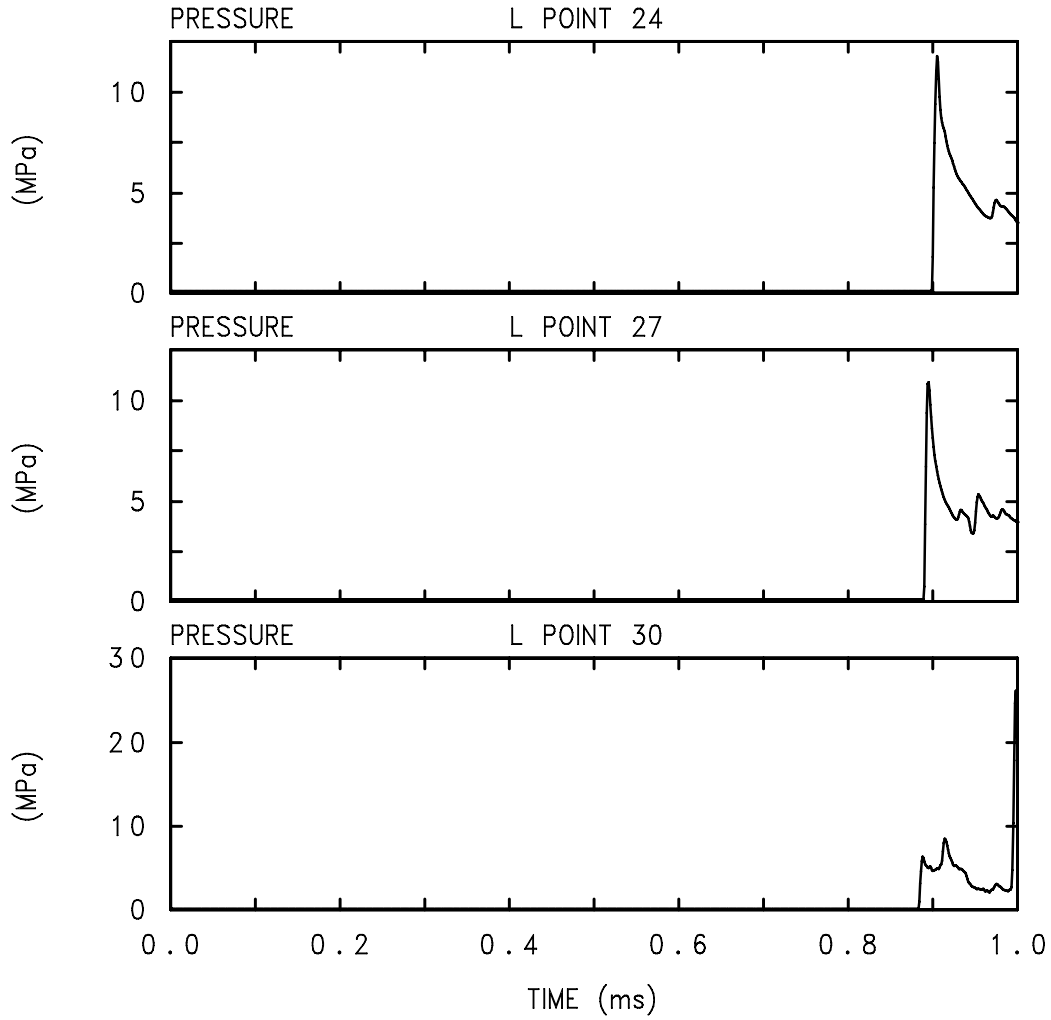

Fig. 8. Case 1 (detonation at upper region of the front-end tube)—pressure profile near the bottom window.

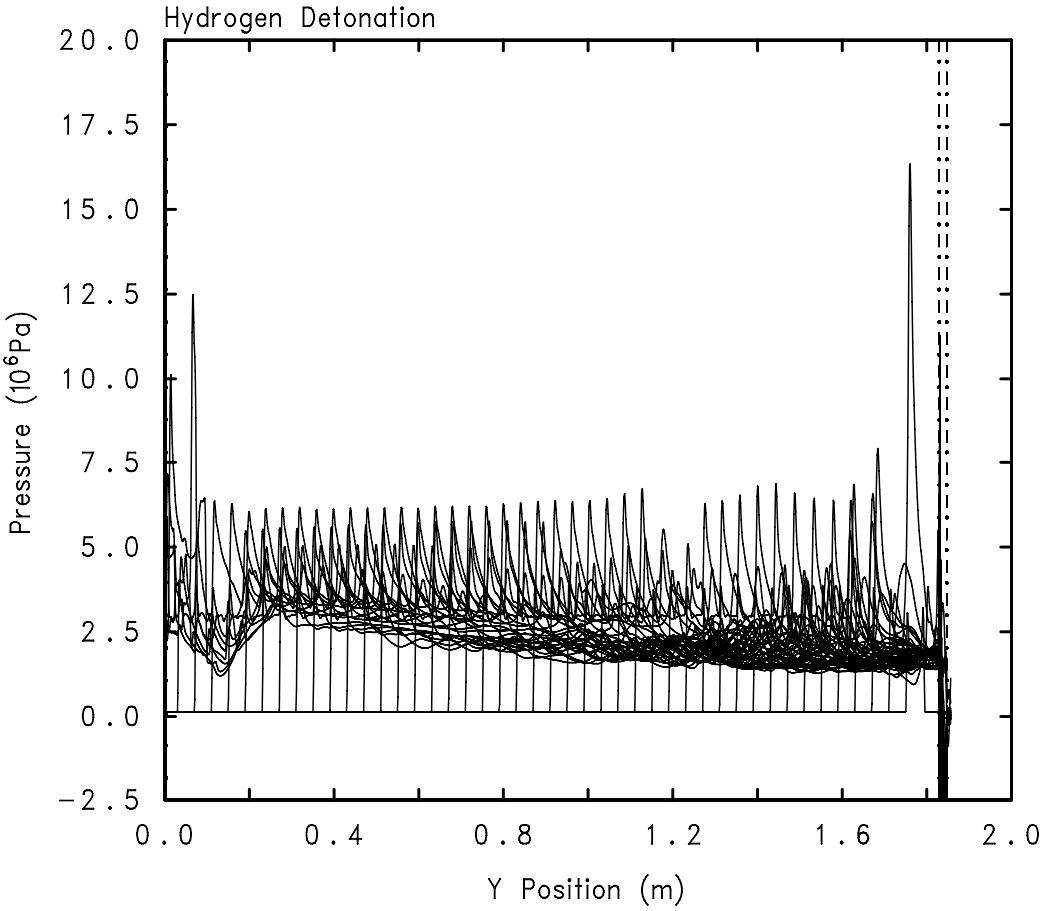

Fig. 9. Case 1 (detonation at upper region of the front-end tube)—pressure profile at centerline along y-axis from 0 to 0.97 ms with 0.02-ms interval.

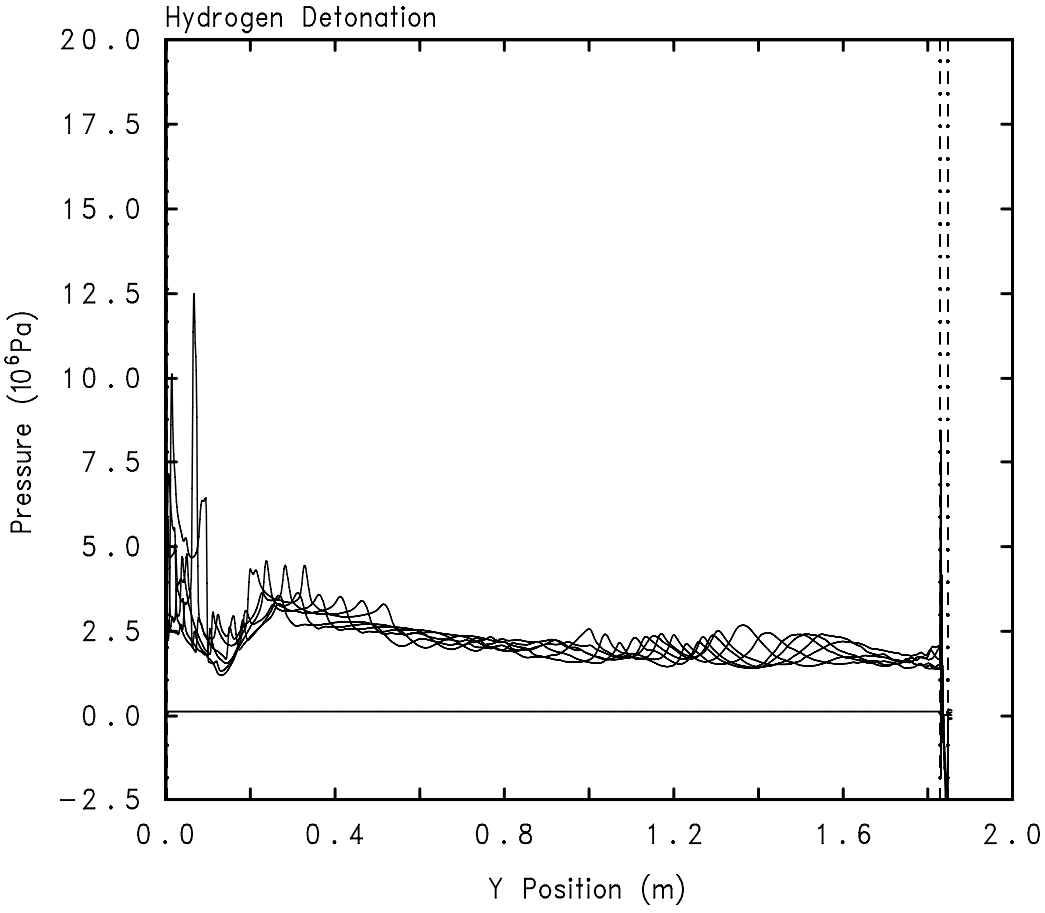

Fig. 10. Case 1 (detonation at upper region of the front-end tube)—pressure profile at centerline along y-axis from 0.89 ms to 0.99 ms with 0.02-ms interval.

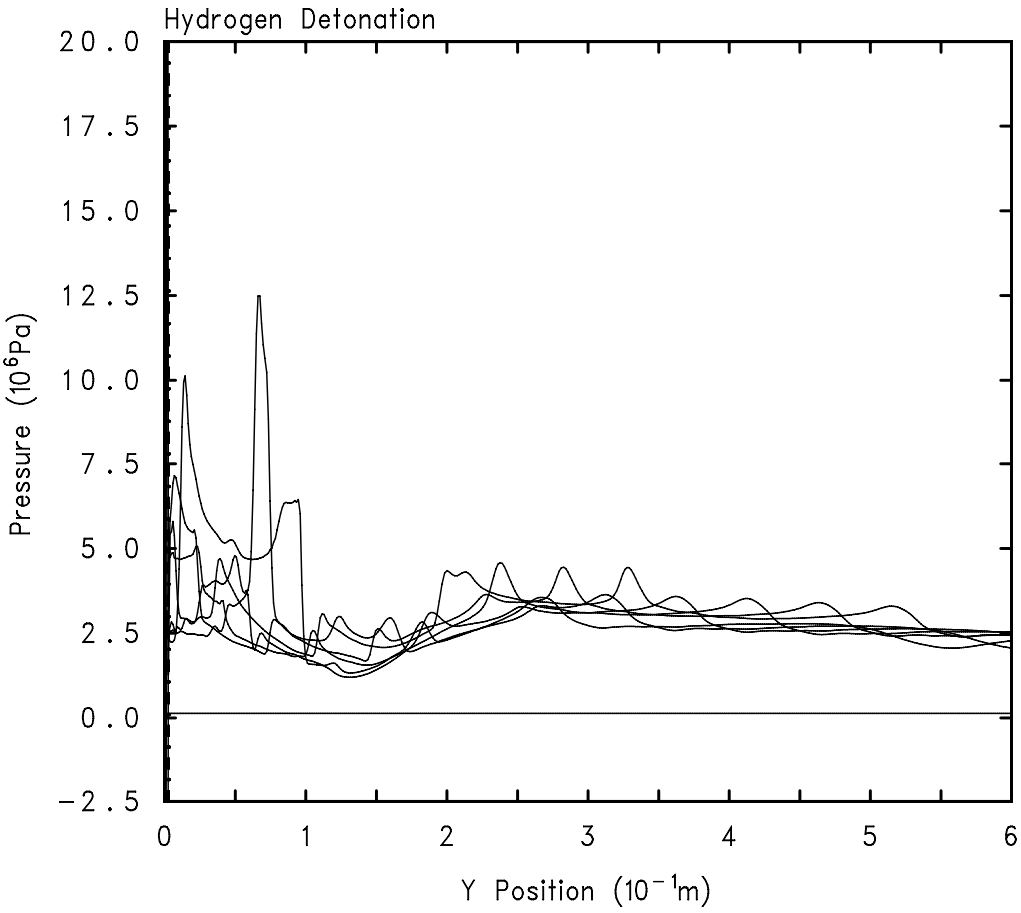

Fig. 11. Case 1 (detonation at upper region of the front-end tube)—pressure profile at centerline along y-axis from 0.89 ms to 0.99 ms with 0.02-ms interval (expanded view).

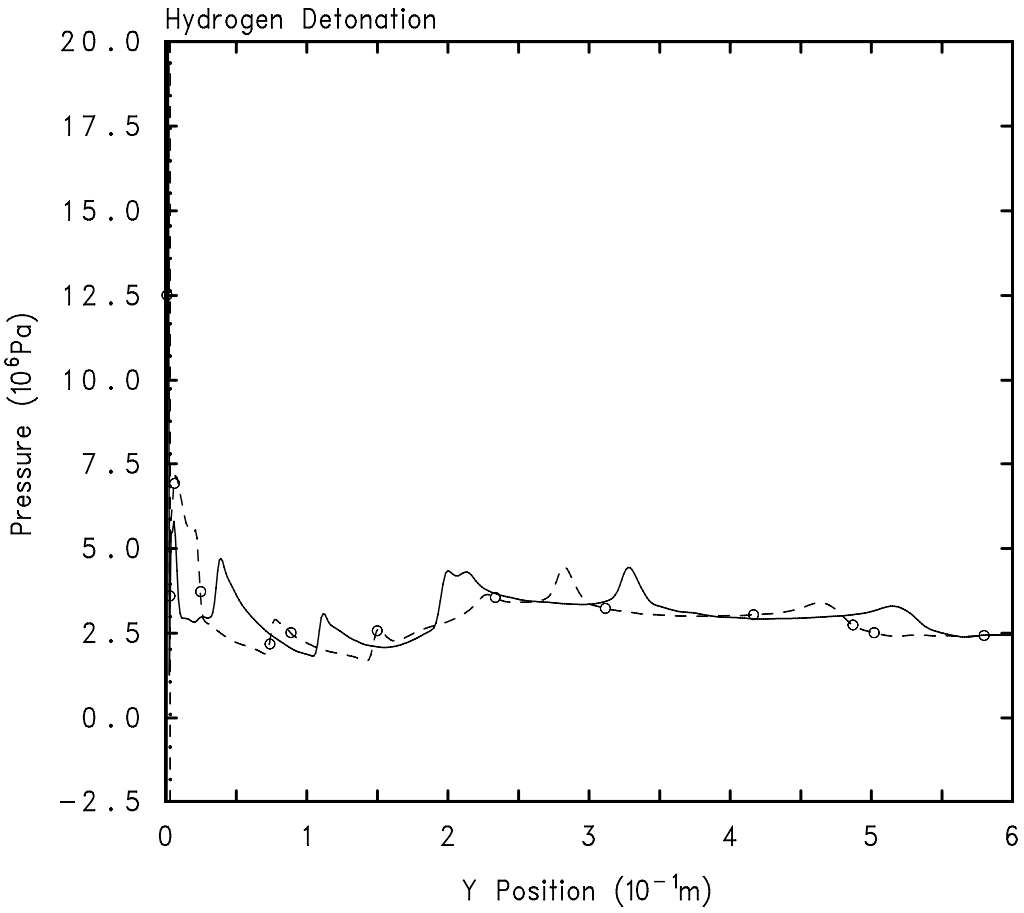

Fig. 12. Case 1 (detonation at upper region of the front-end tube)—pressure profile at centerline along y-axis from 0.89 ms (solid line) and 0.91 ms (dotted line).

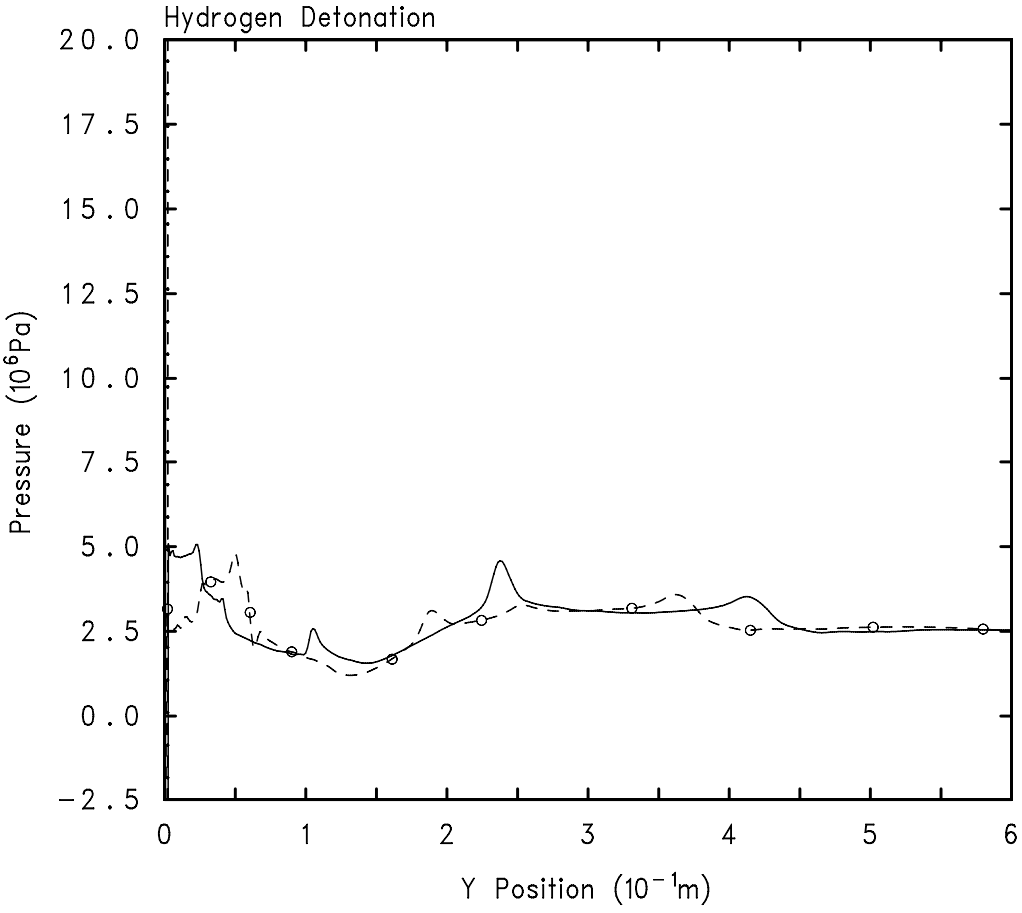

Fig. 13. Case 1 (detonation at upper region of the front-end tube)—pressure profile at centerline along y-axis from 0.93 ms (solid line) and 0.95 ms (dotted line).

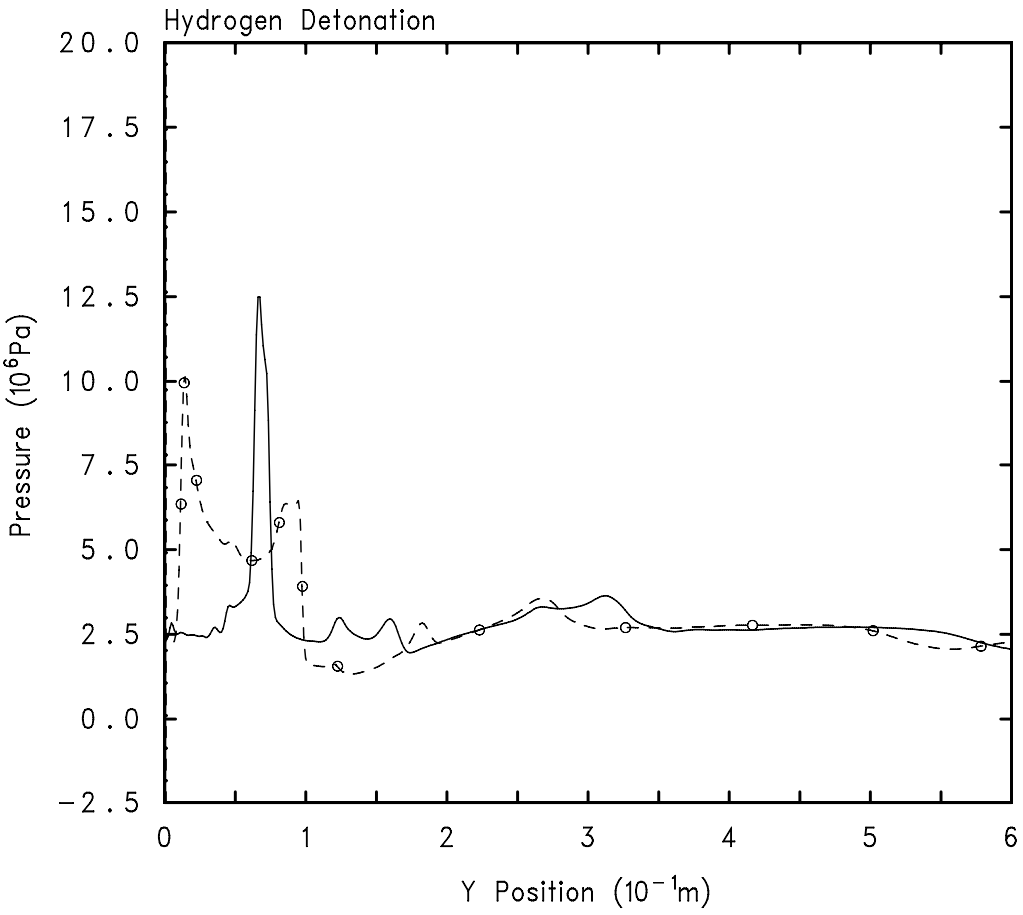

Fig. 14. Case 1 (detonation at upper region of the front-end tube)—pressure profile at centerline along y-axis from 0.97 ms (solid line) and 0.99 ms (dotted line).

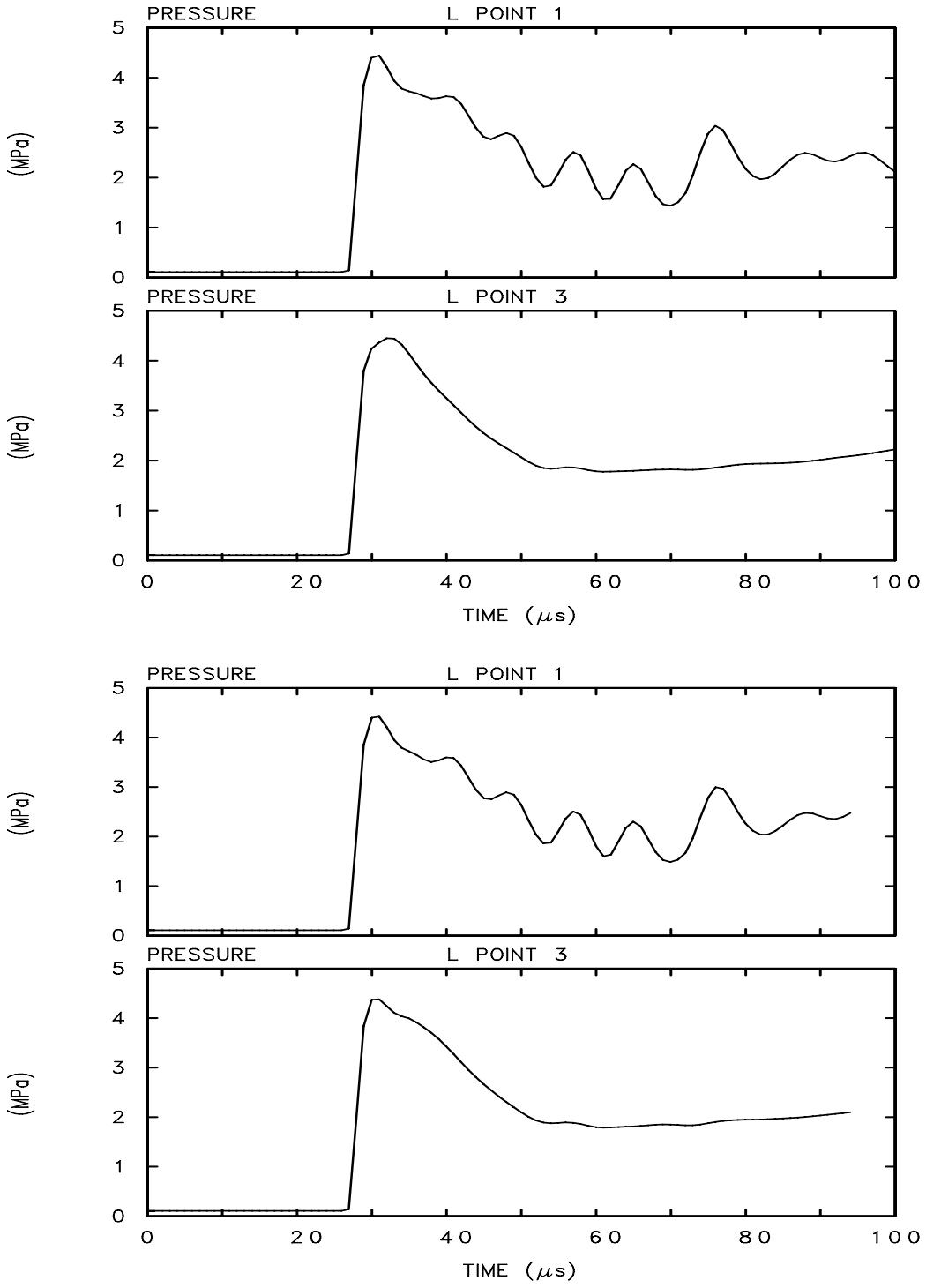

Fig. 15. Case 1 (detonation at upper region of the front-end tube)—pressure profiles in the gas mixture near the hemispherical nose region for the cases with 0.1 MPa of the water pressure (upper two plots) and with 3.45 MPa (500 psia) of the water pressure (lower two plots).

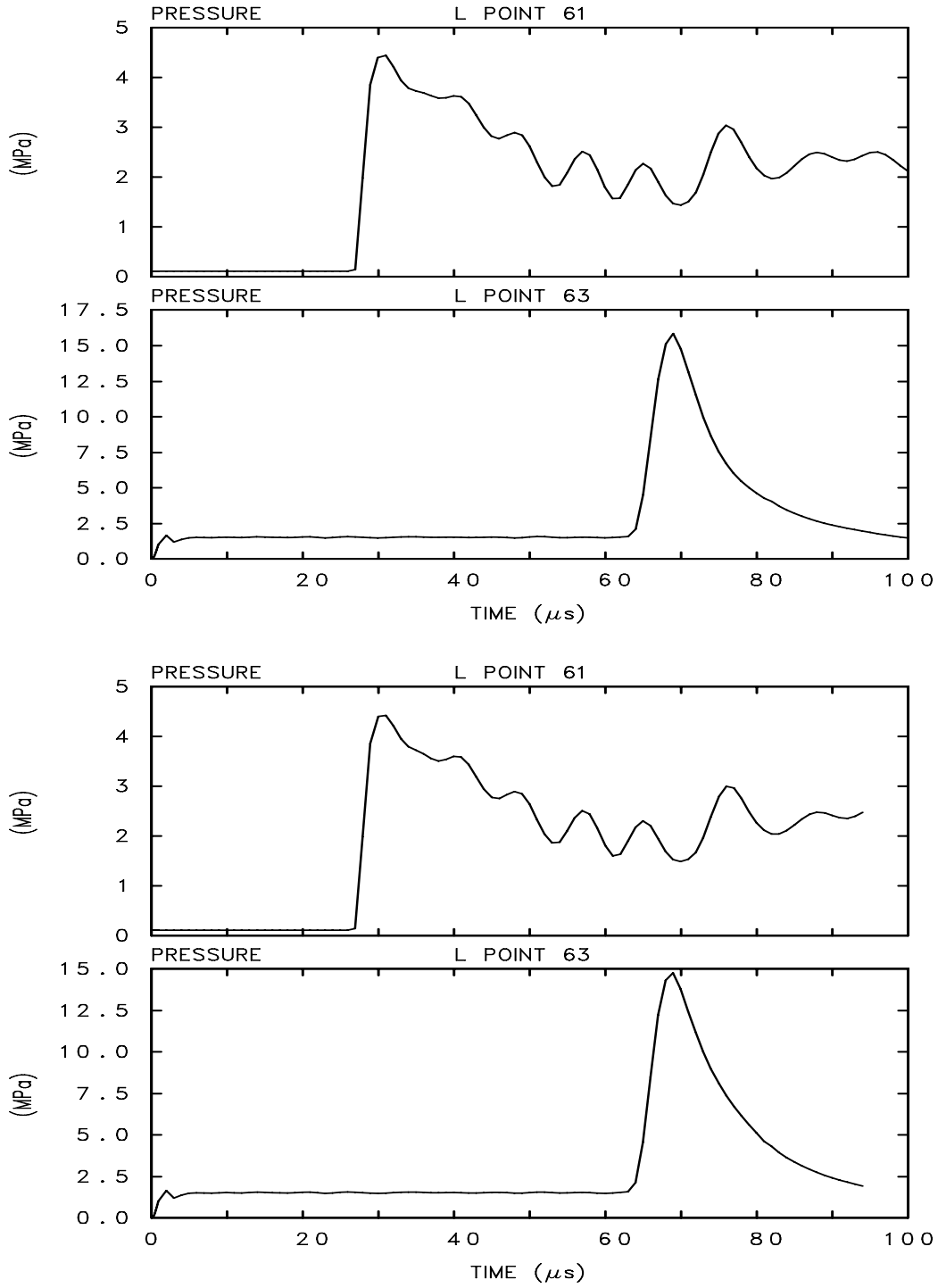

Fig. 16. Case 1 (detonation at upper region of the front-end tube)—pressure profiles in the gas mixture along the y-axis for the cases with 0.1 MPa of the water pressure (upper two plots) and with 3.45 MPa (500 psia) of the water pressure (lower two plots).

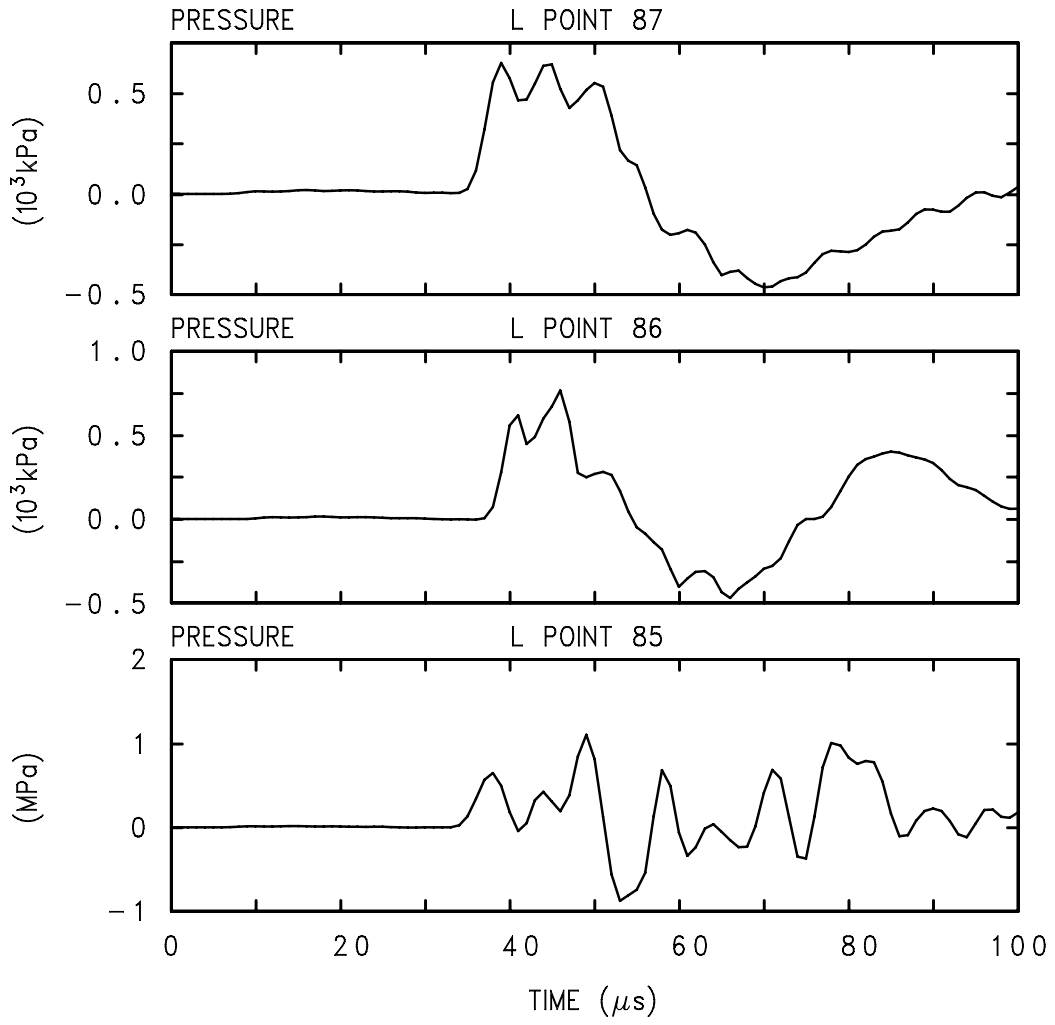

Fig. 17. Case 1 (detonation at upper region of the front-end tube)—pressure profiles in the water around the hemispherical region for the case with 0.1 MPa of the water pressure.

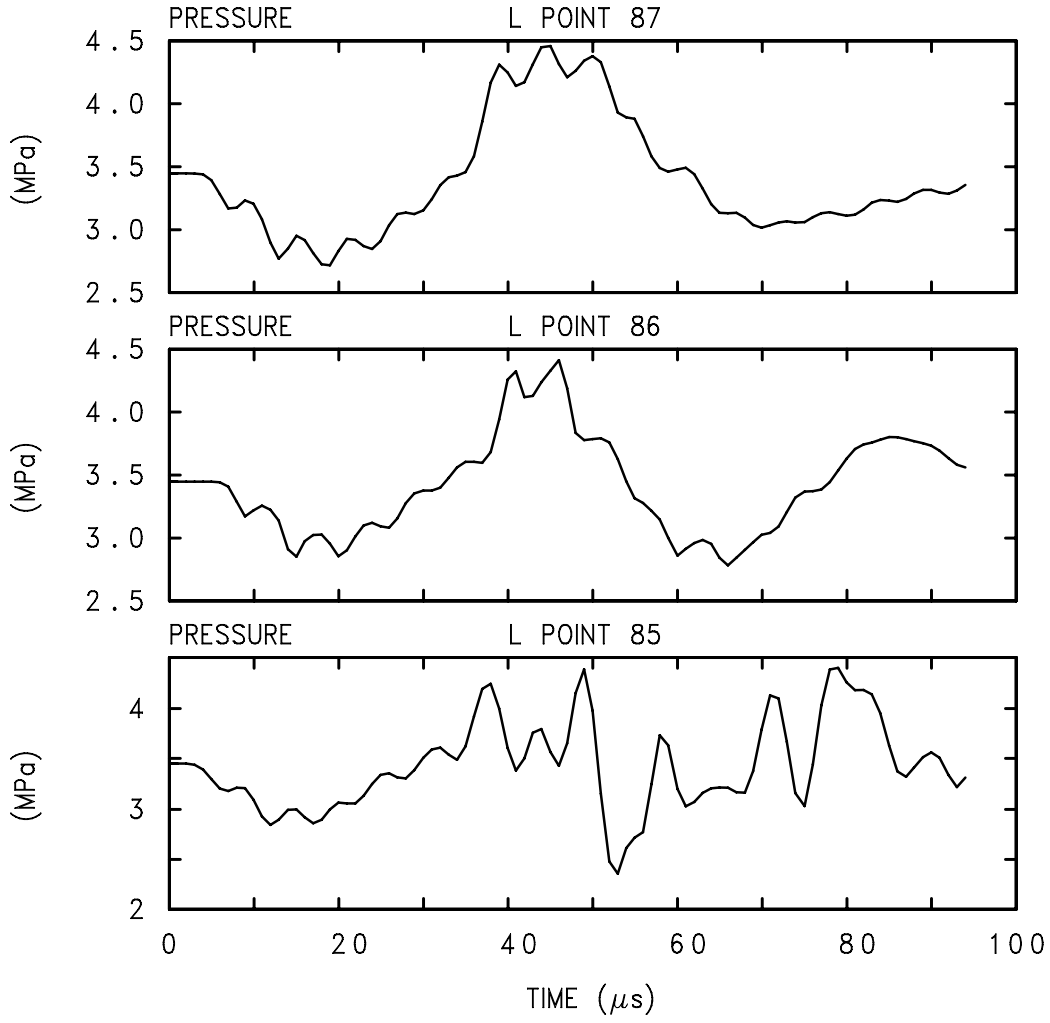

Fig. 18. Case 1 (detonation at upper region of the front-end tube)—pressure profiles in the water around the hemispherical region for the case with 3.45 MPa (500 psia) of the water pressure.

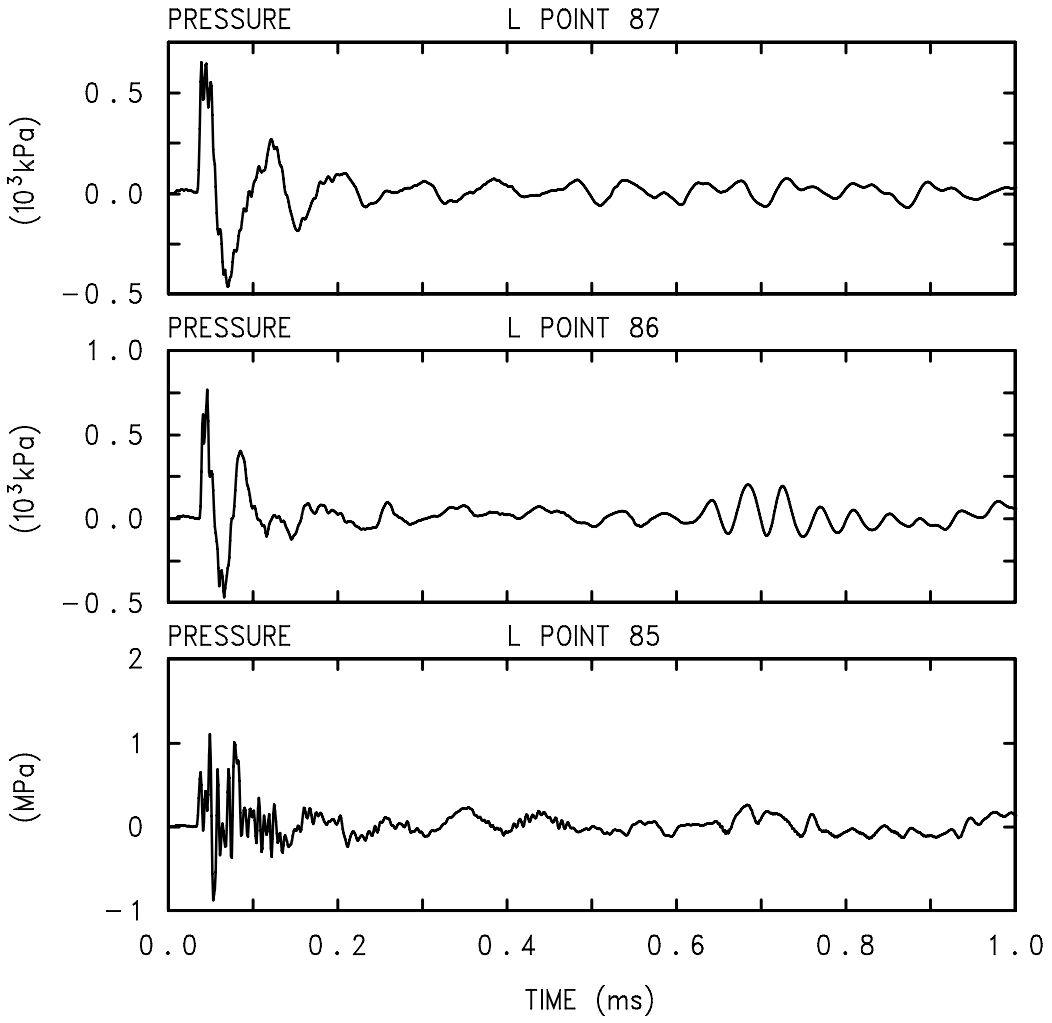

Fig. 19. Case 1 (detonation at upper region of the front-end tube)—pressure profiles in the water around the hemispherical region for the case with 0.1 MPa of the water pressure for extended period of time.

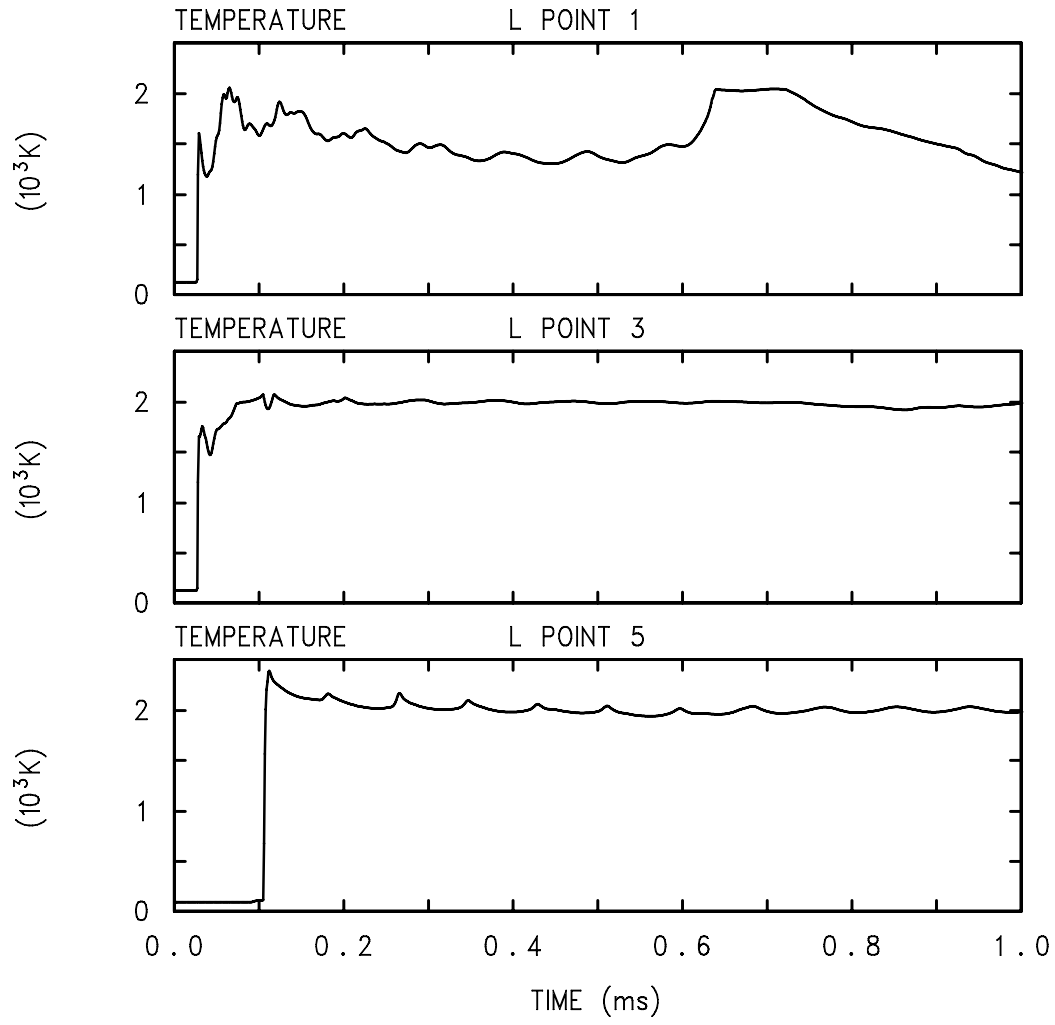

Fig. 20. Case 1 (detonation at upper region of the front-end tube)—gas mixture temperature profiles near the wall at the upper section of the vacuum tube.

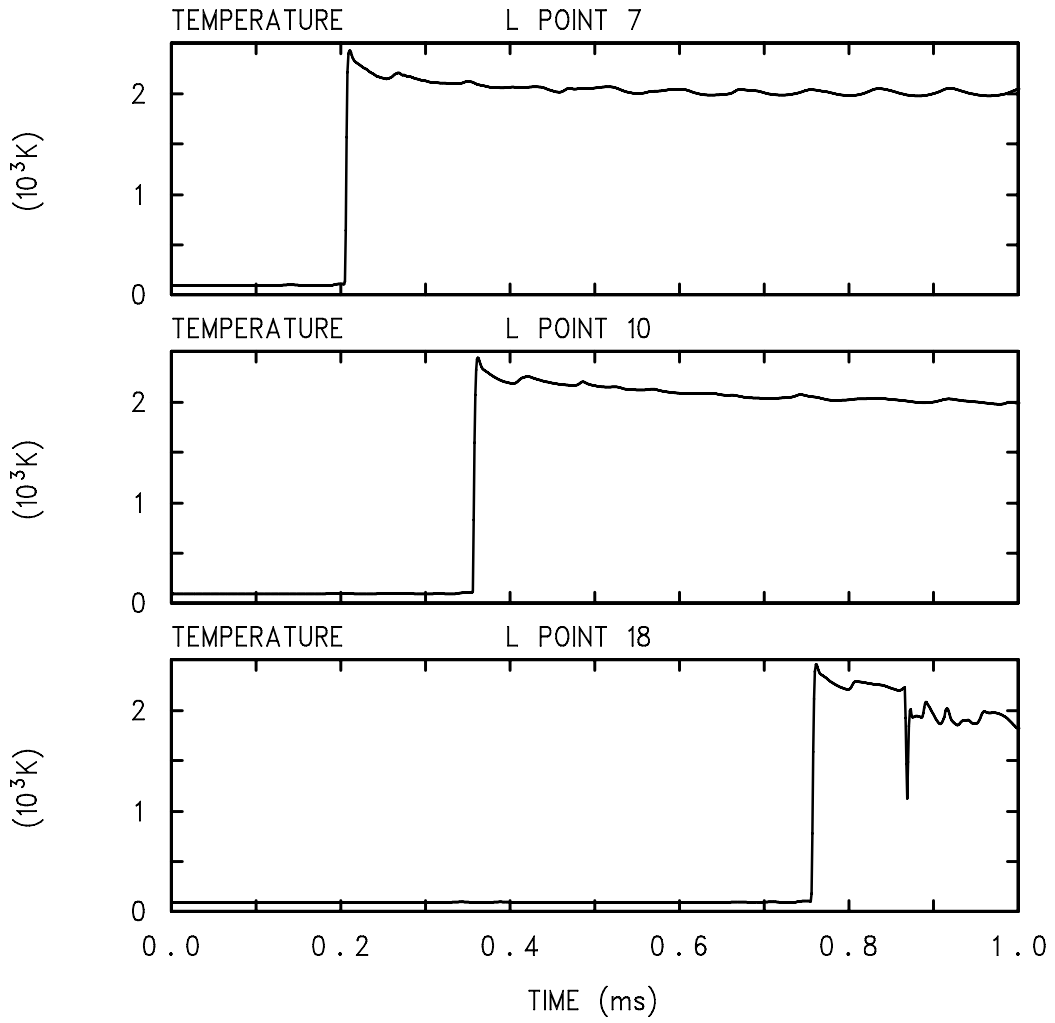

Fig. 21. Case 1 (detonation at upper region of the front-end tube)—gas mixture temperature profiles near the wall at the lower section of the vacuum tube.

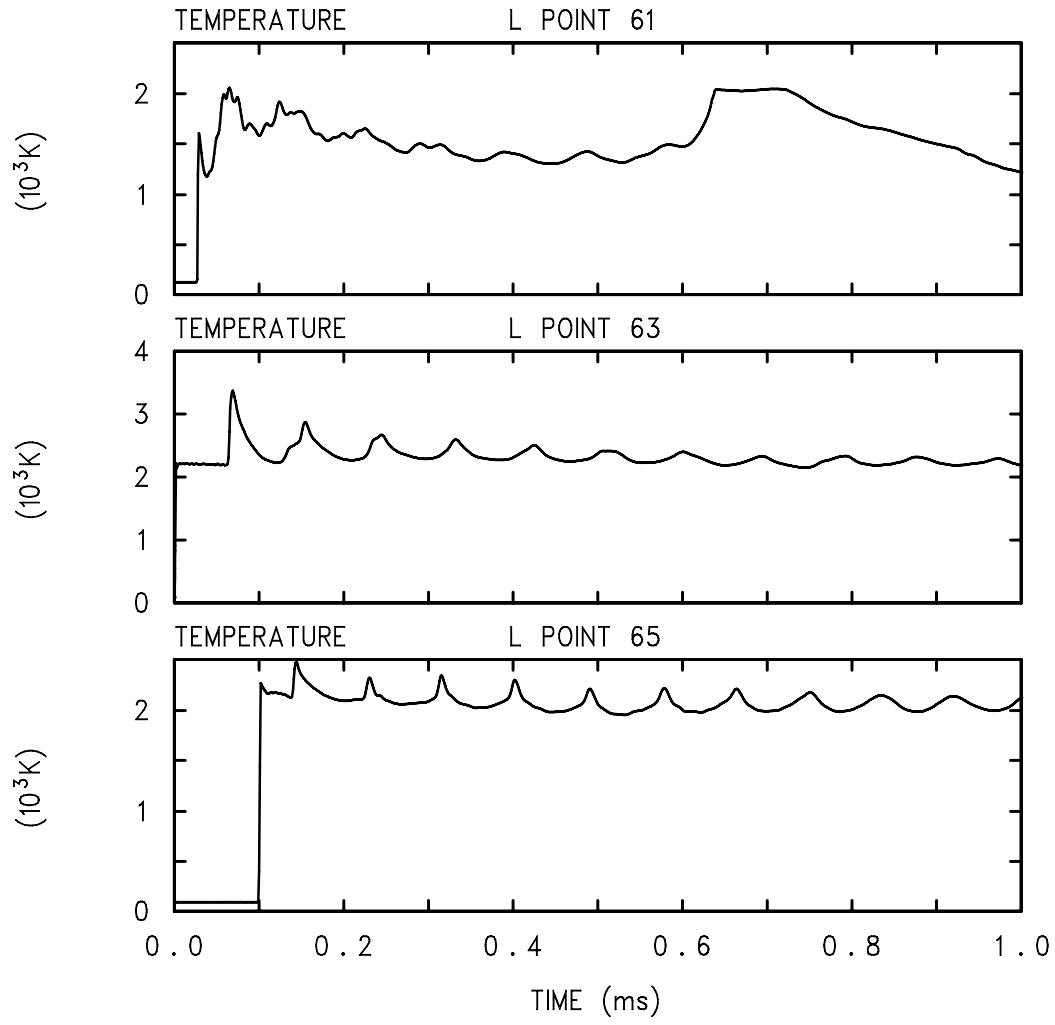

Fig. 22. Case 1 (detonation at upper region of the front-end tube)—gas mixture temperature profiles in the upper section along the y = 0 axis.

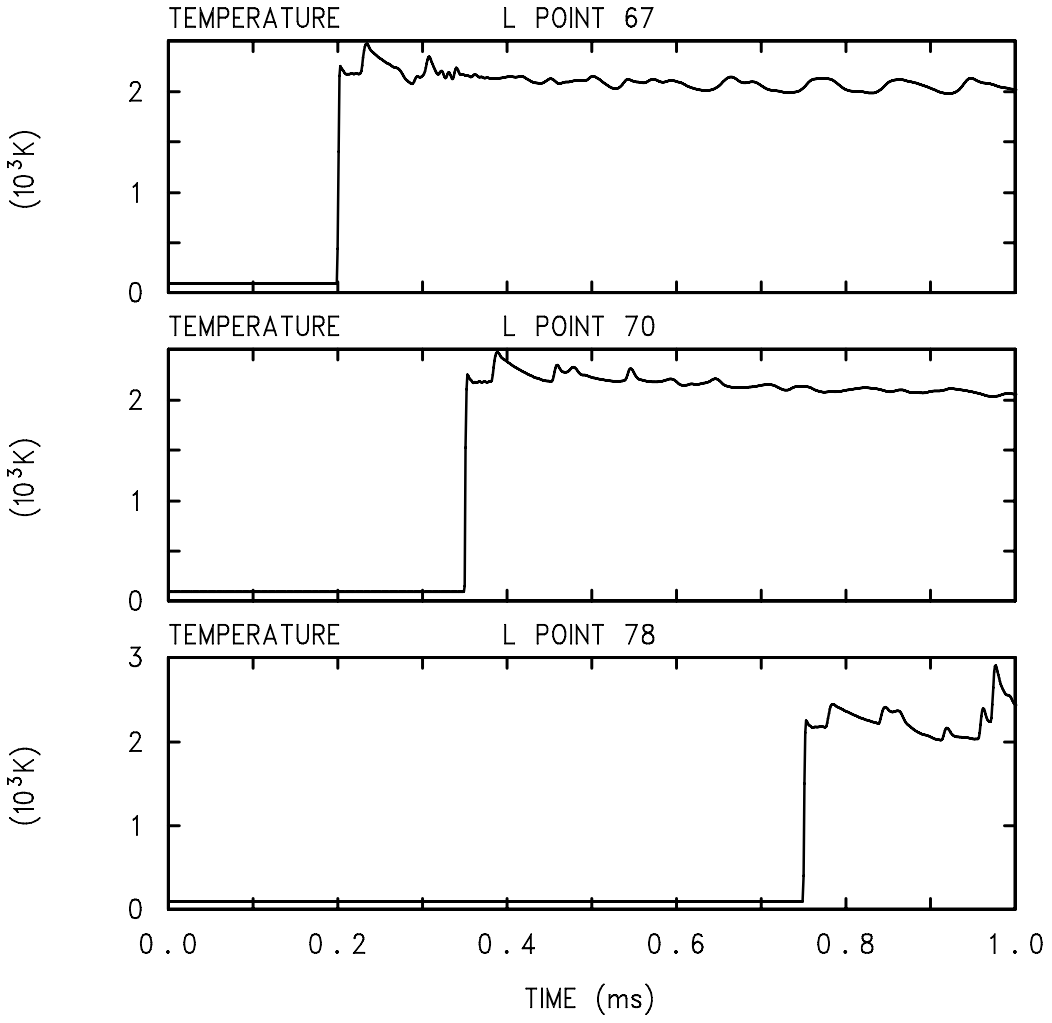

Fig. 23. Case 1 (detonation at upper region of the front-end tube)—gas mixture temperature profiles in the lower section along the y = 0 axis.

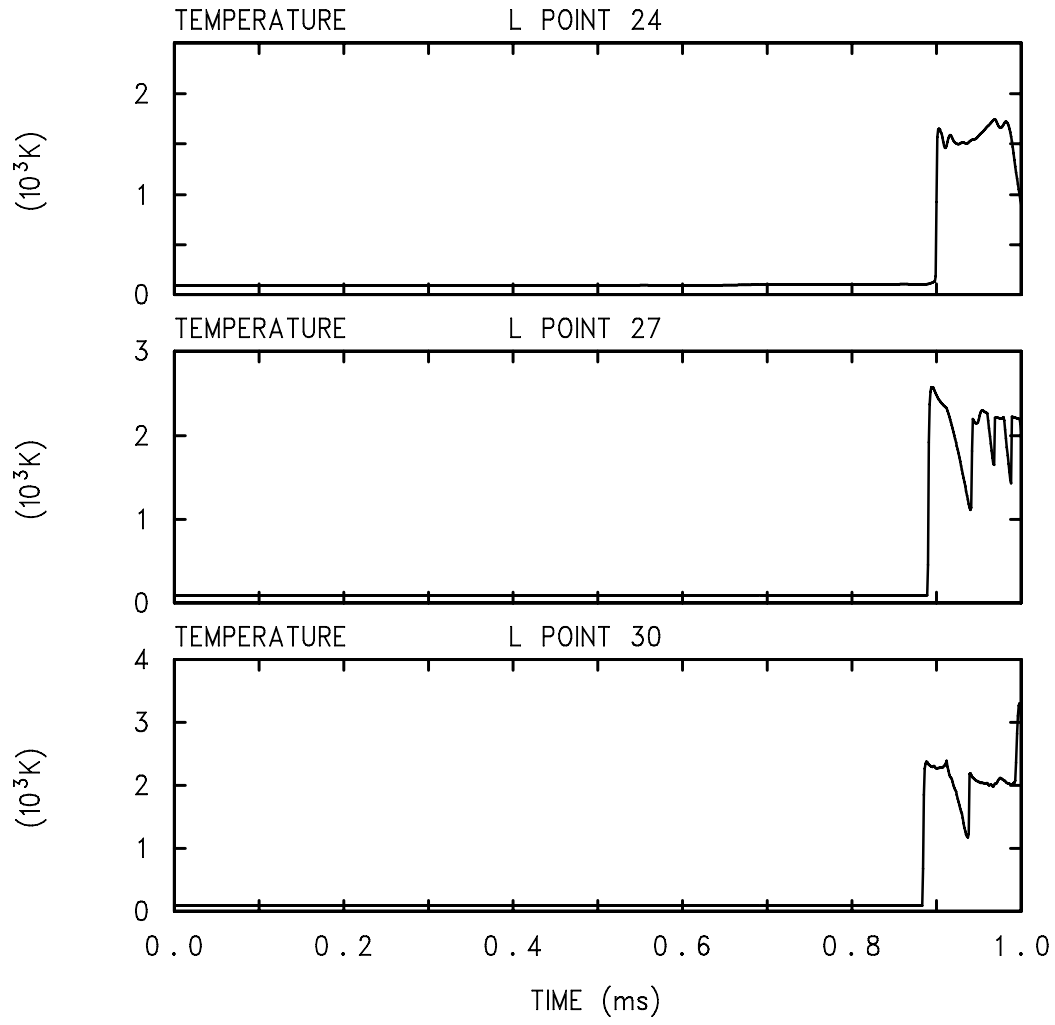

Fig. 24. Case 1 (detonation at upper region of the front-end tube)—gas mixture temperature profiles near the bottom window.

mixture properties were specified as the values averaged between the preburn and the postburn gas mixture properties. To have CTH predict the C-J pressure consistent with the CET89 prediction, the detonation velocity in CTH was arbitrarily raised to 2,400 m/s. However, it has been found that in CTH modeling, it is more appropriate to specify the properties of the postburn mixture because the pressure wave propagates through the postburn gas mixture (the detonation wave propagates through the preburn mixture, and its velocity is correctly specified as 2,000 m/s as predicted by CET89). With the current CTH modeling, it was previously shown that CTH correctly predicts the C-J pressure consistent with the value predicted by CET89. Furthermore, the behavior of the pressure wave behind the detonation front (based on the sound speed) is also correctly predicted with the current CTH model.

Figure 10 shows the pressure profiles for a few time moments before and after the wave reaching the bottom window. The same pressure profiles are magnified in Fig. 11. To understand the pressure wave behavior near the bottom window more clearly, two curves of the same profiles are plotted in Figs. 12–14. In Fig. 12, it is seen that the wave arrives at the window at 0.89 ms with amplitude of about 5.5 MPa. Upon being reflected, in the same figure, it becomes magnified to about 7.5 MPa at 0.91 ms. The reflected wave disperses to about 5 MPa quickly at 0.93 ms (Fig. 13) and keeps moving with the same magnitude (at 0.95 ms in Fig. 13). However, the complex geometrical configuration around the bottom window allows the pressure wave to overlap with the waves reflected from elsewhere, and the wave becomes as large as around 13 MPa at 0.97 ms (Fig. 14). It is also seen in the same figure that the pressure wave immediately splits into two at 0.99 ms; one moving upward with around 5.5 MPa and another moving toward the bottom window with around 10 MPa of the amplitude. This wave when it arrives at the bottom window is reflected, becoming as large as 25 MPa as already seen in Fig. 8 (history point-30 that is a central location near the bottom window).

3.1.2 Water Pressure Profiles

The side wall of the aluminum tube is surrounded by water that is at ~3.45 MPa (500 psia). Other structures are located outside in the vicinity of the hemispherical section of the front-end beam tube. To evaluate the safety implication of those structures to hydrogen/air detonation in the vacuum tube, estimates are required for the pressure amplitude in water as a result of transmission of mechanical energy of the detonation wave. The CTH model was executed assuming with a water pressure of 3.45 MPa; however, the calculation failed when the shock wave passed through the tube wall section at around the y = 128-cm location. Currently, a simple constitutive material model is assumed for aluminum wall behavior subject to the shocks. The model incorporates a simple von-Mises yield criterion with quasi-static structural properties, which may not be appropriate for modeling the dynamic response of solid materials to shocks. Instead of further investigating this CTH failure with high water pressure back, it was decided to perform the CTH calculations assuming that the water pressure is in equilibrium with the gas mixture pressure inside the tube (0.1 MPa). To estimate the pressure amplitude outside the hemispherical section of the tube, however, the pressure profiles have been obtained until the moment that CTH failed. Also to measure the effects of high water pressure on detonation wave propagation inside the tube, the pressure profiles of the gas mixtures were compared between two cases with a low and a high water pressure. Figure 15 compares the gas mixture pressure near the wall in the hemispherical section (history points of 1 and 3). In the figure, the two plots on top represent the low water pressure case (0.1 MPa), and the bottom two plots are for a high water pressure case (3.45 MPa). The detonation wave and following pressure profiles in the midsection of the tube are also shown in Fig. 16 for both cases. As seen in the figures, the detonation wave and pressure profiles for both cases are almost identical. Therefore, it was concluded that high water pressure effects on the detonation wave propagation inside the tube and the following

and the following pressure profiles are almost negligible. Figure 17 shows the pressure profiles in the water around the hemispherical section of the tube for the low water pressure case, and Fig. 18 shows similar profiles for the high water pressure case. The water pressure profiles for an extended time period for the low pressure case are shown in Fig. 19. As seen in Fig. 19, the water pressure associated with the earlier time period represents the highest during the transient. Therefore, the water pressure profiles in Fig. 18 could be conservatively used for the safety evaluation of surrounding structures.

3.1.3 Temperature Profiles

Transient temperature profiles in the gas mixture are shown in Figs. 20–24. Because the postburn gas mixture is expected to behave closely to the ideal gas, temperature response is shown closely to follow the pressure profile. Heat conduction (or thermal dissipation) through the tube wall is not modeled because the timescale associated with thermal conduction is much longer than the timescale with the detonation and shock wave transport. As mentioned above, CTH predicts a C-J temperature lower than CET89; therefore, it is recommended to use the CTH predicted temperatures multiplied by 1.25 (i.e., 2,937 K from CET89 divided by 2,346 K from CTH) for any safety applications. In general, the gas temperatures are predicted to be around 2,500 K except for the middle location near the bottom window where the predicted temperature can go above 3,000 K as seen in Fig. 24.

3.2 CASE 2 RESULTS: POINT DETONATION AT (0, 57.27) IN FRONT-END VACUUM TUBE

For case 2, the detonation was assumed to start at the location y = 57.27 cm along the centerline (r = 0), history point of 75. The calculation was performed for 0.64 ms of detonation transient. Similar to case 1, the results show detonation wave propagation, amplification, reflection, and focusing. Figures 25–28 show transient profiles of the detonation pressure wave at various history points; detonation pressure wave behaviors when the wave arrives at the bottom window are illustrated in Figs. 29–32. Figures 33–36 show gas mixture temperature variations at the same history points as for the pressure profiles shown in Figs. 25–28.

As seen in Fig. 25, detonation initiated at history point-75 propagates upward (history point-70) and downward (history point-80). Geometrical focusing amplifies the wave to as high as 9 MPa at history point-75, following reflection back from the nearby cylindrical walls. If we only consider the reflection from the side wall, the wave focusing is expected to occur at every 0.12 ms (i.e., diameter of the tube, 13 cm, divided by the sound speed, 1,092 m/s). The pressure profile of history point-75 clearly indicates that CTH predicts the wave transport behavior correctly. In Fig. 25, it is seen that the history point-80 experiences about 18 MPa of the pressure peak due to overlapping (or focusing) of the waves reflected from various surfaces including the side wall and the bottom window. Figure 26 shows the pressure profiles of the history points-9, -14, and -19 that are near the cylindrical tube wall. The detonation wave initiated at history point-75 is expected to arrive to the bottom window at around 0.28 ms (distance, 57.27 cm, divided by the detonation velocity, 2000 m/s). The detonation wave and following pressure profiles near the bottom window wall are shown in Fig. 27. As seen in the figure, CTH predicts that the detonation wave arrives at around 0.28 ms to the midlocation of the bottom window as indicated in the pressure profile of the history point-30. Along the edges of the bottom window, the pressure amplitude goes up as high as 10 ~ 14 MPa as seen from the history points-24 and -27; however, the midlocation (history point-30) experiences as high as 21 MPa due to the wave reflected from the surrounding tube walls. Figure 28 shows the pressure profiles at the history points-1, -3, and -5, which are along the top hemispherical wall. In general, the wall experiences

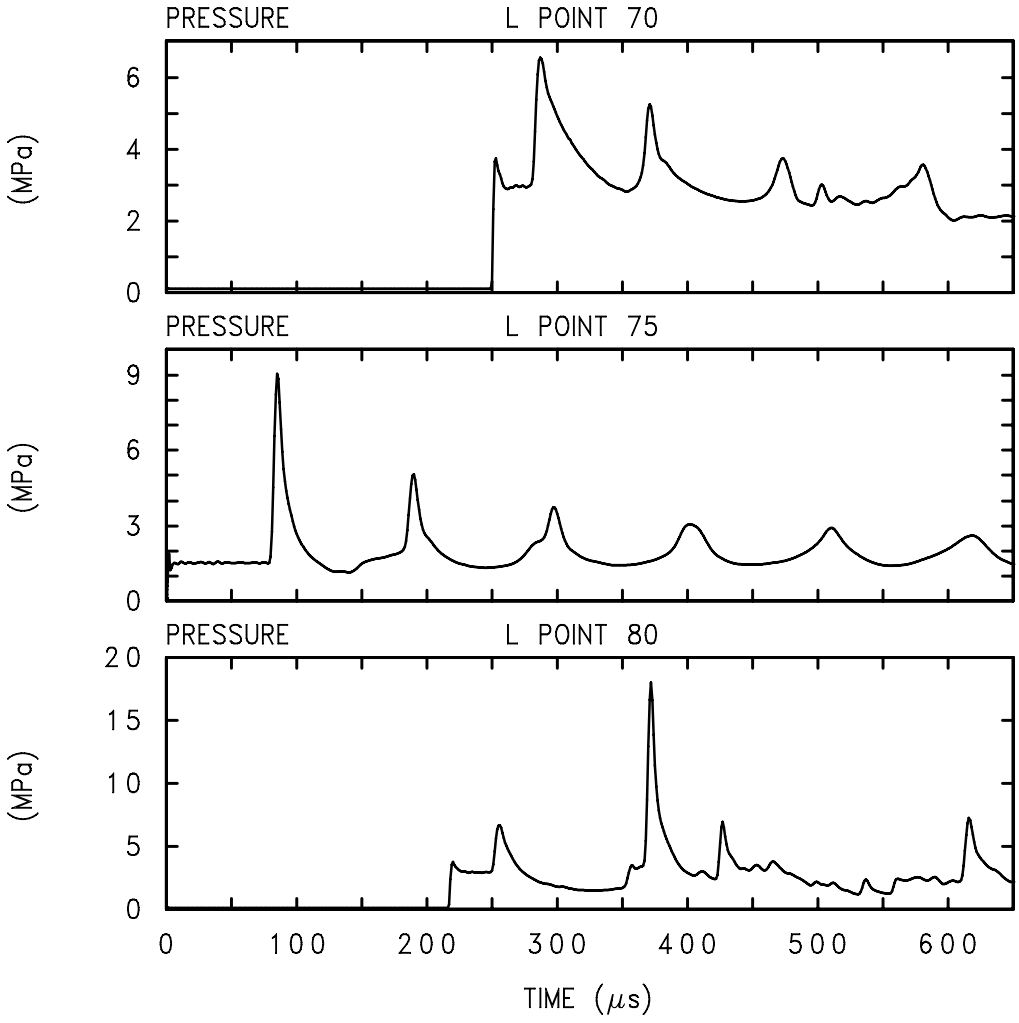

Fig. 25. Case 2 (detonation at lower region of the front-end tube)—pressure profile in lower section at the centerline (x = 0) along the y-axis.

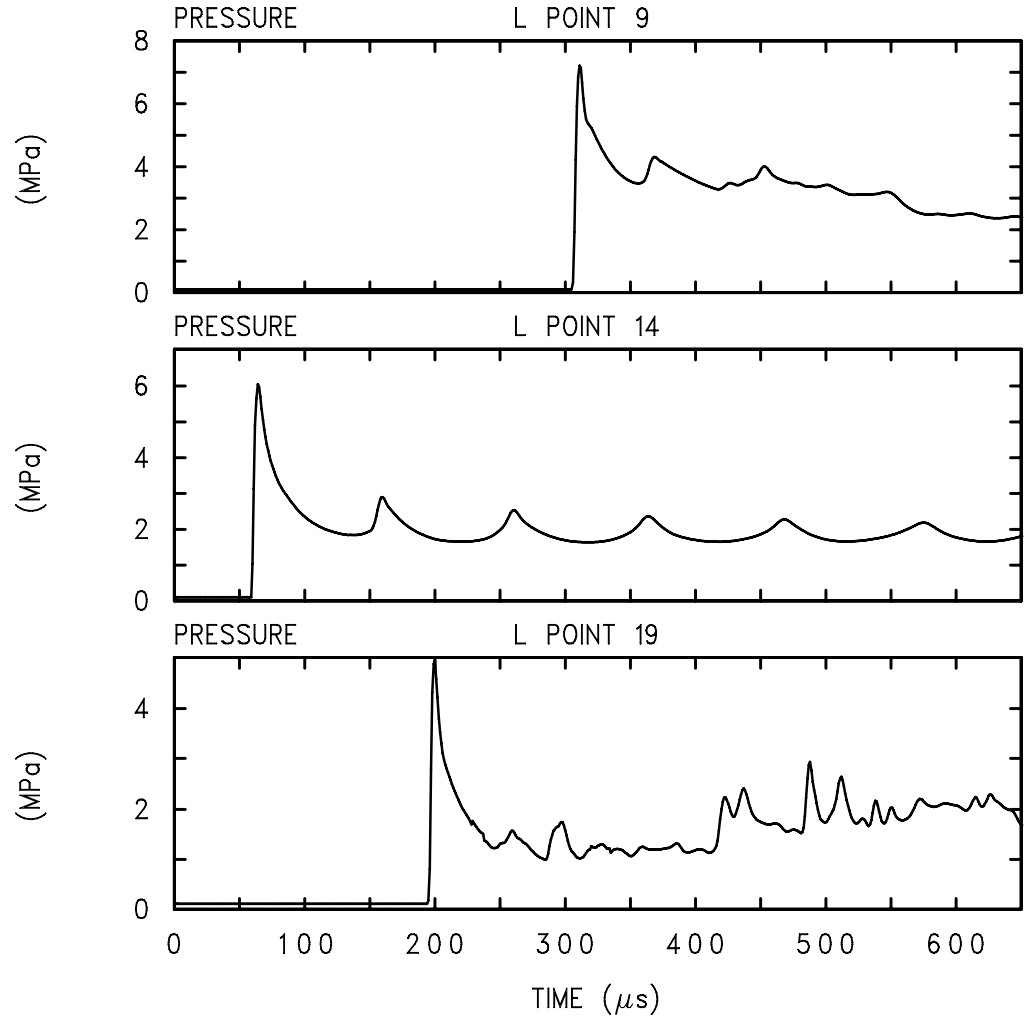

Fig. 26. Case 2 (detonation at lower region of the front-end tube)—pressure profile near the side wall in lower section.

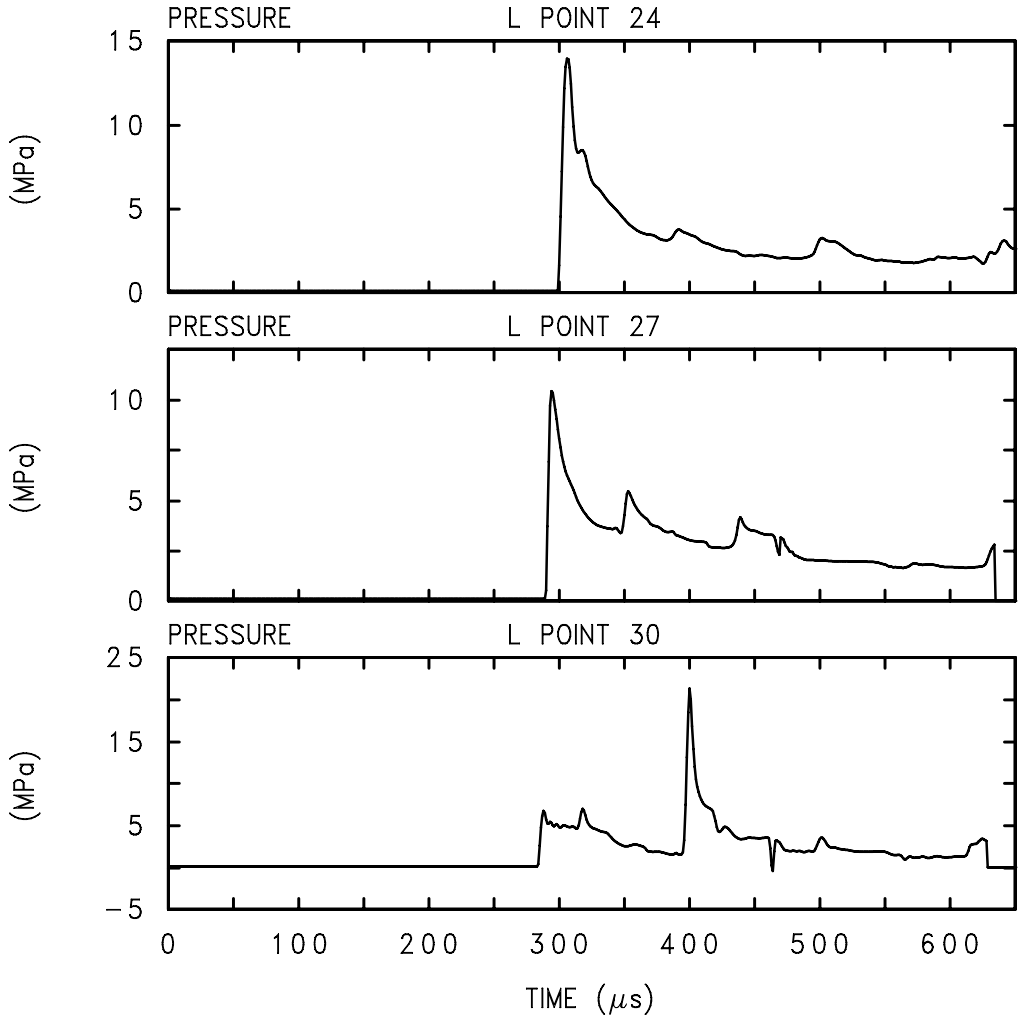

Fig. 27. Case 2 (detonation at lower region of the front-end tube)—pressure profile near the bottom window.

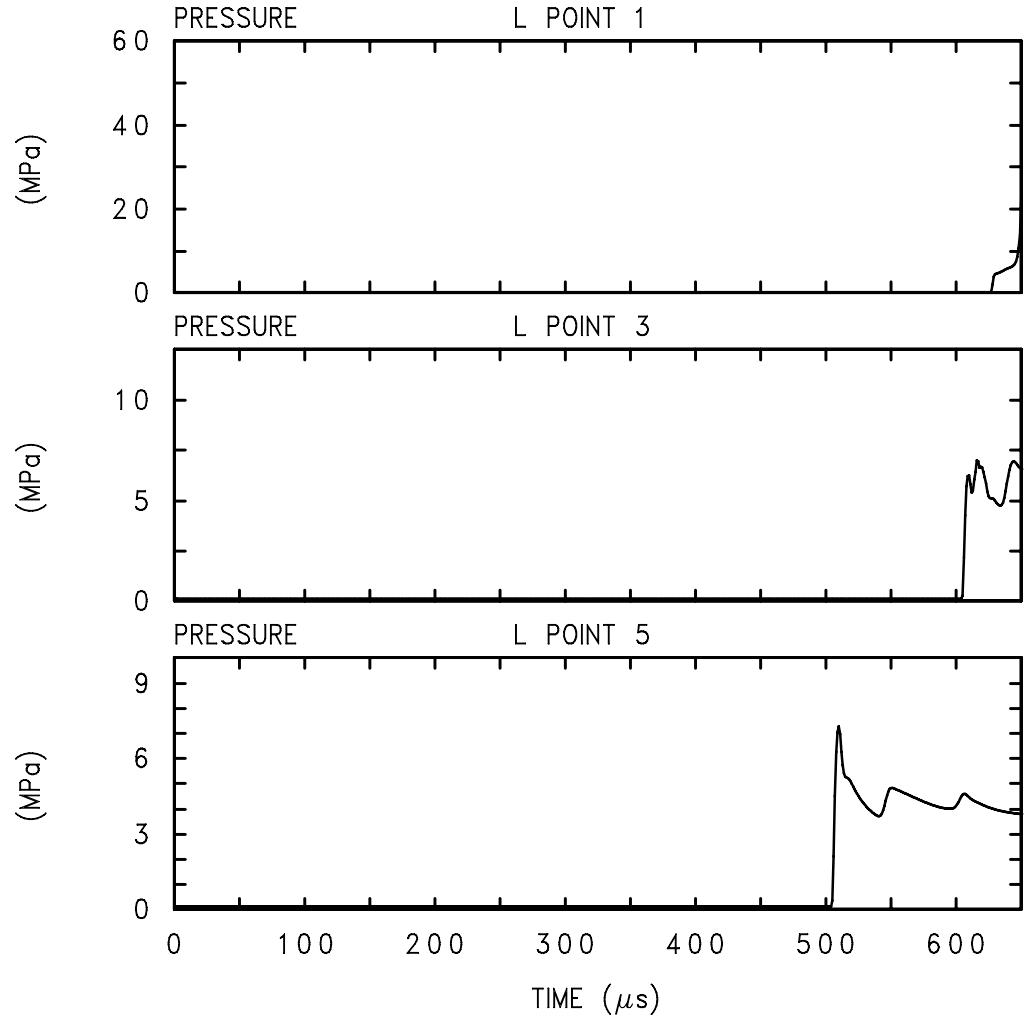

Fig. 28. Case 2 (detonation at lower region of the front-end tube)—pressure profile near the wall at the upper hemispherical region.

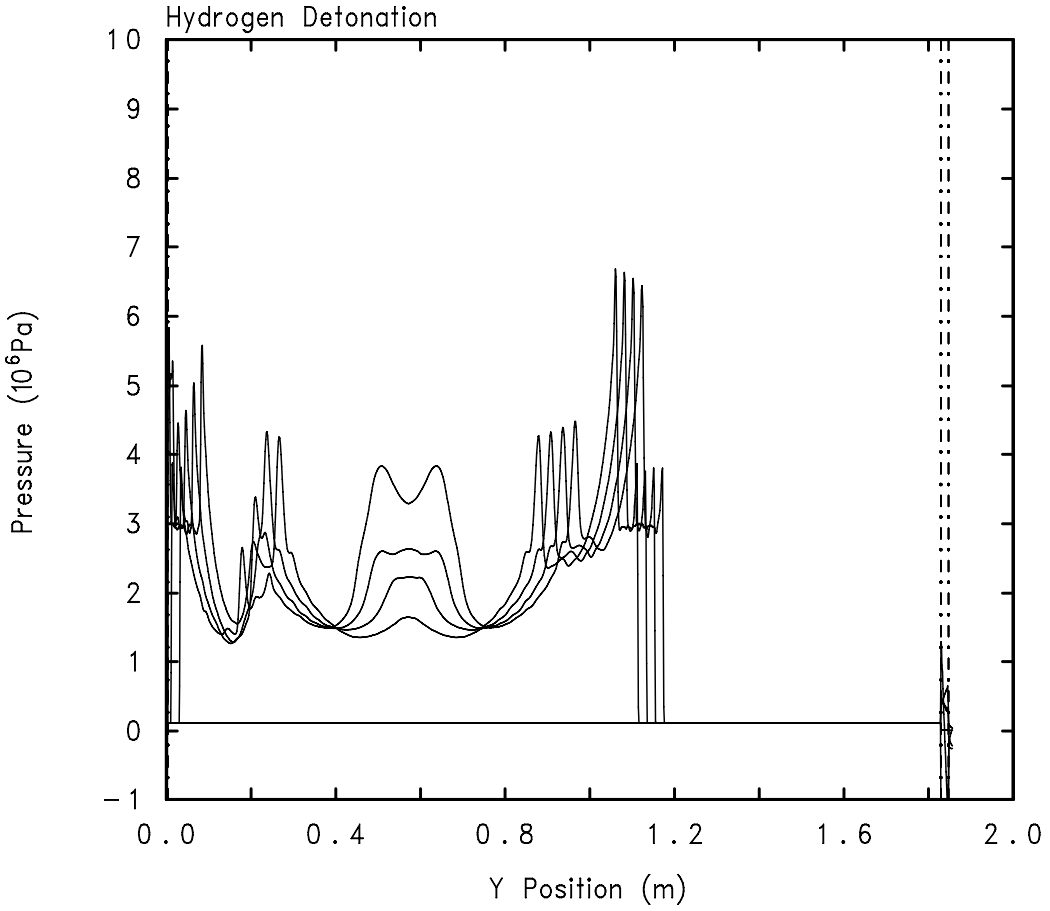

Fig. 29. Case 2 (detonation at lower region of the front-end tube)—pressure profile at centerline along y-axis from 0.27 ms to 0.30 ms with 0.01-ms interval.

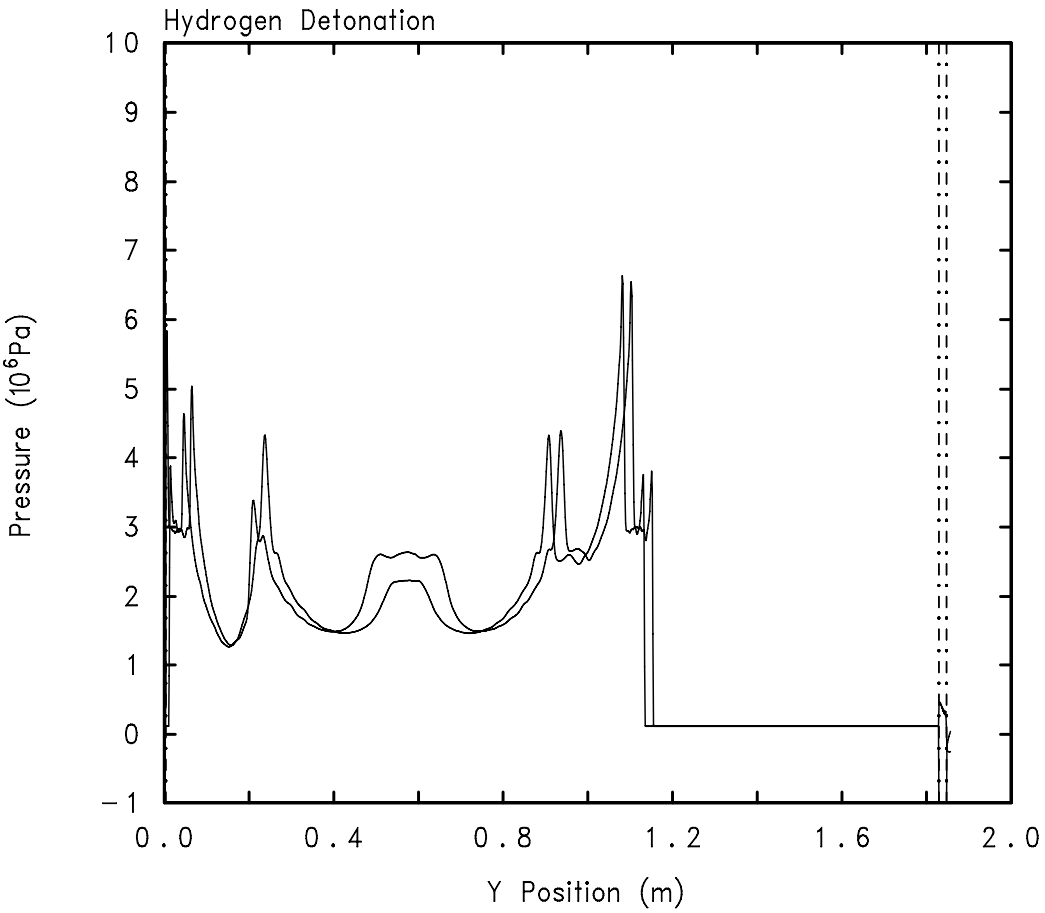

Fig. 30. Case 2 (detonation at lower region of the front-end tube)—pressure profile at centerline along y-axis at 0.28 (before arriving at the bottom window) and 0.29 ms (after being reflected).

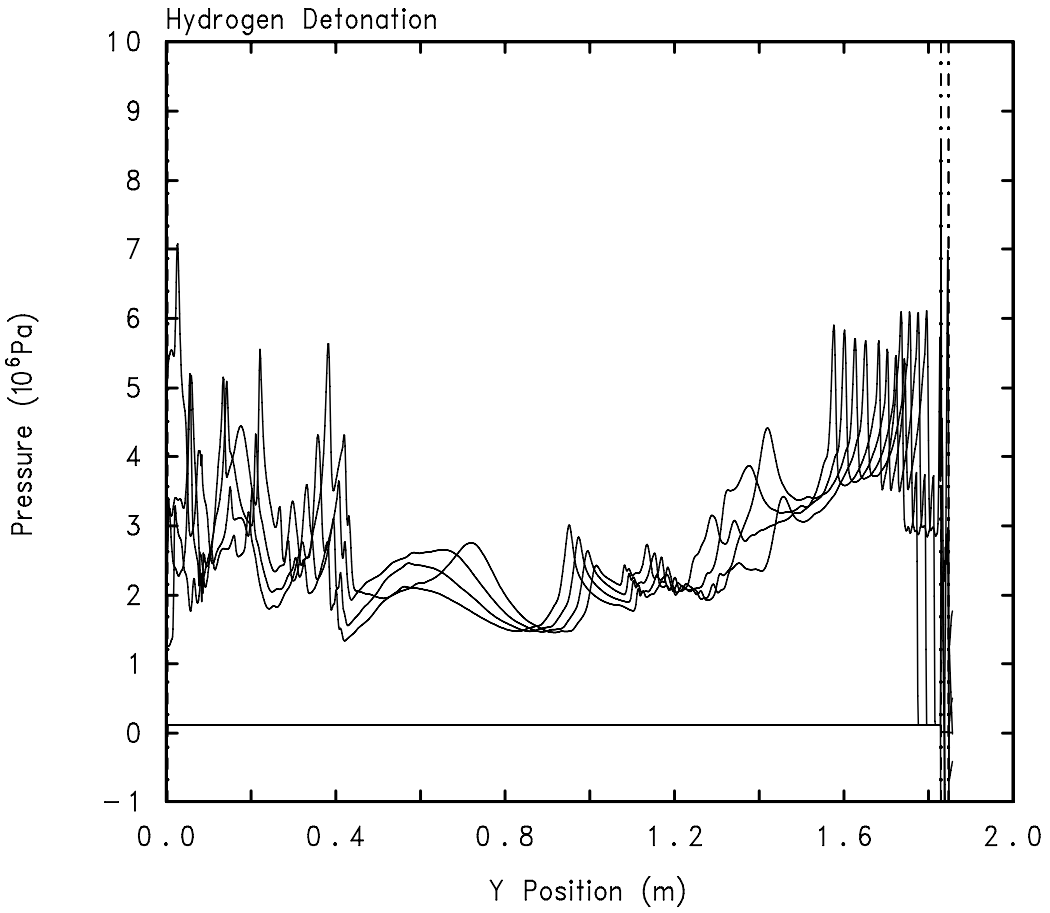

Fig. 31. Case 2 (detonation at lower region of the front-end tube)—pressure profile at centerline along y-axis from 0.6 ms to 0.63 ms with 0.01-ms interval.

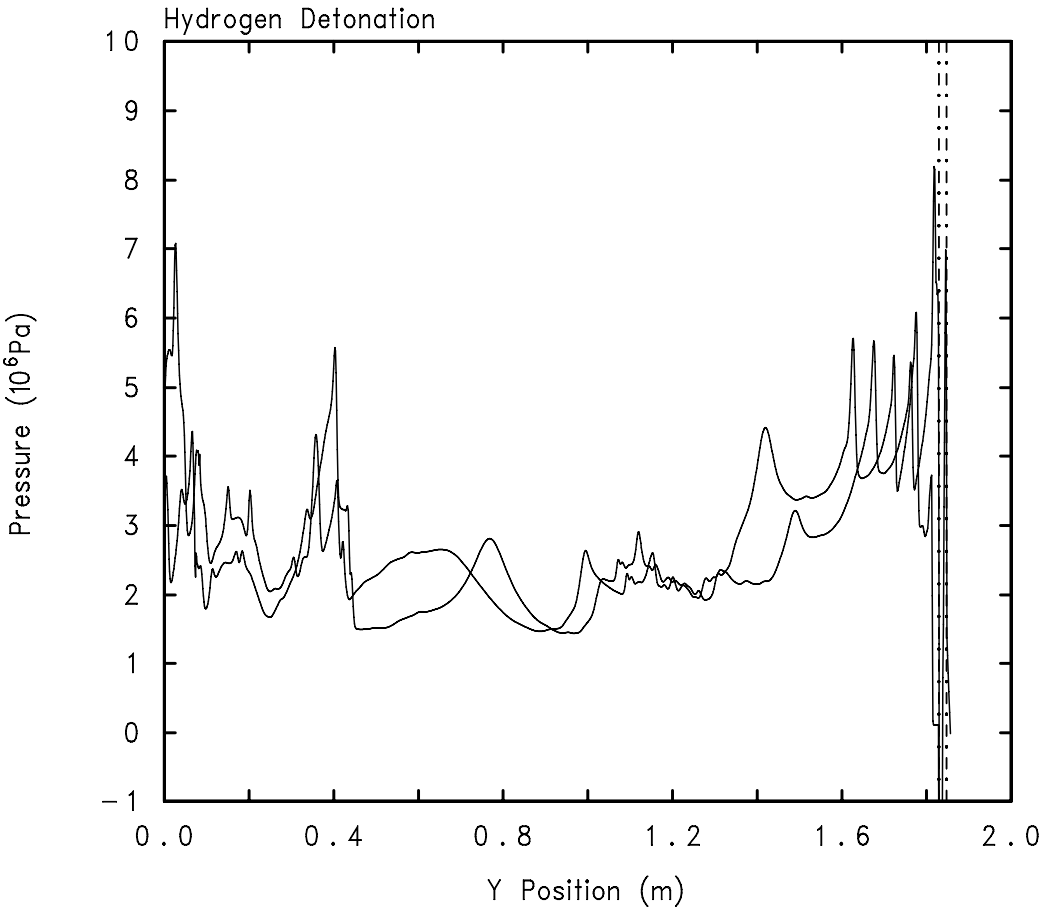

Fig. 32. Case 2 (detonation at lower region of the front-end tube)—pressure profile at centerline along y-axis at 0.62 (before arriving at the top hemispherical wall) and 0.64 ms (after being reflected).

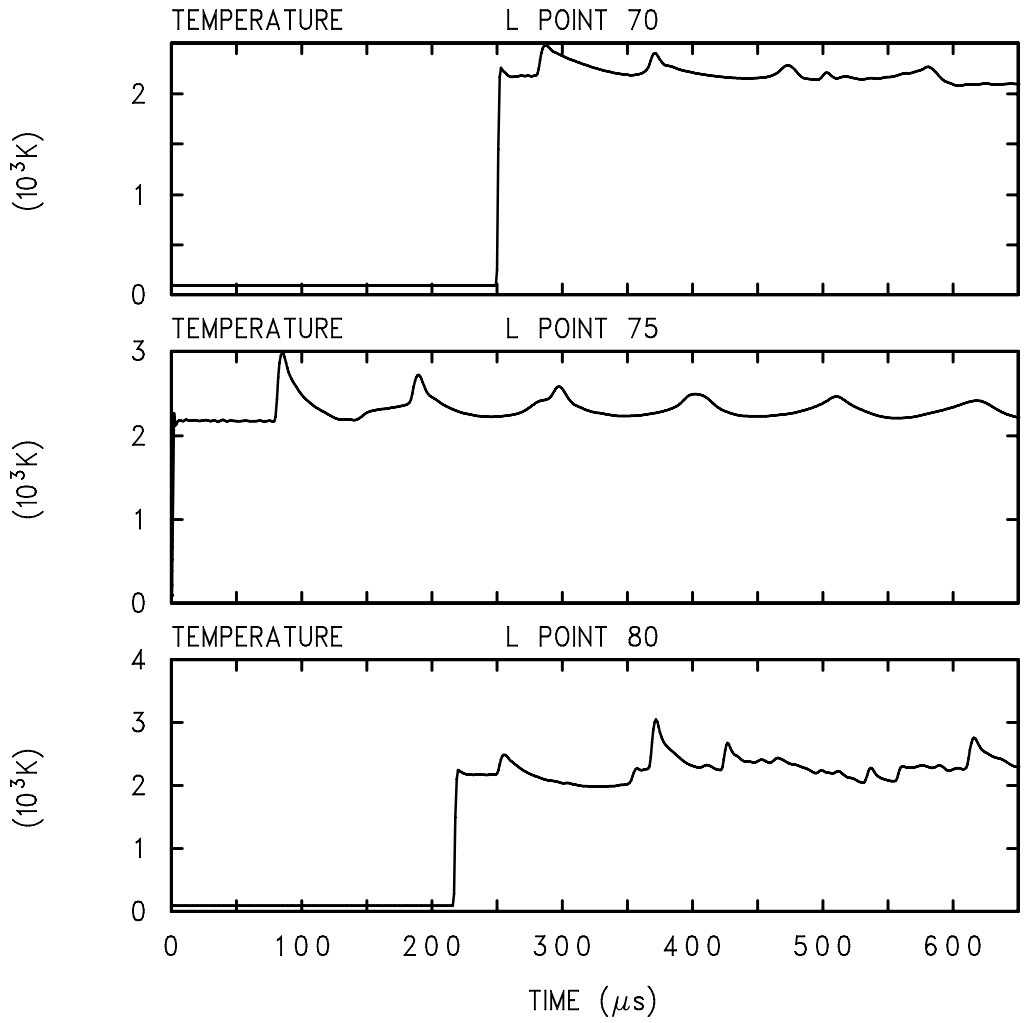

Fig. 33. Case 2 (detonation at lower region of the front-end tube)—temperature profile in lower section at the centerline (x = 0) along the y-axis.

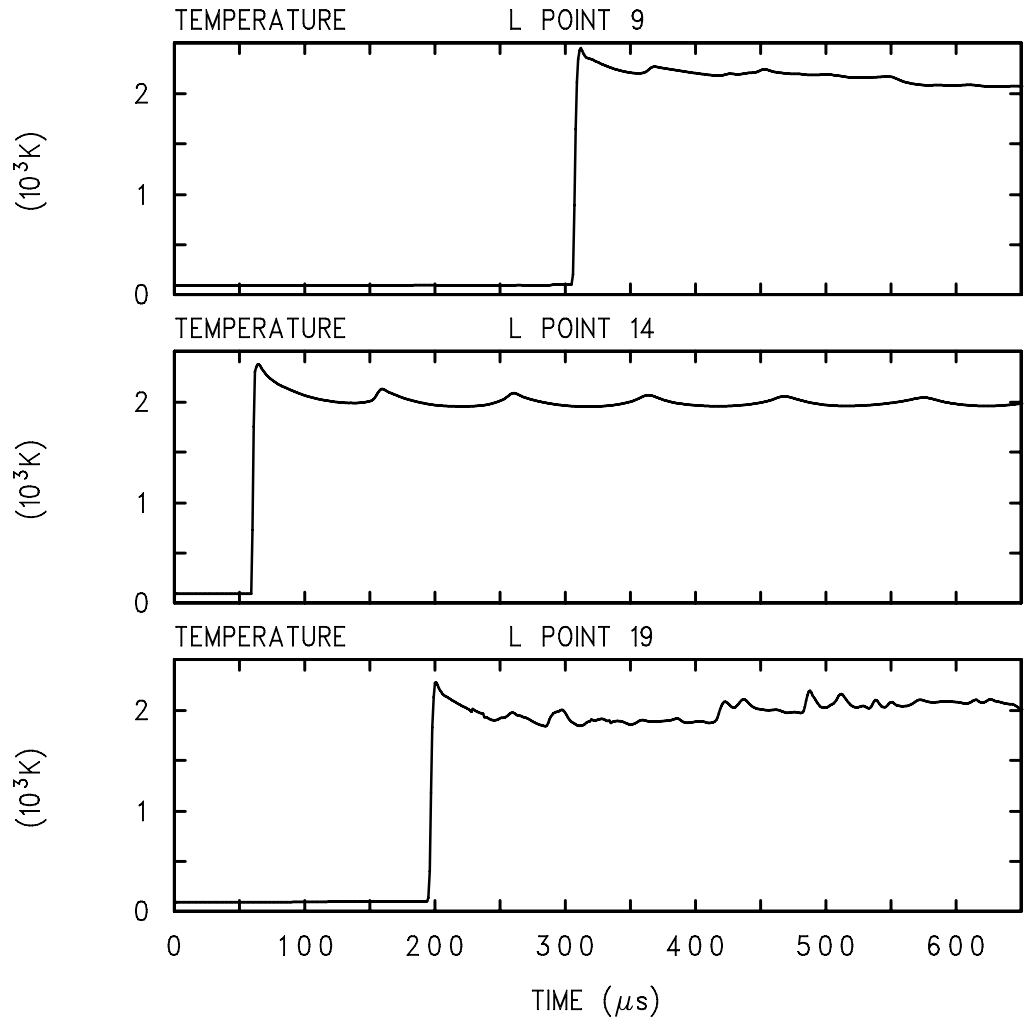

Fig. 34. Case 2 (detonation at lower region of the front-end tube)—temperature profile near the side wall in lower section.

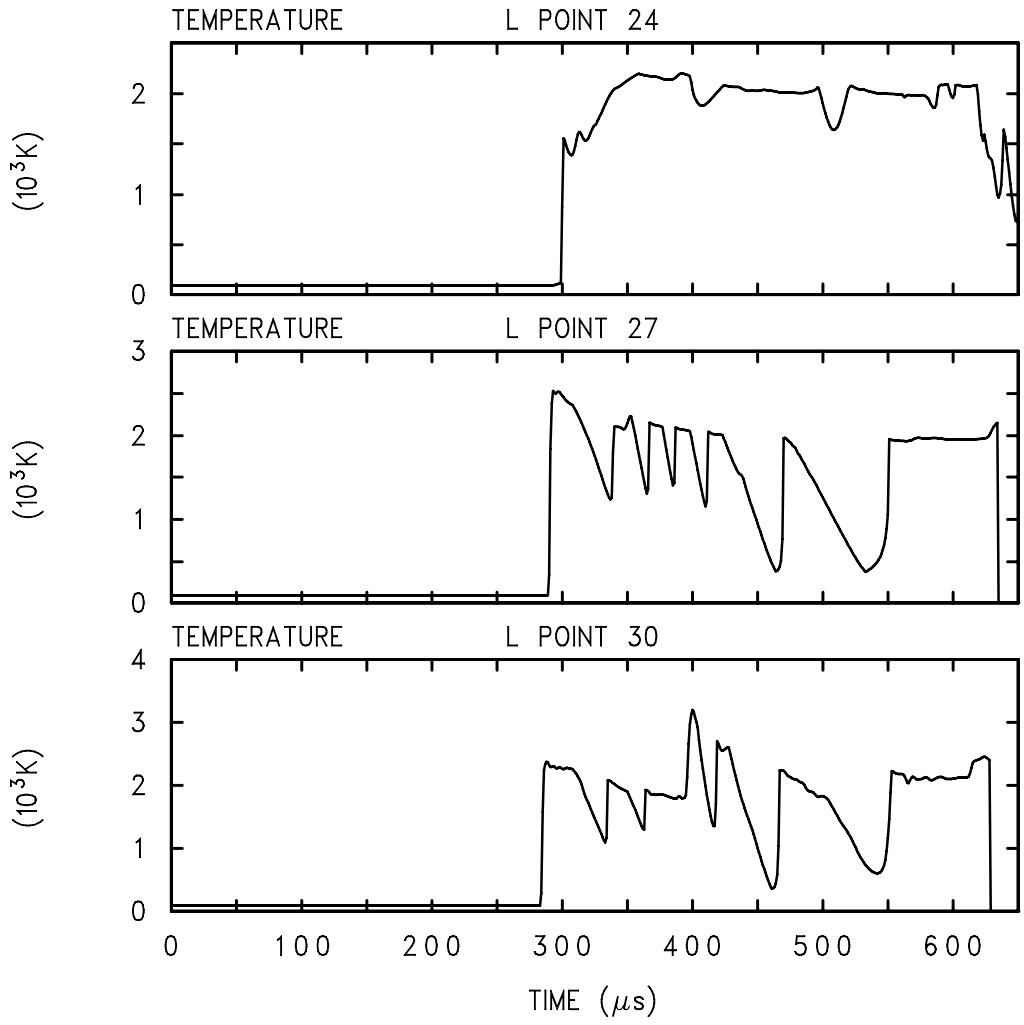

Fig. 35. Case 2 (detonation at lower region of the front-end tube)—temperature profile near the bottom window.

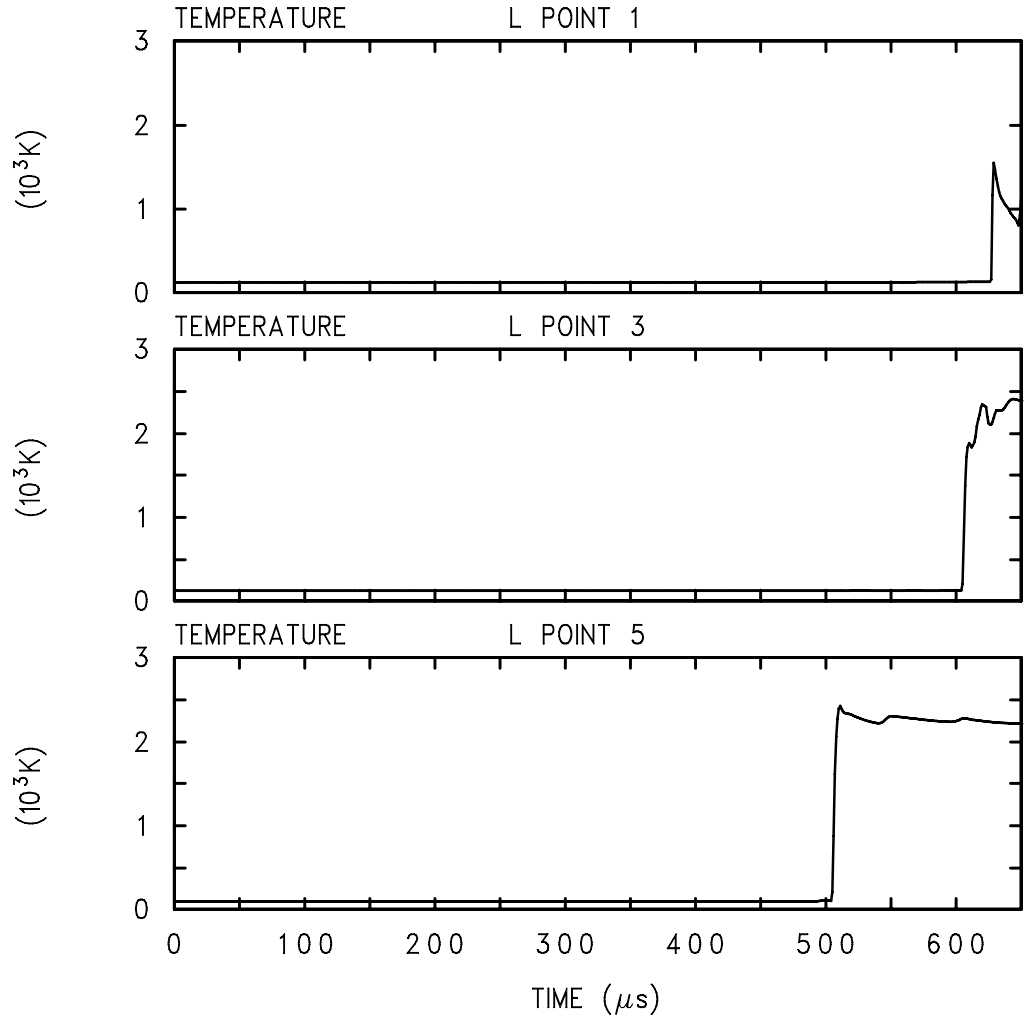

Fig. 36. Case 2 (detonation at lower region of the front-end tube)—temperature profile near the wall at the upper hemispherical region.

the pressure wave, as high as ~8 ~ 13 MPa. The detonation wave arrives at the wall at around 0.63 ms [i.e., a distance, (182.91–57.27) cm, divided by the detonation velocity, 2,000 m/s]. CTH predicts the arrival time correctly as seen in the pressure profile of the history point-1. Figures 29 and 30 show several snapshots of the pressure profile at the centerline (x = 0) along the y-axis from 0.27 ms to 0.30 ms. This time period corresponds to the time the detonation wave reaches the bottom window and is reflected back. Similar plots are shown in Figs. 31 and 32 for the time moments around when the detonation wave reaches the top hemispherical wall. These figures do not plot the peak pressure near the wall. Therefore, it is suggested to use the pressure peak of 10 ~ 14 MPa at the bottom window edges and around 21 MPa in the middle as indicated in Fig. 27. Similarly, a peak of 10 ~ 13 MPa near the top hemispherical wall is suggested by Fig. 28.

Transient temperature profiles of the gas mixtures at various locations are shown in Figs. 33–36. It is seen that the temperature can go up as high as 3,000 K.

3.3 CASE 3 RESULTS: POINT DETONATION AT (0, 128.1) IN BACK-END BEAM TUBE

The detonation of this case for the back-end vacuum tube was assumed to start at the location y = 128.1 cm along the centerline (x = 0), at history point of 13 (Fig. 3). The calculation was performed for 1.5 ms into the transient. Figures 37–41 show transient variations of detonation pressure at various history points. In Figs. 42–46, similar pressure profiles are illustrated at various time moments along the centerline (i.e., x = 0). Transient profiles of the gas mixture temperatures are illustrated in Figs. 47–51.

Initial conditions of the hydrogen/air gas mixture in the back-end beam tube are 300 K and 0.1 MPa. The C-J conditions predicted by CET89 are, as seen in Table 1, 1.55 MPa and 2,946 K for the C-J pressure and temperature, respectively. Using the detonation velocity and the transport property values predicted by CET89, CTH predicts 1.53 MPa and 2,033 K for the C-J pressure and temperature, respectively. CTH's C-J pressure is in good agreement with that of CET89; as also seen in the case 1, a difference is observed in the C-J temperature between the values predicted by CTH and CET89. Therefore, it is suggested to use a safety factor of 1.45 to be multiplied to the CTH predicted temperature values for any safety implications.

Detonation started at the history point-13 propagates through the gas mixture, and resulting pressure waves are reflected from the surrounding tube walls as seen in Fig. 37. The gas pressure goes up as high as 4 MPa at the history point-13. The top window experiences ~6 MPa of pressure as seen in the history point-1 that is near the top window. The pressure wave behind the detonation front is expected to travel at 1,092 m/s as seen in Table 1. Therefore, the focusing due to reflection from the side wall is expected to occur every 0.29 ms according to the CET89 predictions (i.e., tube diameter, 31.75 cm, divided by a sound speed, 1,092 m/s). Looking at the pressure profiles at the history points-1, -13, and -14 in Fig. 37, CTH predicts such geometrical focusing at about 0.27 ms. This means that CTH predicts the sound speed in the postburn gas mixture about 7% higher than CET89. Figure 38 shows the pressure profiles of the gas mixture inside the collimator along the centerline (x = 0). Ringing behavior inside the collimator has a higher frequency because the diameter inside the collimator is smaller than the tube diameter. Pressure focusing is expected to be every 0.13 ms according to CET89 (i.e., the collimator inside diameter, 14.1 cm, divided by the sound speed, 1,092 m/s). Figure 38 shows that CTH predicts geometrical focusing at about 0.11 ~ 0.13 ms.

The gas mixture pressure profiles near the side wall, top window, and bottom window are shown in Figs. 39–41. On the side wall, the gas pressure goes up to about 1.5 ~ 3 MPa, depending on location. The detonation wave is expected to arrive at the top window at around 0.28 ms [i.e., a distance (182.71–128.1) cm, divided by the detonation velocity, 1,970 m/s]. CTH

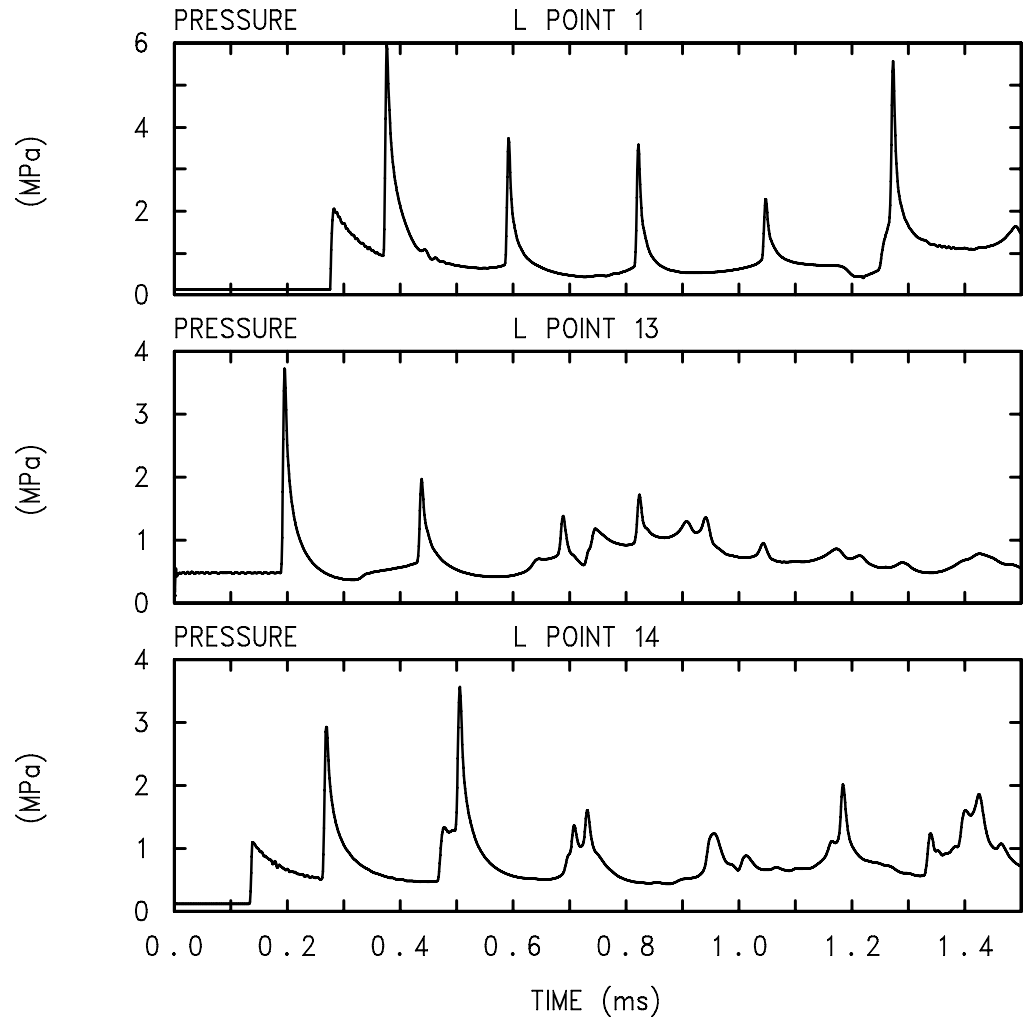

Fig. 37. Case 3 (detonation at upper region of the back-end tube)—pressure profile at the centerline (x = 0) along the y-axis.

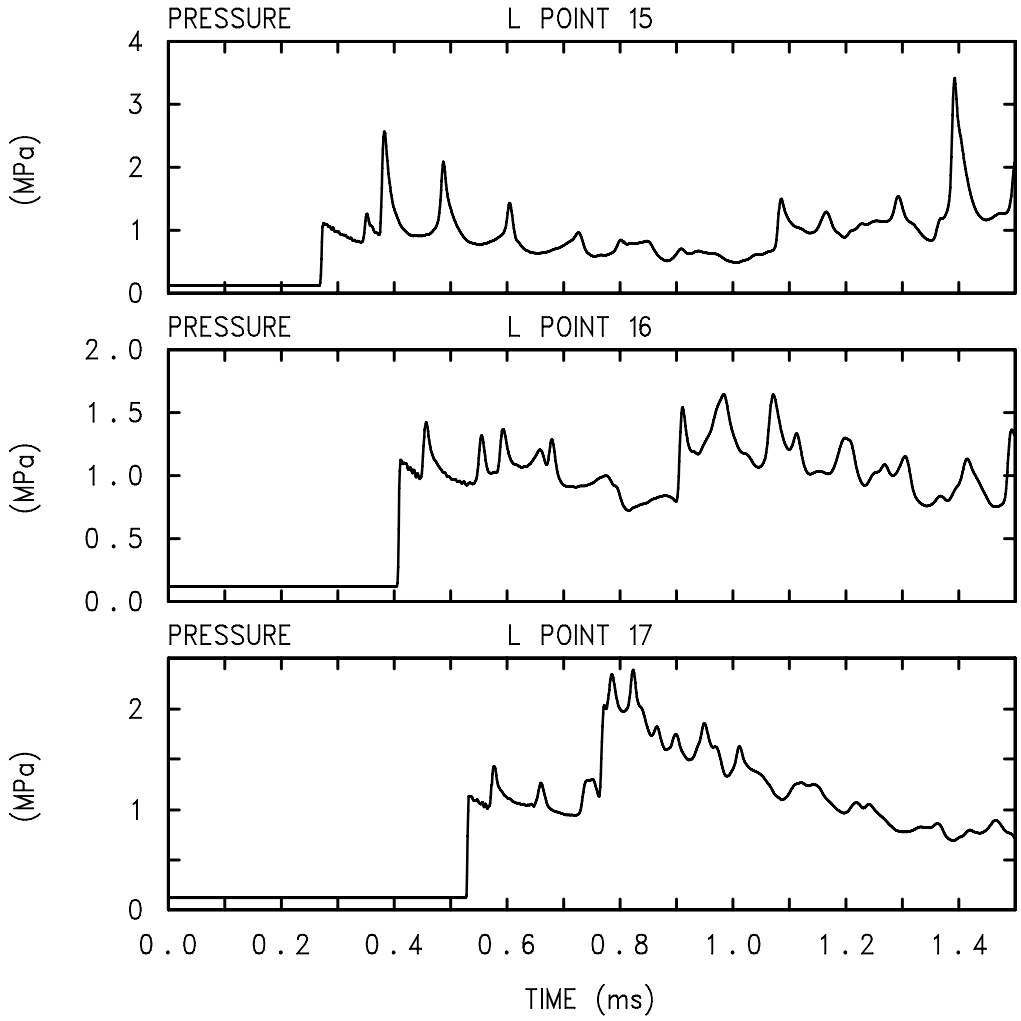

Fig. 38. Case 3 (detonation at upper region of the back-end tube)—pressure profile at the centerline (x = 0) in the collimator along the y-axis.

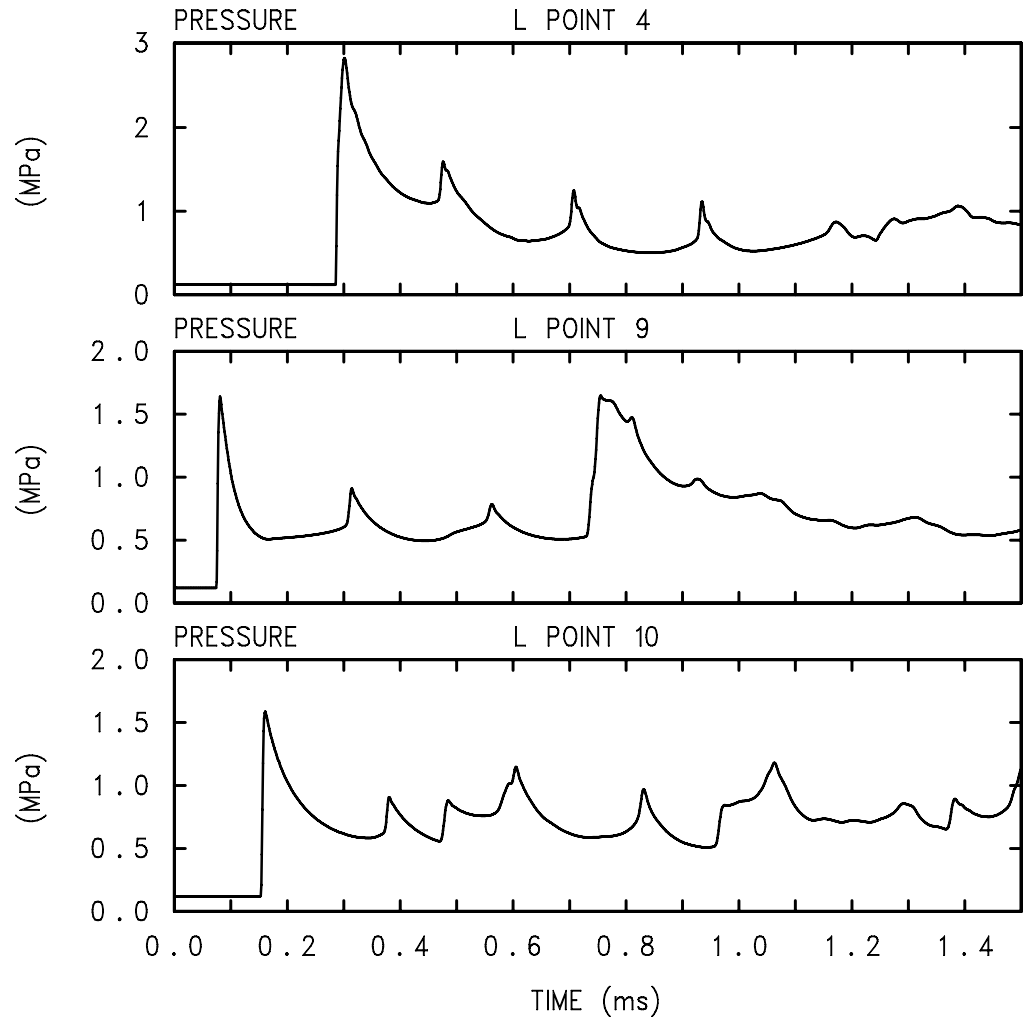

Fig. 39. Case 3 (detonation at upper region of the back-end tube)—pressure profile along the side wall.

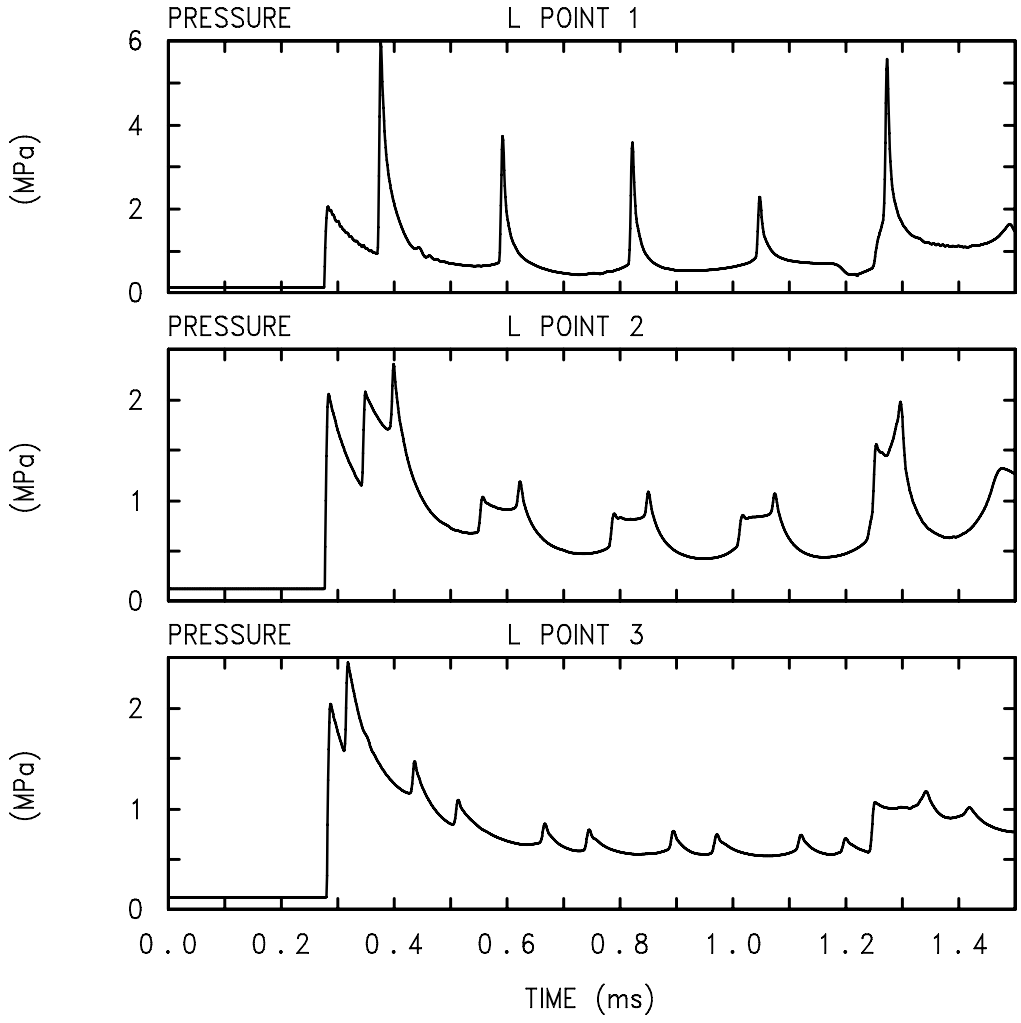

Fig. 40. Case 3 (detonation at upper region of the back-end tube)—pressure profile near the top window.

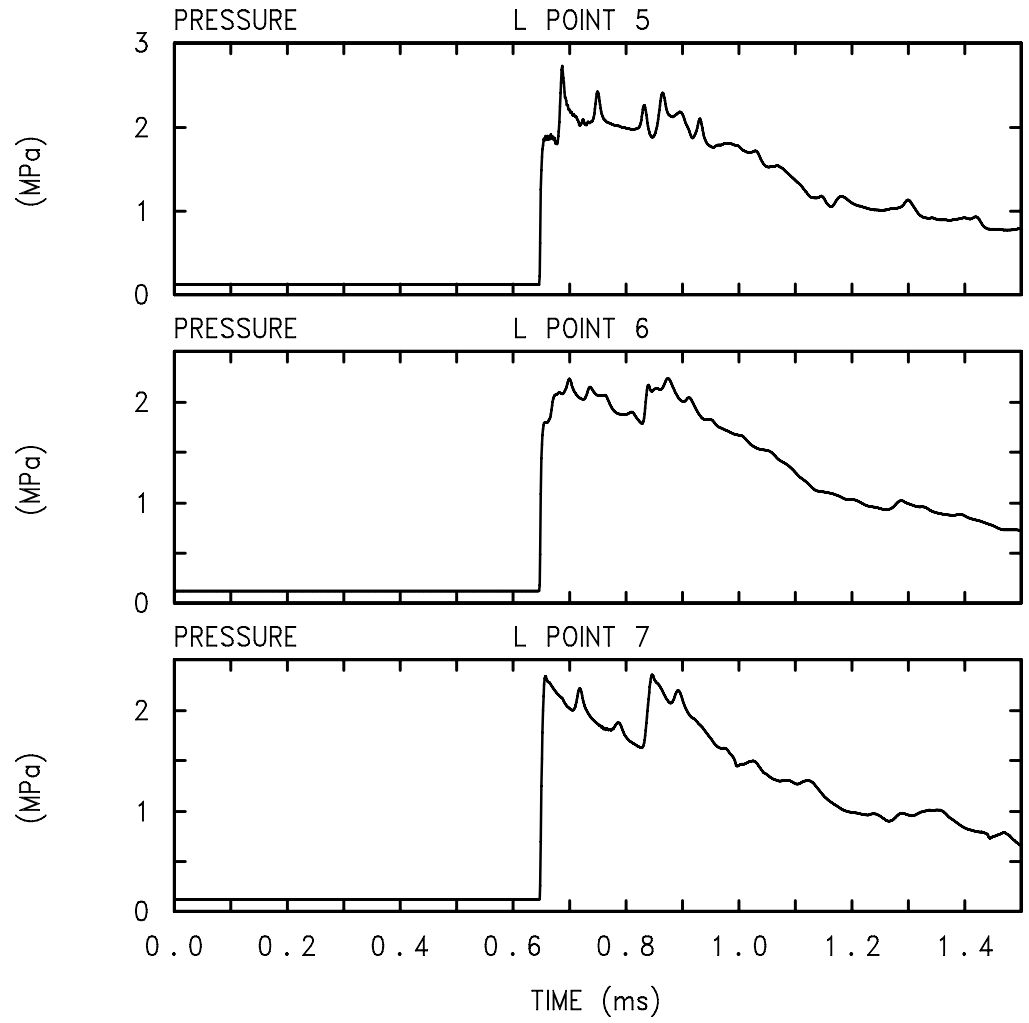

Fig. 41. Case 3 (detonation at upper region of the back-end tube)—pressure profile near the bottom window.

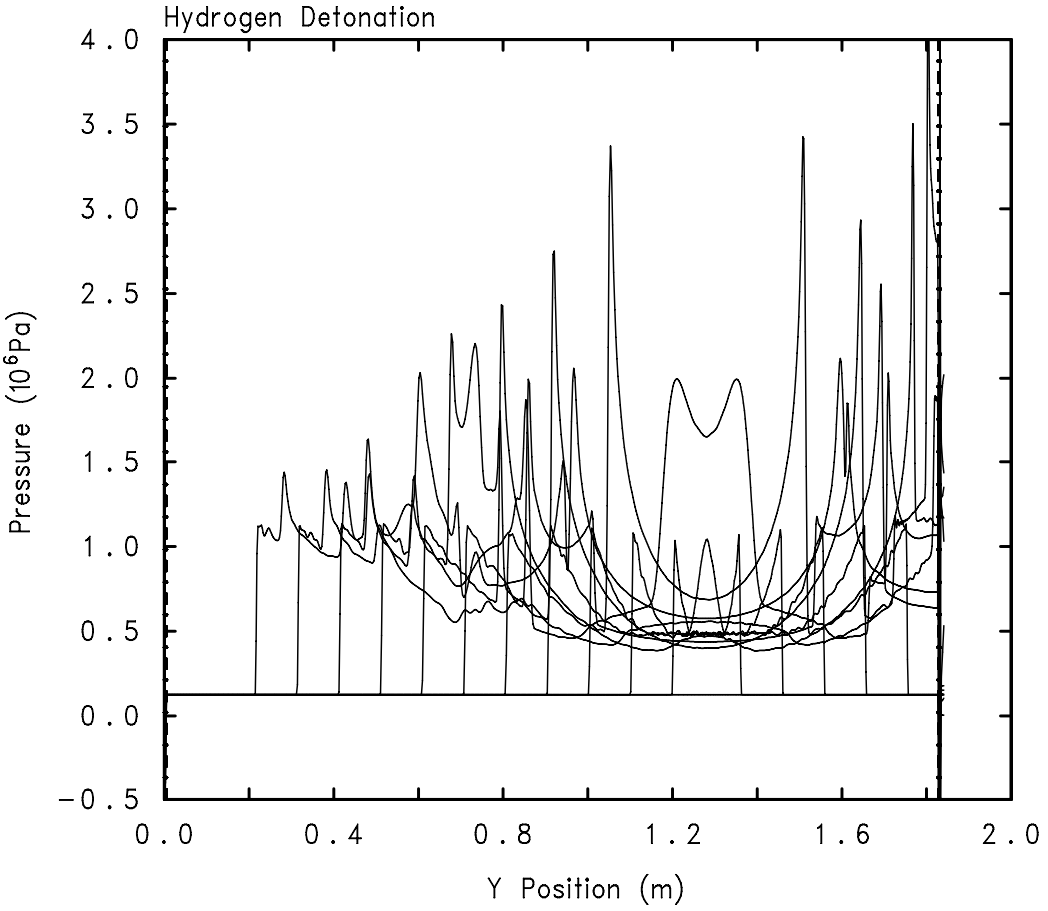

Fig. 42. Case 3 (detonation at upper region of the back-end tube)—pressure profile at the centerline along y-axis from 0.04 ms to 0.54 ms with 0.05-ms interval.

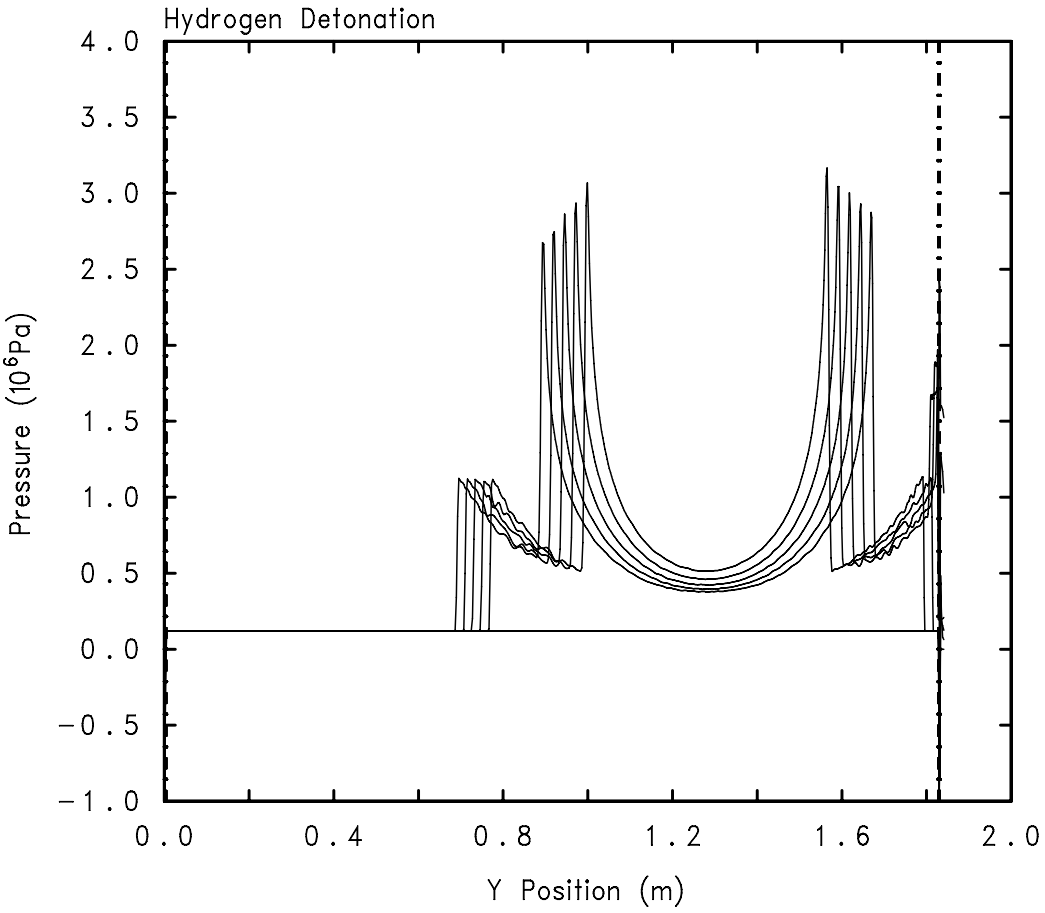

Fig. 43. Case 3 (detonation at upper region of the back-end tube)—pressure profile at the centerline along y-axis from 0.26 ms to 0.3 ms with 0.01-ms interval when the detonation wave reaches to the top window.

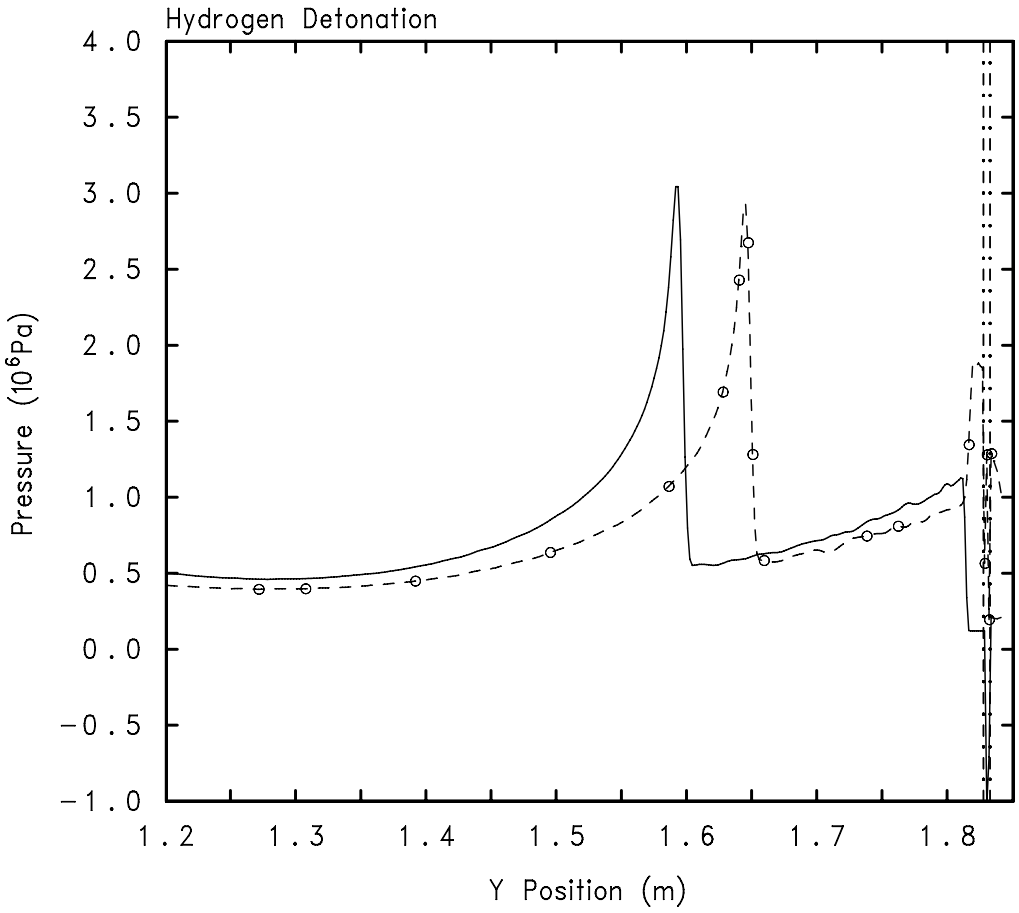

Fig. 44. Case 3 (detonation at upper region of the back-end tube)—pressure profile at the centerline along y-axis at 0.27 ms (solid line, before the wave arrives at the top window) and 0.29 ms (dotted line, after the wave being reflected at the top window).

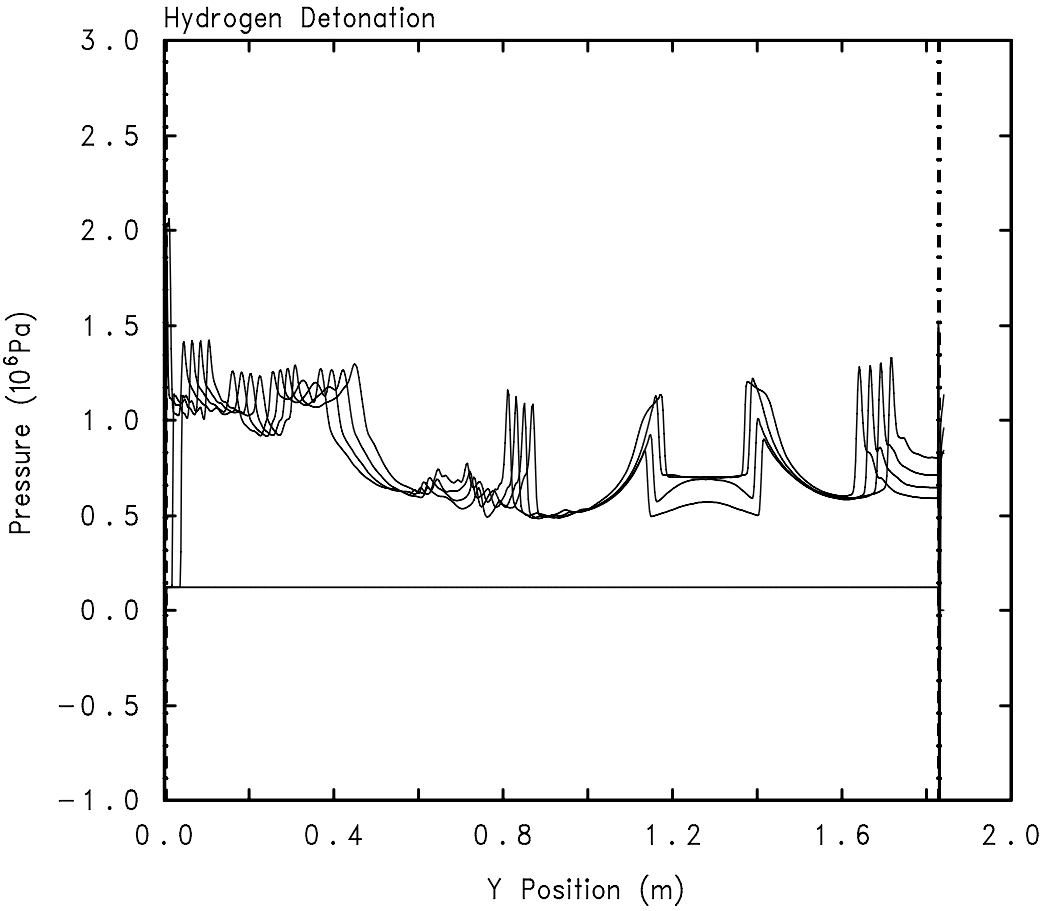

Fig. 45. Case 3 (detonation at upper region of the back-end tube)—pressure profile at the centerline along y-axis from 0.63 ms to 0.66 ms with 0.01-ms interval when the detonation wave reaches to the bottom window.

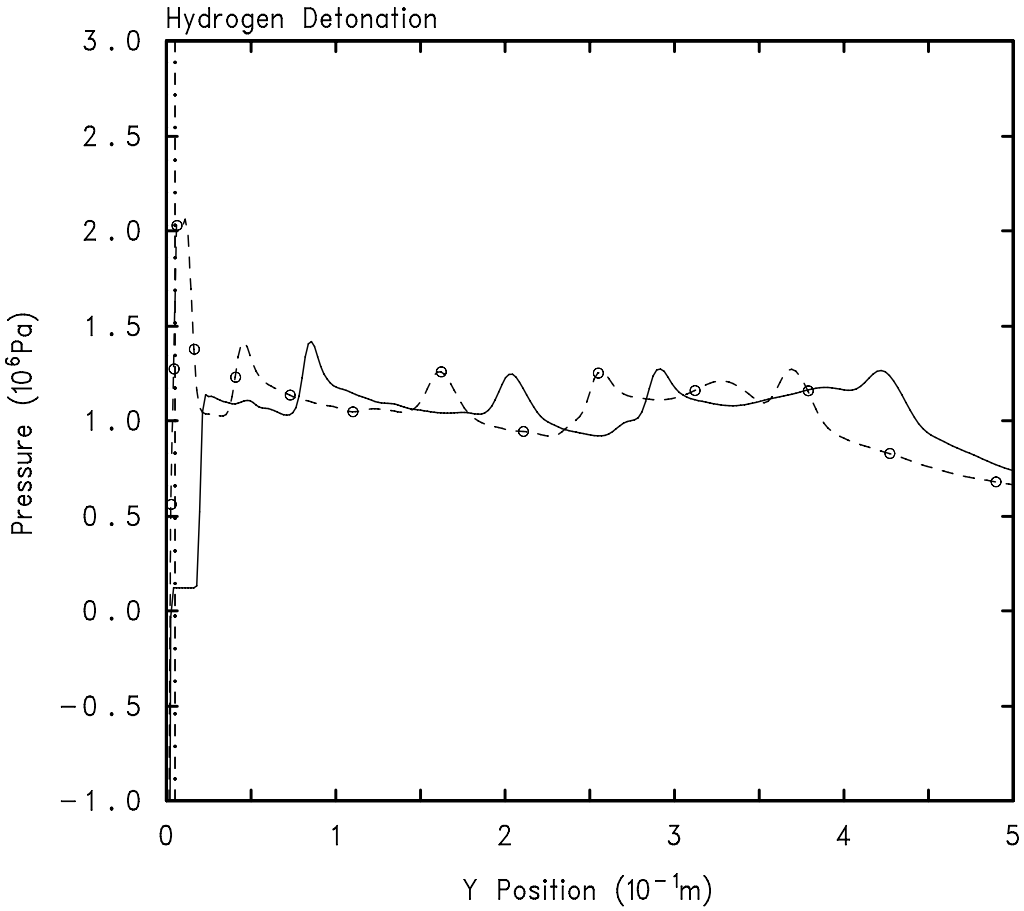

Fig. 46. Case 3 (detonation at upper region of the back-end tube)—pressure profile at the centerline along y-axis at 0.64 ms (solid line, before the wave arrives at the bottom window) and 0.66 ms (dotted line, after the wave being reflected at the bottom window).

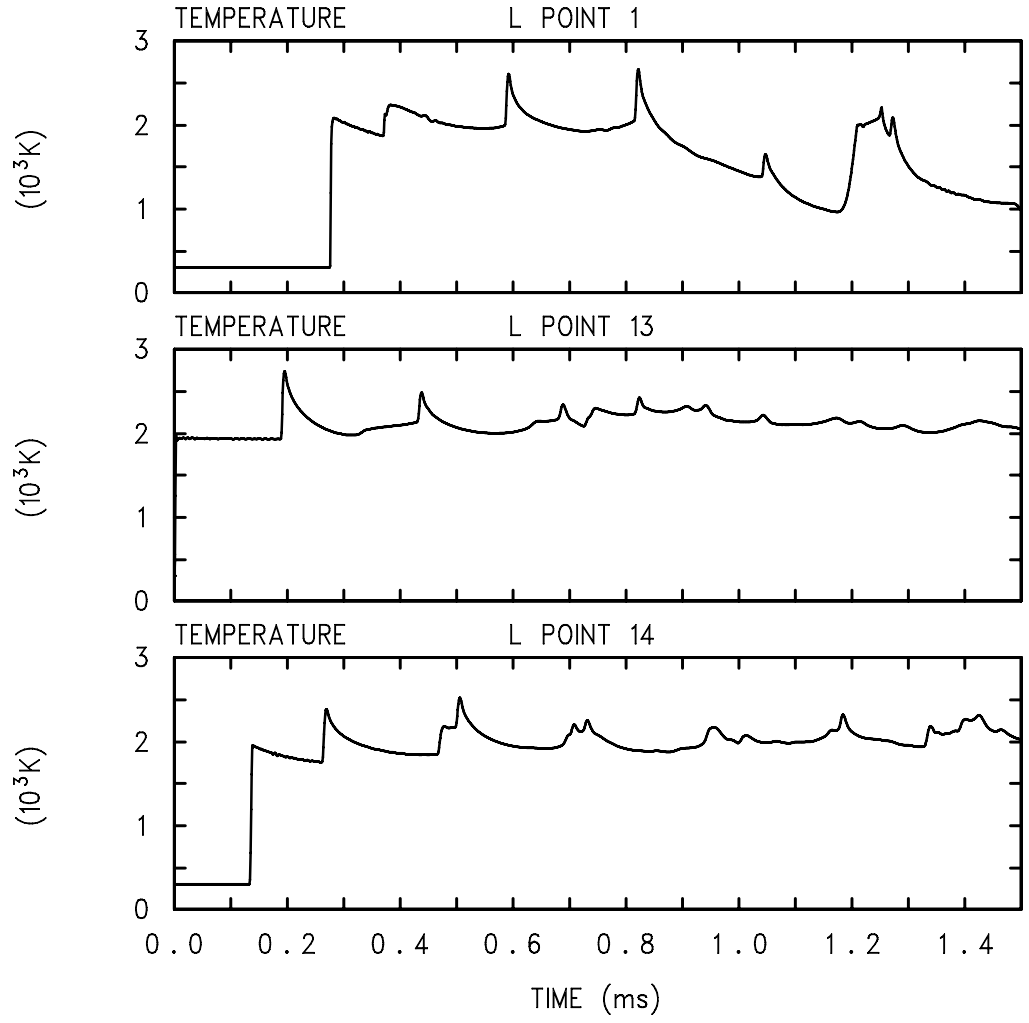

Fig. 47. Case 3 (detonation at upper region of the back-end tube)—gas mixture temperature profile at the centerline (x = 0) along the y-axis.

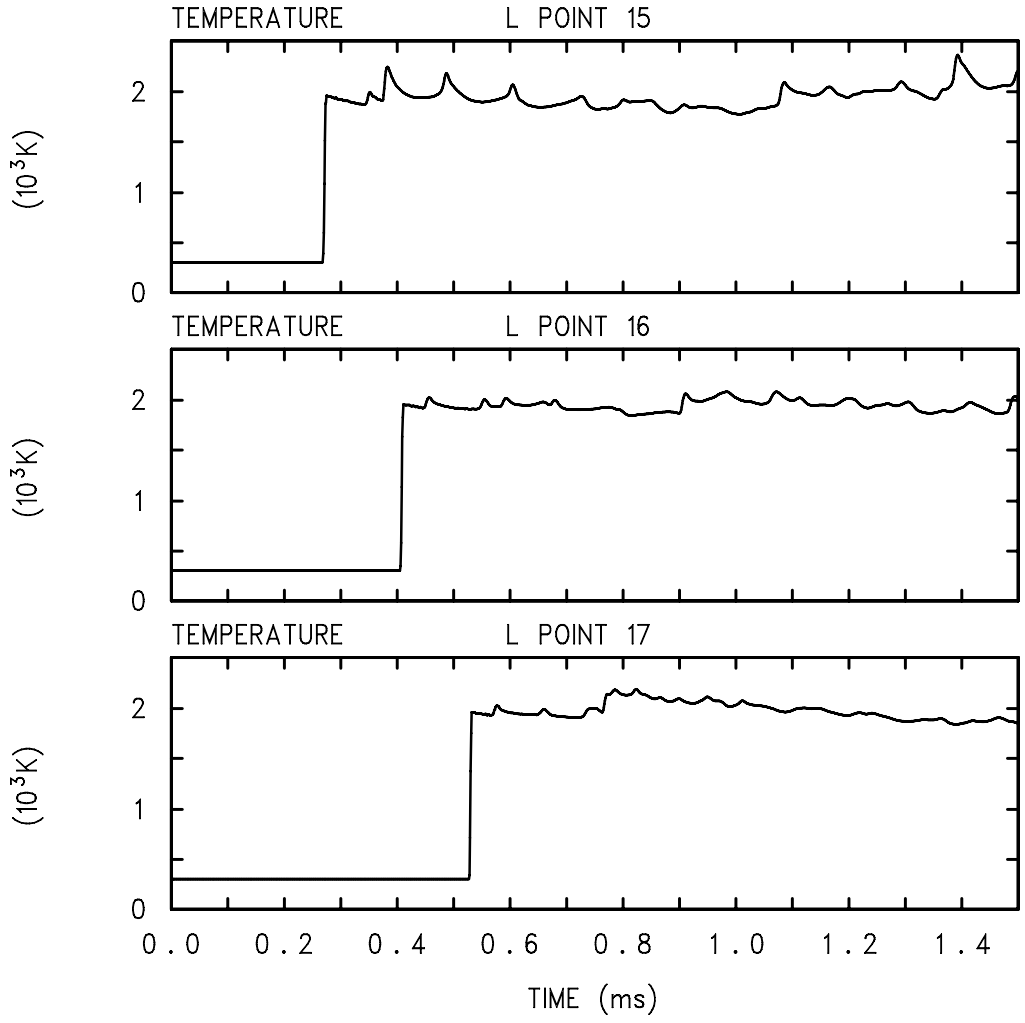

Fig. 48. Case 3 (detonation at upper region of the back-end tube)—gas mixture temperature profile at the centerline (x = 0) along the y-axis inside the collimator.

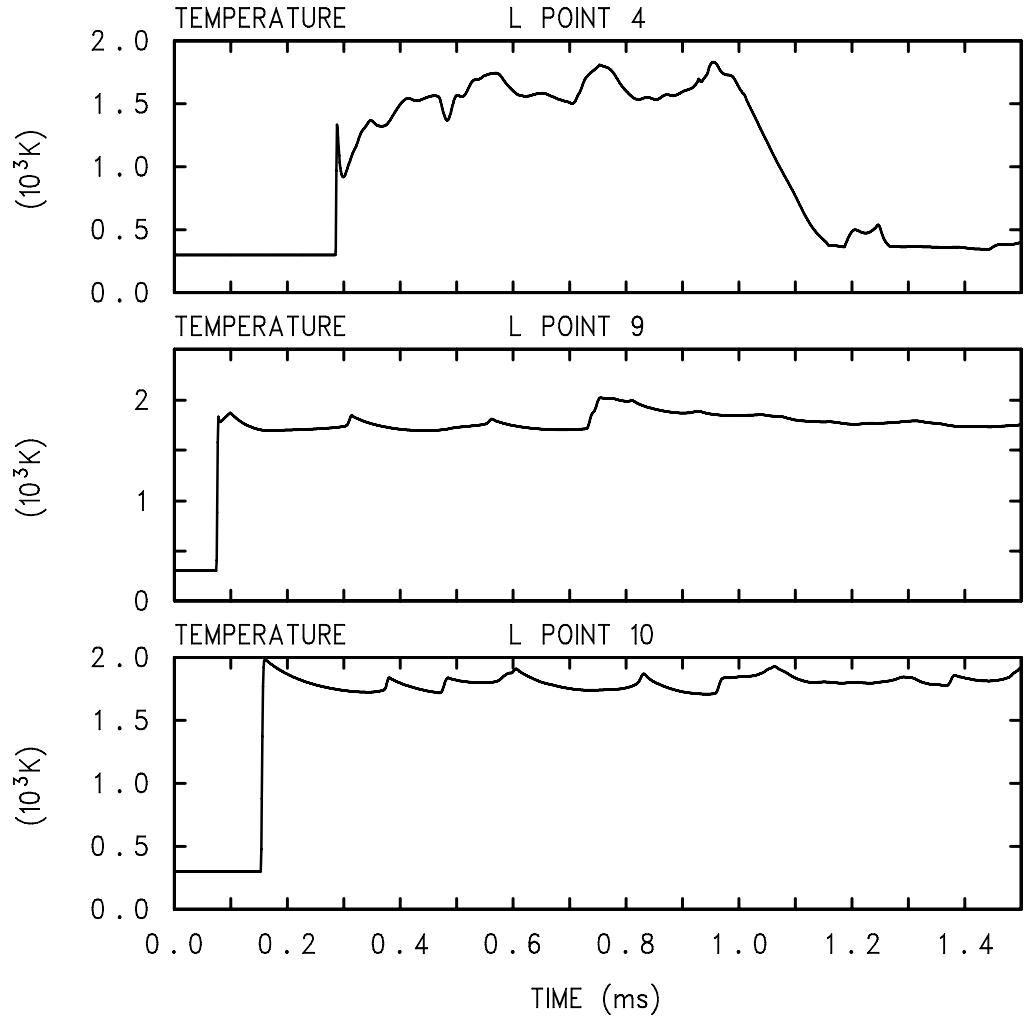

Fig. 49. Case 3 (detonation at upper region of the back-end tube)—gas mixture temperature profile near the tube wall.

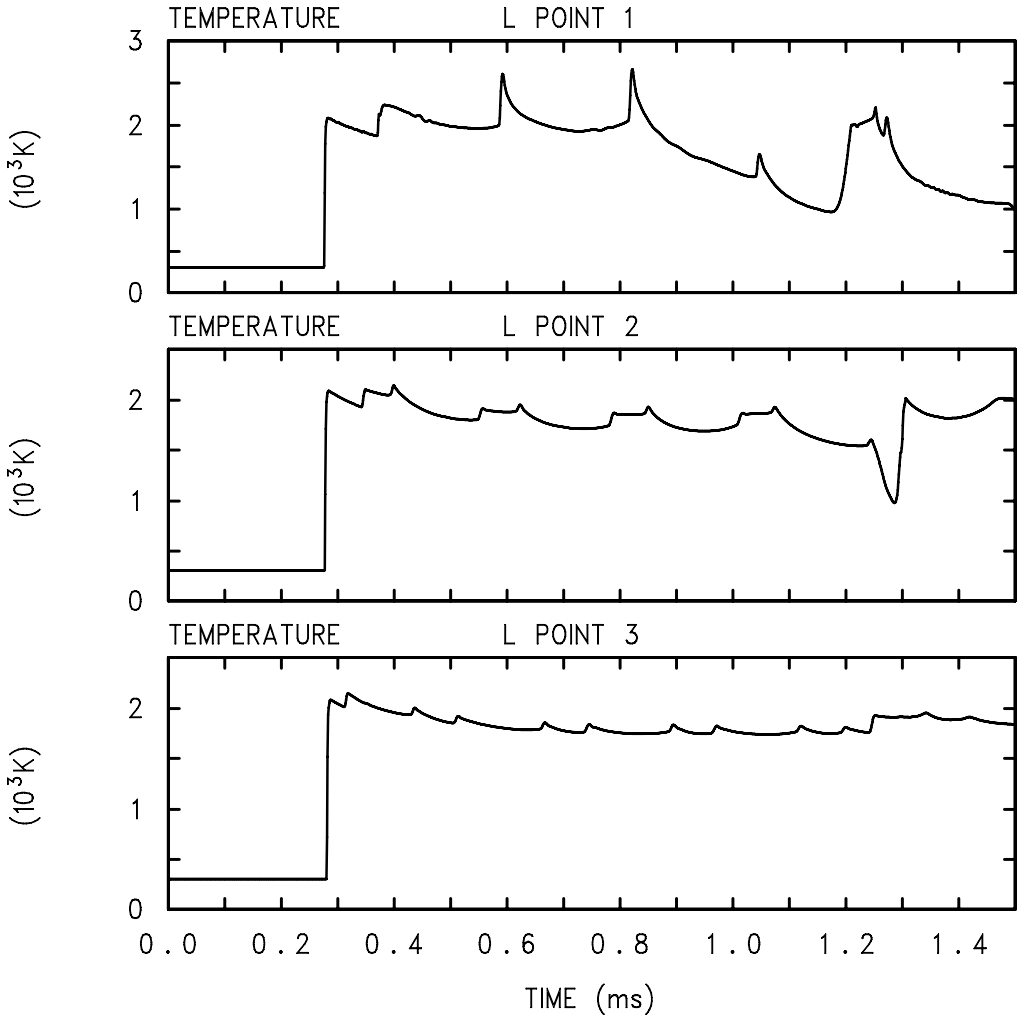

Fig. 50. Case 3 (detonation at upper region of the back-end tube)—gas mixture temperature profile near the upper window.

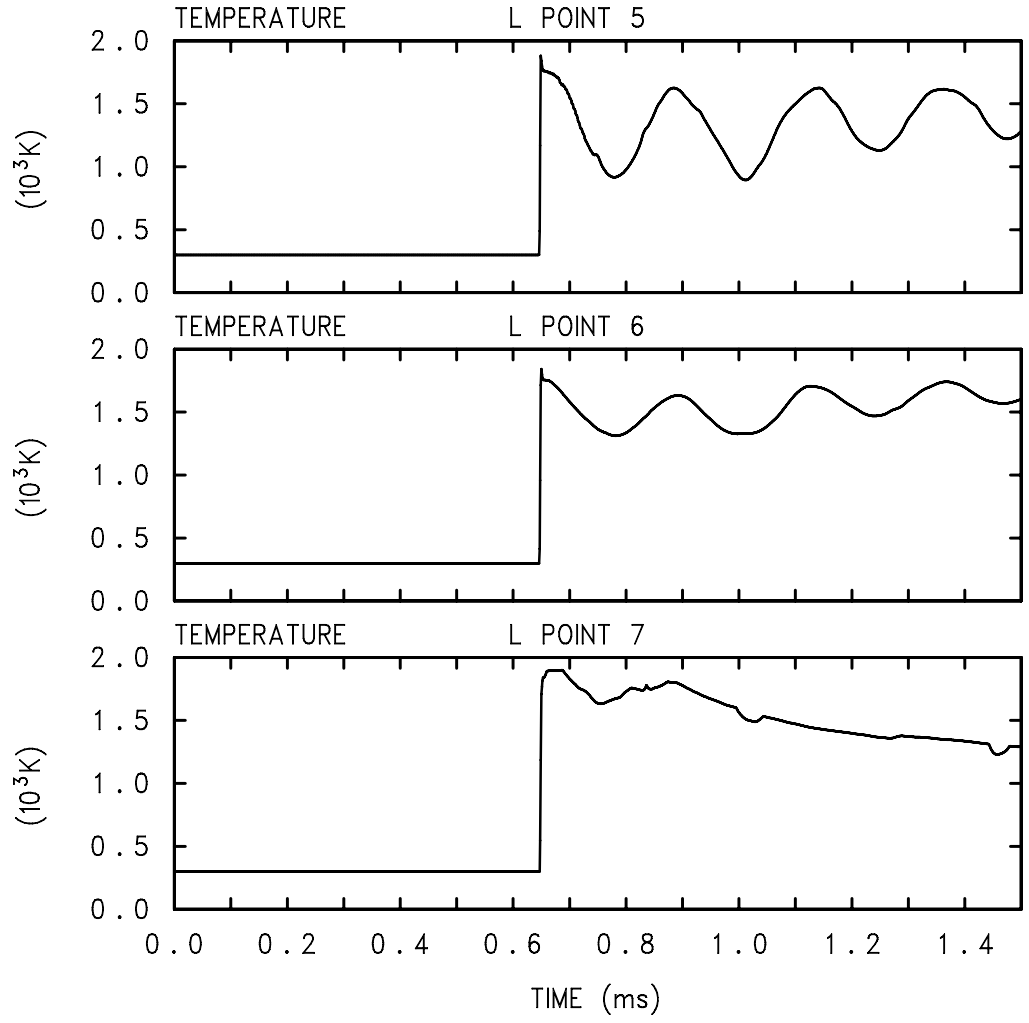

Fig. 51. Case 3 (detonation at upper region of the back-end tube)—gas mixture temperature profile near the bottom window.

is shown to predict the arrival time correctly as seen in Fig. 40. The top window experiences the gas pressure as high as 6 MPa at the center (history point-1) and about 2.5 MPa at the edge as seen in the Fig. 40. Several snapshots of the pressure profiles at around the time when the detonation wave reaches to the top window are shown in Figs. 43 and 44. As seen in the Fig. 44, the initial wave incident on the top window is more than 1 MPa that is reflected at about 2.2 MPa. Also seen in the same figure, another wave approaches the top window with the amplitude of about 3 MPa, which is expected to be reflected at about 6 MPa. Such behavior is also seen in the second pressure peak of about 6 MPa at the history point-1 in Fig. 40. The detonation wave arrives at the bottom window at around 0.65 ms (i.e., a distance, 128.1 cm, divided by the detonation velocity, 1,970 m/s). A correct arrival time is predicted by CTH as seen in Fig. 41. In the same figure, it is shown that the bottom window experiences a pressure as high as about 3 MPa at history point 5. Figures 45 and 46 show several snapshots of the pressure profiles around the time when the detonation wave arrives at the bottom window. In addition to various snapshots of the pressure profiles when the detonation wave arrives at the top and bottom windows, multiple pressure profiles at the centerline (x = 0) along the y-axis are also shown in Fig. 42, from 0.04 ms to 0.54 ms, in which the propagation and focusing of the detonation wave and the following pressure waves are well seen.

Transient temperature profiles in the gas mixtures are shown in Figs. 47–51. It is seen in the figures that the gas mixture temperatures go up as high as about 2,700 K.

3.4 CASE 4 RESULTS: POINT DETONATION AT (0, 75) IN BACK-END BEAM TUBE

For the case 4, the detonation was assumed to start at the location y = 75 cm along the centerline (x = 0), the history point of 15. This is the location around where the collimator is placed in the tube. The calculation was performed for 1.5 ms of detonation transient. Figures 52–56 show transient variations of detonation pressure at various history points. In Figs. 57–60, similar pressure profiles are illustrated at various time moments along the centerline (i.e., x = 0). Transient profiles of the gas mixture temperatures are illustrated in Figs. 61–65.

As in other similar cases, the results show the detonation/pressure wave propagation and amplification as the reflected wave is focused. Figures 52 and 53 show transient profiles of detonation pressure wave at various history points at the centerline (x = 0) along the y-axis. The detonation starts at the history point-15 in Fig. 53. As seen in the figures, the gas pressure goes up to around 3.8 MPa at the history point-1 that is near the top window (Fig. 52). In the middle region of the tube, the pressure gets amplified to as high as around 3 MPa, as seen in Fig. 52. Similar ringing behaviors to those exhibited in case 3 due to reflections and focusing are also seen in Fig. 53. The gas pressure goes up ~1.5 ~ 2 MPa in the middle region of the collimator as seen in Fig. 53 (the history points-16 and -17).

Figures 54–56 show the gas pressure profiles near the walls. The detonation wave arrives at the top window at around 0.55 ms [i.e., a distance, (128.71–75) cm, divided by the detonation velocity, 1,970 m/s]. CTH predicts the arrival time correctly as seen in Fig. 55. A peak pressure near the side tube wall is predicted to be about 2.5 MPa as seen in the history point-4 of Fig. 54. The top window is predicted to experience about 4 MPa of a pressure peak at the central region (at the history point-1) and less than 3 MPa at the edges (at the history points-2 and -3). Snapshots of several pressure profiles when the detonation wave arrives at the top window are shown in Figs. 57 and 58. The pressure profiles near the bottom window are shown in Figs. 56, 59, and 60. The detonation wave arrives at the bottom window at around 0.38 ms (i.e., a distance, 75 cm, divided by the detonation velocity, 1,970 m/s). CTH predicts the arrival time correctly as seen in Fig. 56. The bottom window is predicted to experience about 3.5 MPa at its central region (history point-5) and about 2.5 MPa at the edges (history points-6 and -7) as seen in

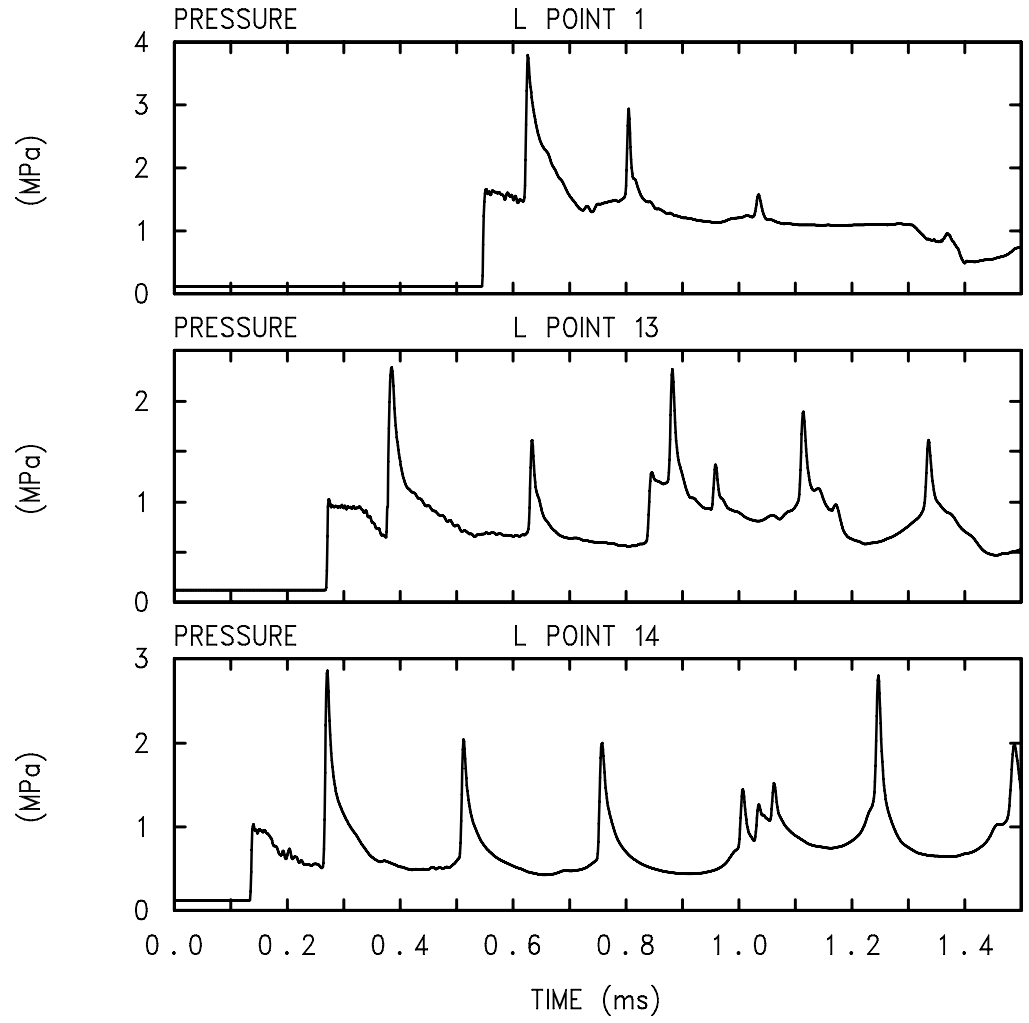

Fig. 52. Case 4 (detonation at lower region of the back-end tube)—pressure profile at the centerline (x = 0) along the y-axis.

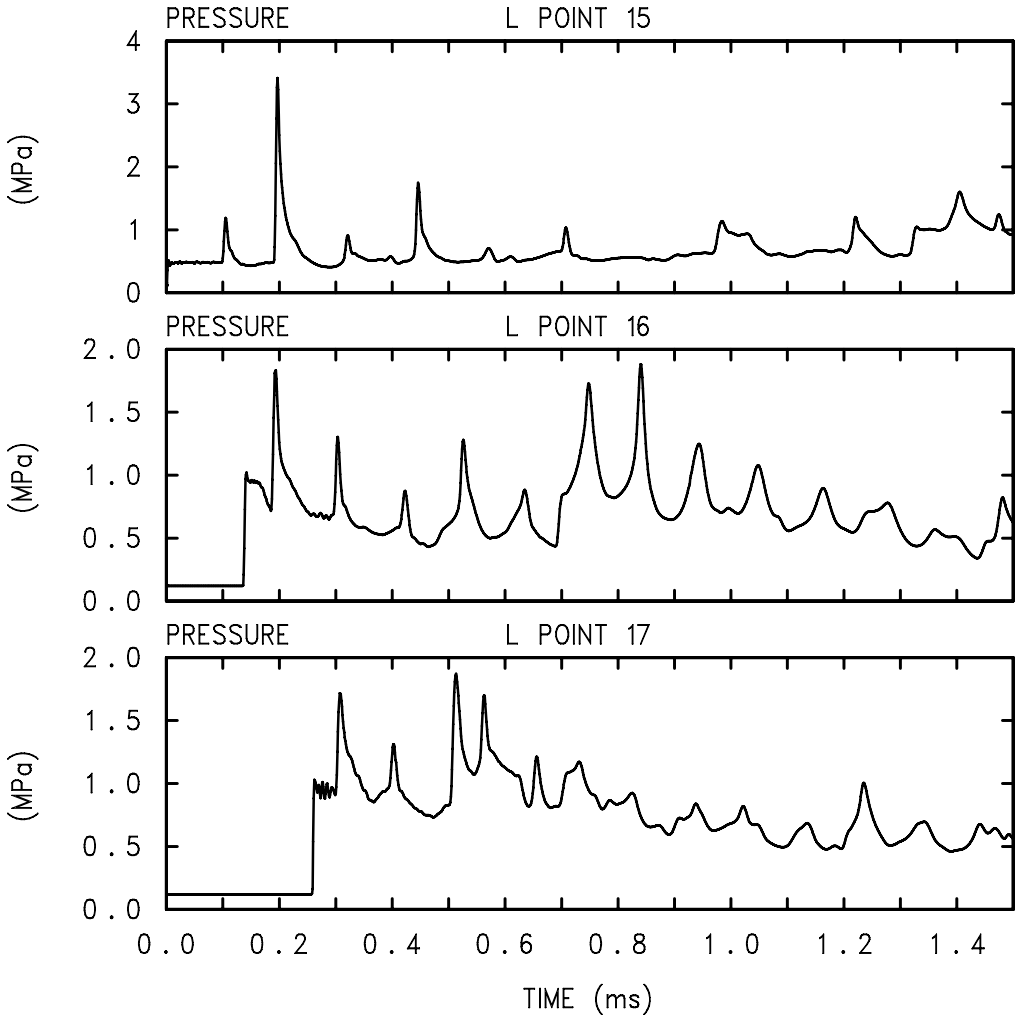

Fig. 53. Case 4 (detonation at lower region of the back-end tube)—pressure profile at the centerline (x = 0) in the collimator along the y-axis.

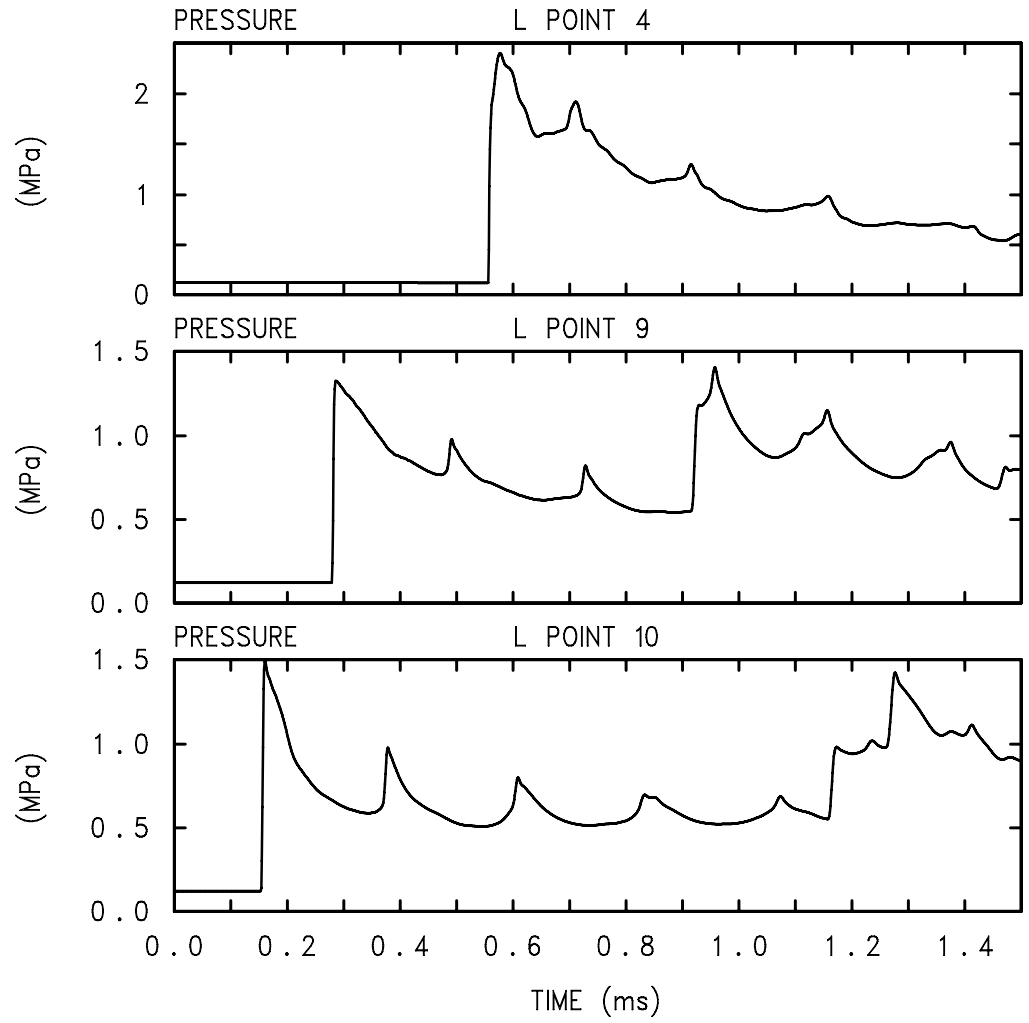

Fig. 54. Case 4 (detonation at lower region of the back-end tube)—pressure profile along the side wall.

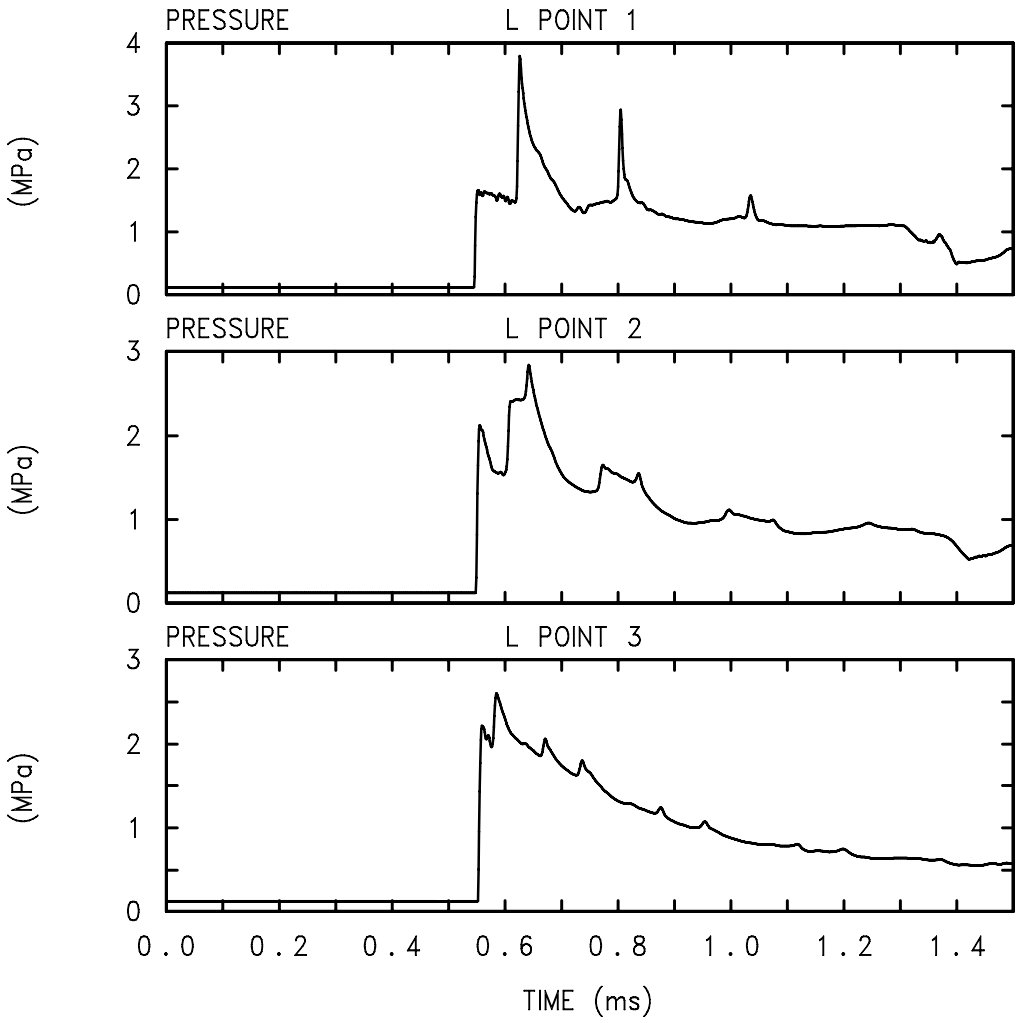

Fig. 55. Case 4 (detonation at lower region of the back-end tube)—pressure profile near the top window.

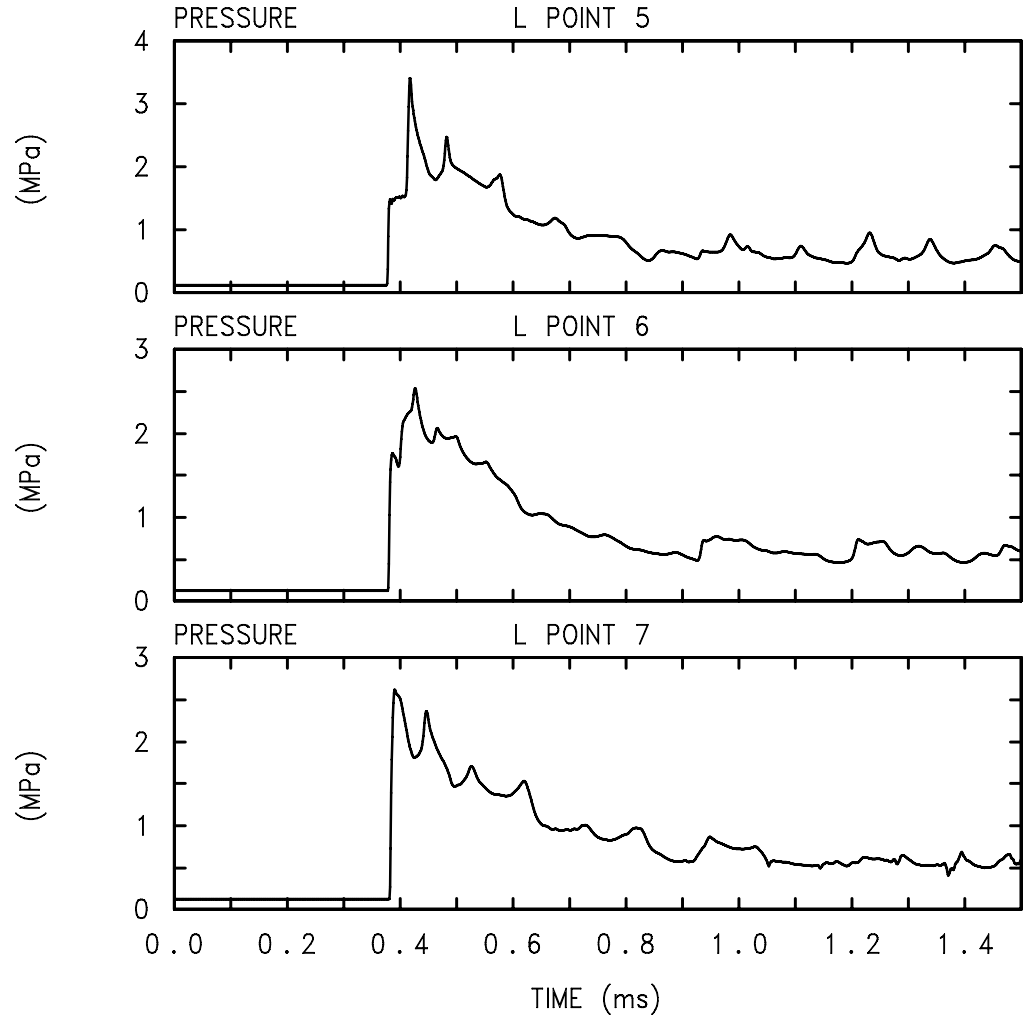

Fig. 56. Case 4 (detonation at lower region of the back-end tube)—pressure profile near the bottom window.

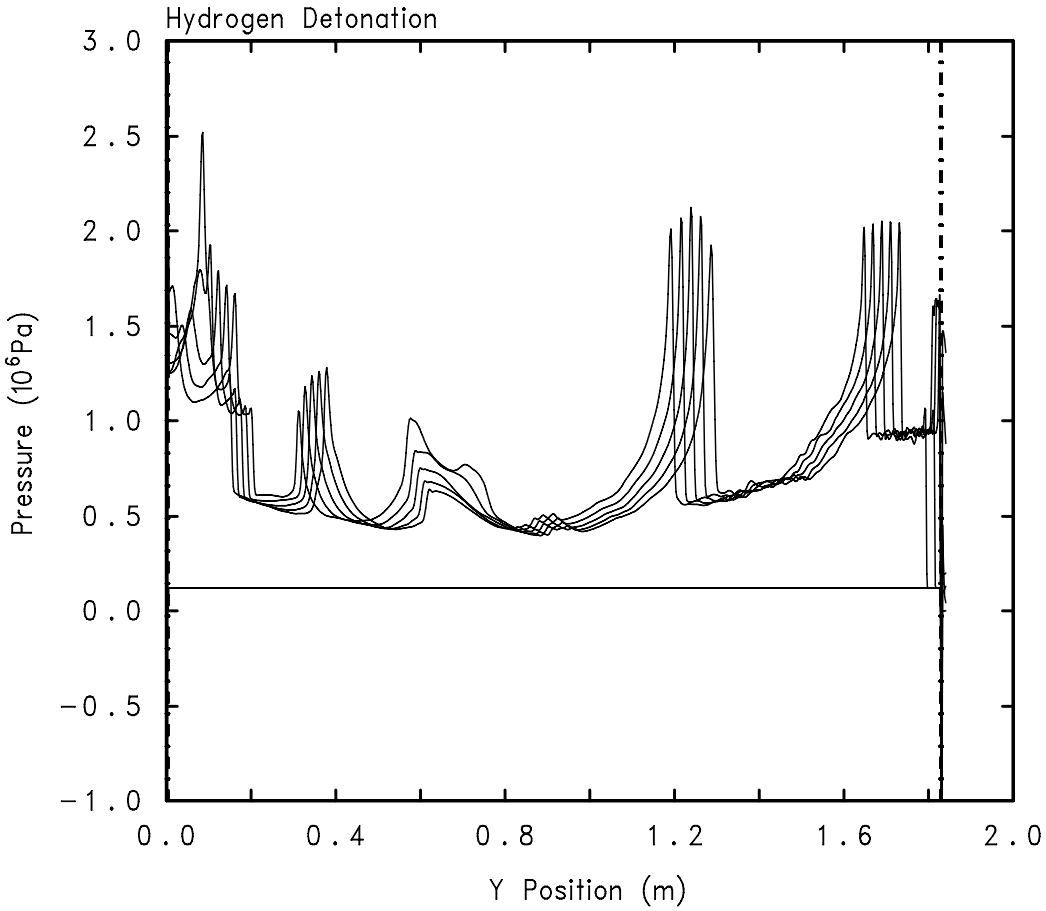

Fig. 57. Case 4 (detonation at lower region of the back-end tube)—pressure profile at the centerline along y-axis from 0.53 ms to 0.57 ms with 0.01-ms interval when the detonation wave reaches to the top window.

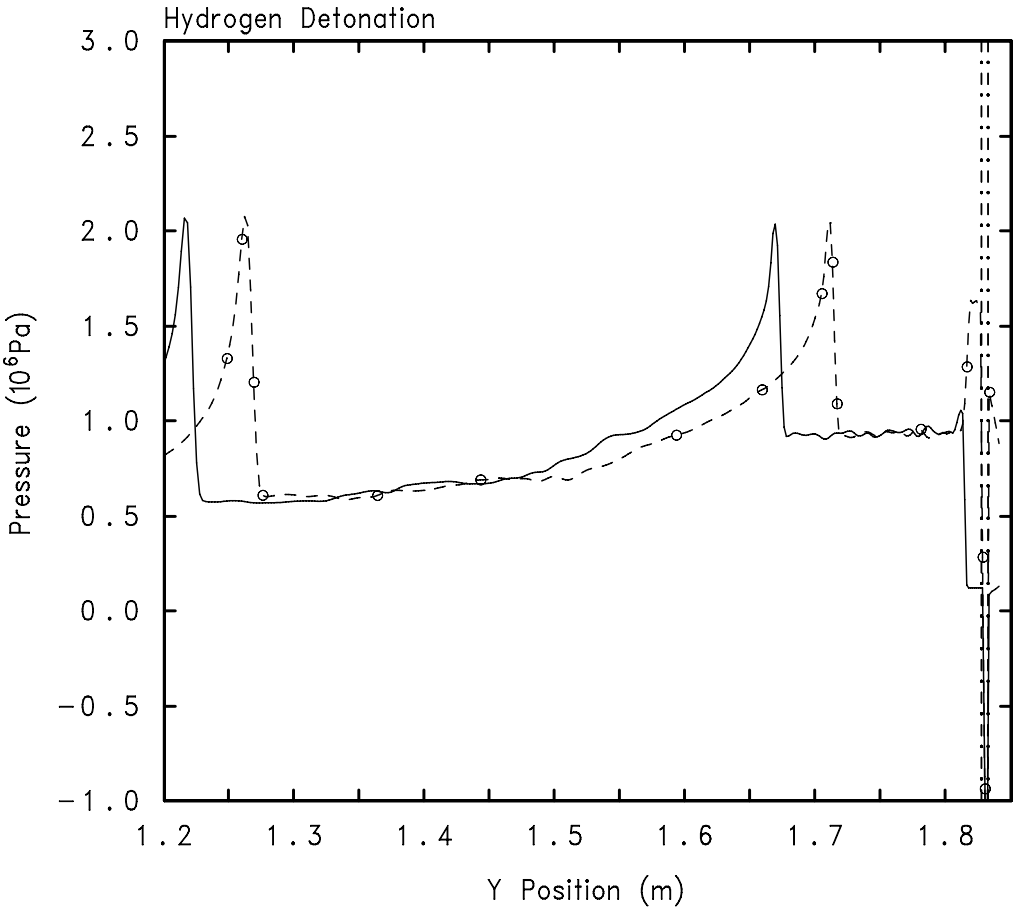

Fig. 58. Case 4 (detonation at lower region of the back-end tube)—pressure profile at the centerline along y-axis at 0.54 ms (solid line, before the wave arrives at the top window) and 0.56 ms (dotted line, after the wave being reflected at the top window).

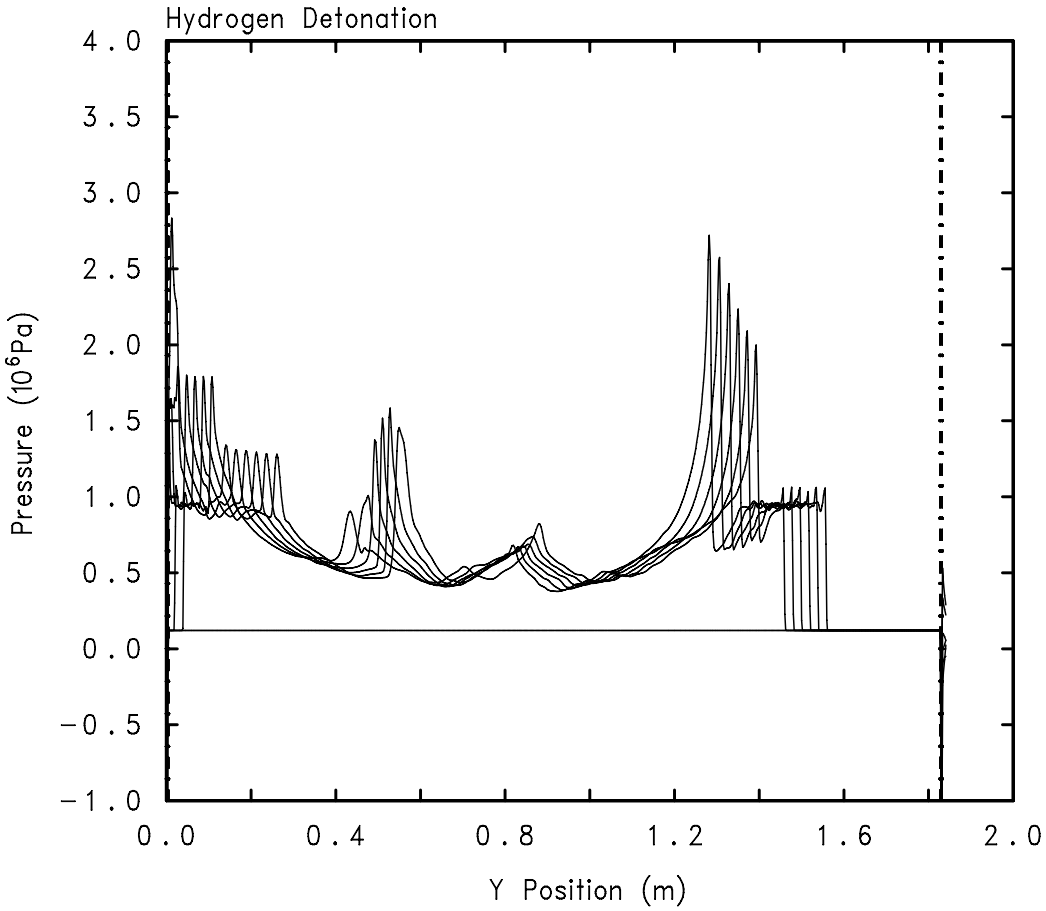

Fig. 59. Case 4 (detonation at lower region of the back-end tube)—pressure profile at the centerline along y-axis from 0.36 ms to 0.41 ms with 0.01-ms interval when the detonation wave reaches to the bottom window.

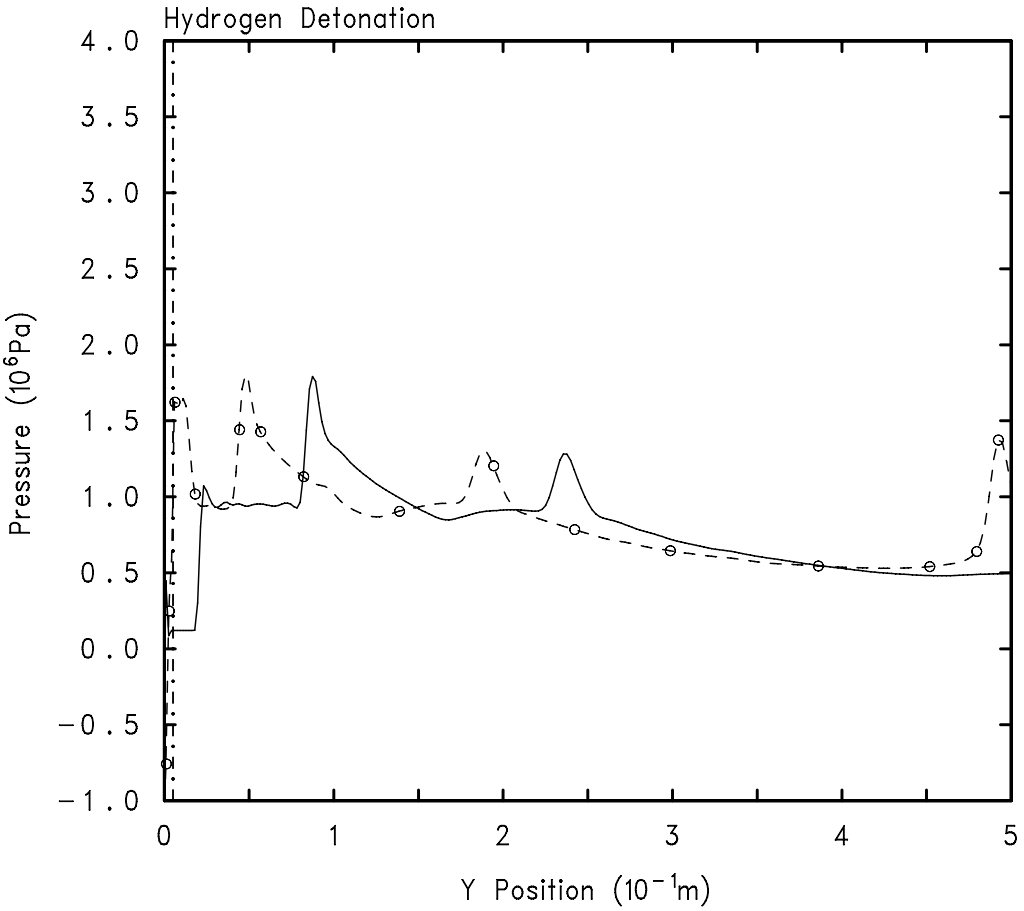

Fig. 60. Case 4 (detonation at lower region of the back-end tube)—pressure profile at the centerline along y-axis at 0.37 ms (solid line, before the wave arrives at the bottom window) and 0.39 ms (dotted line, after the wave being reflected at the bottom window).

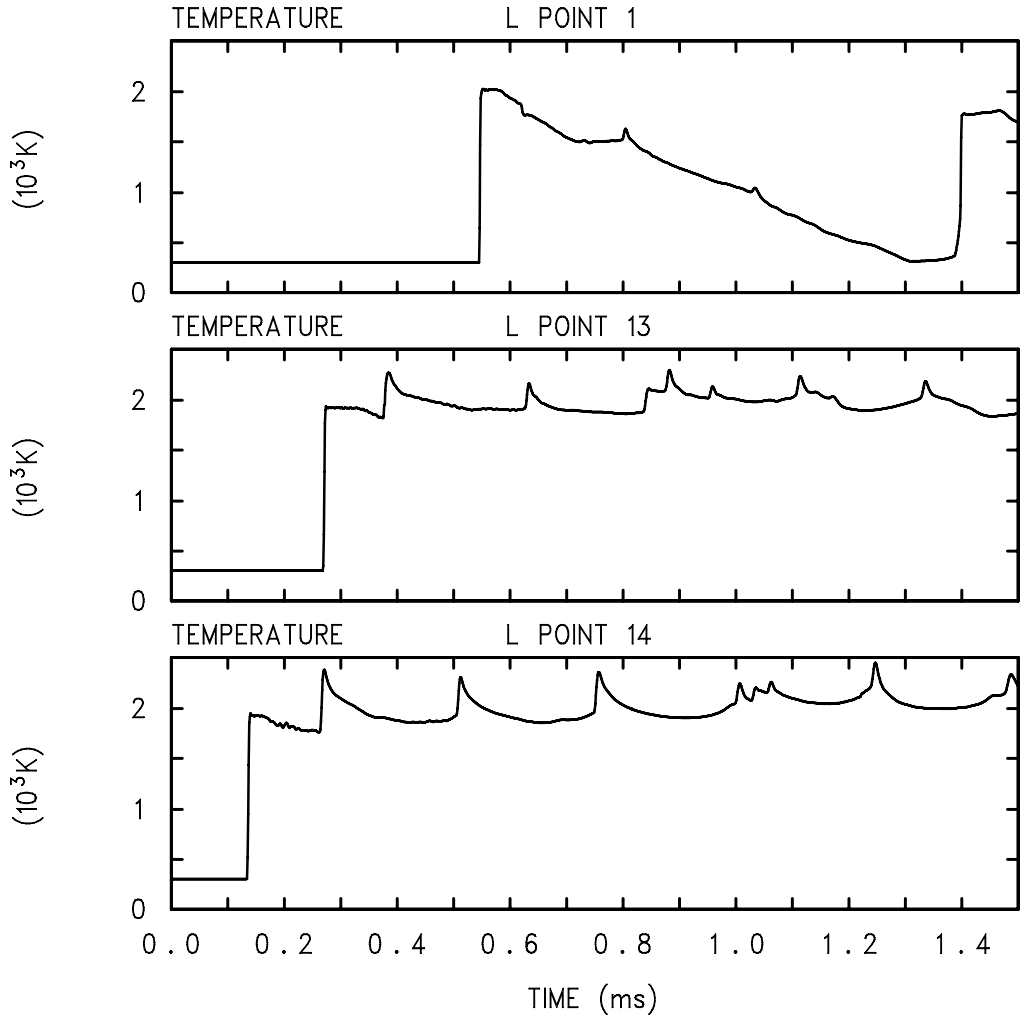

Fig. 61. Case 4 (detonation at lower region of the back-end tube)—gas mixture temperature profile at the centerline (x = 0) along the y-axis.

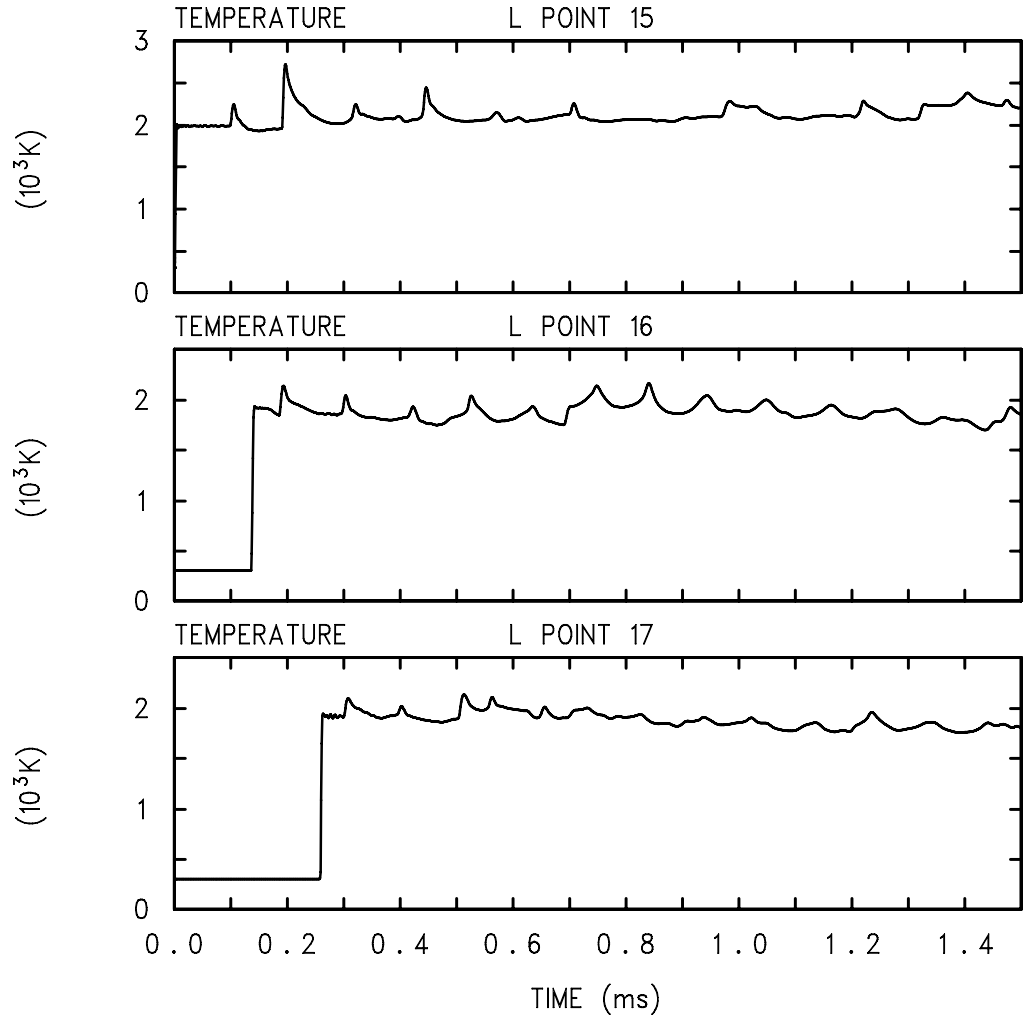

Fig. 62. Case 4 (detonation at lower region of the back-end tube)—gas mixture temperature profile at the centerline (x = 0) along the y-axis inside the collimator.

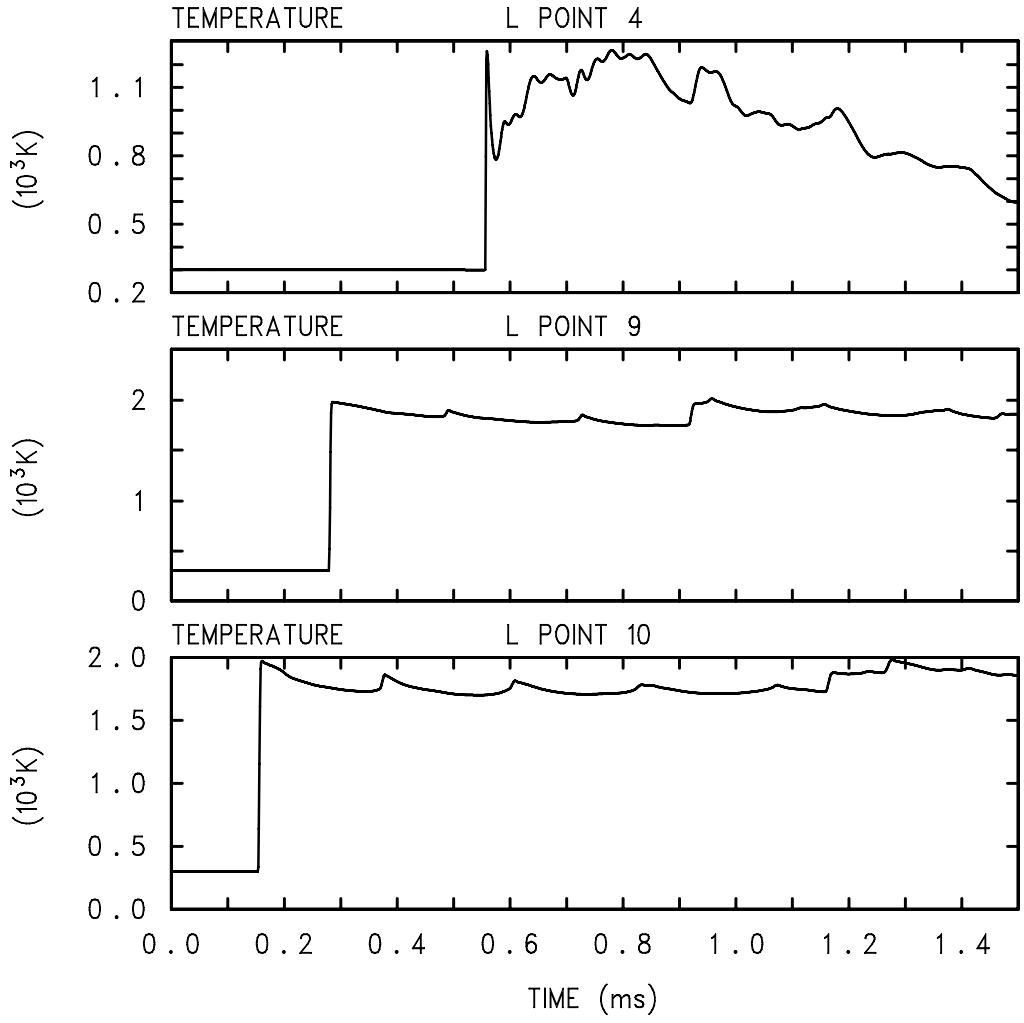

Fig. 63. Case 4 (detonation at lower region of the back-end tube)—gas mixture temperature profile near the tube wall.

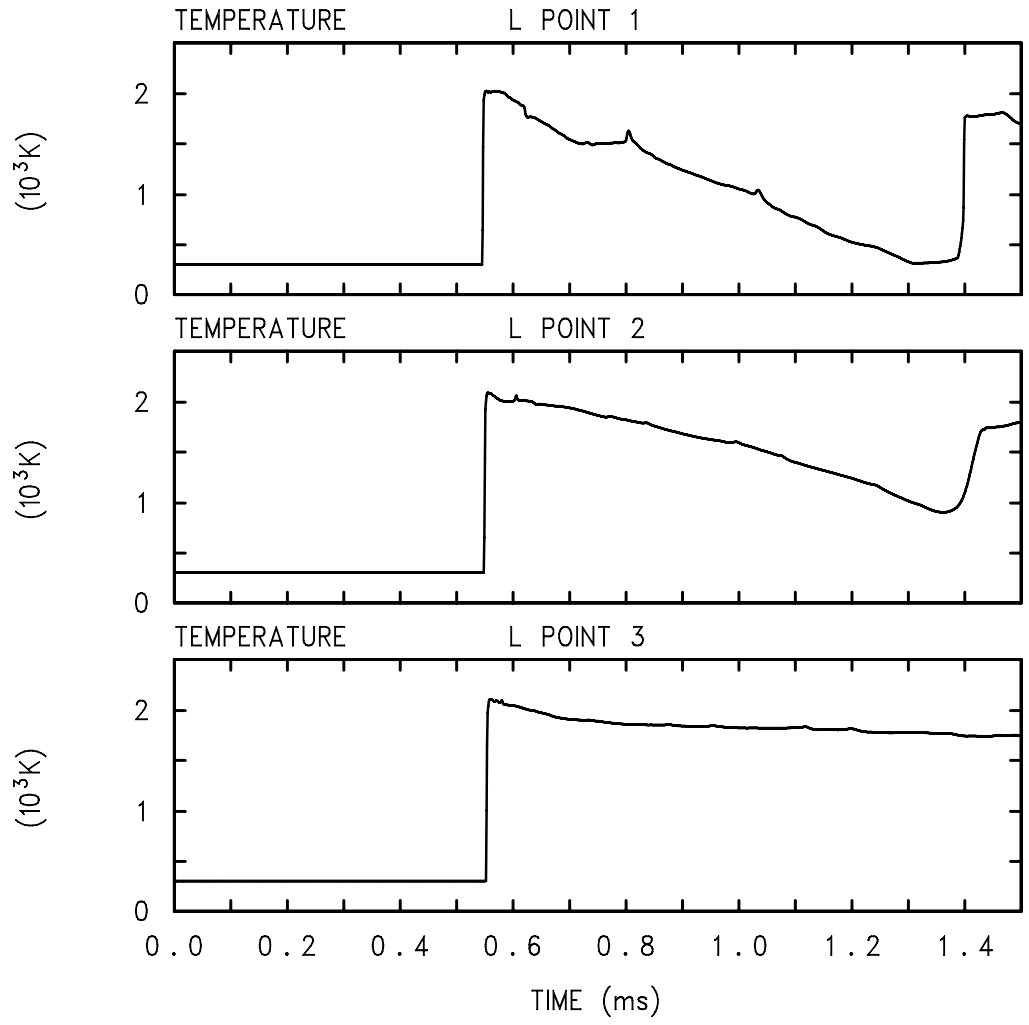

Fig. 64. Case 4 (detonation at lower region of the back-end tube)—gas mixture temperature profile near the upper window.

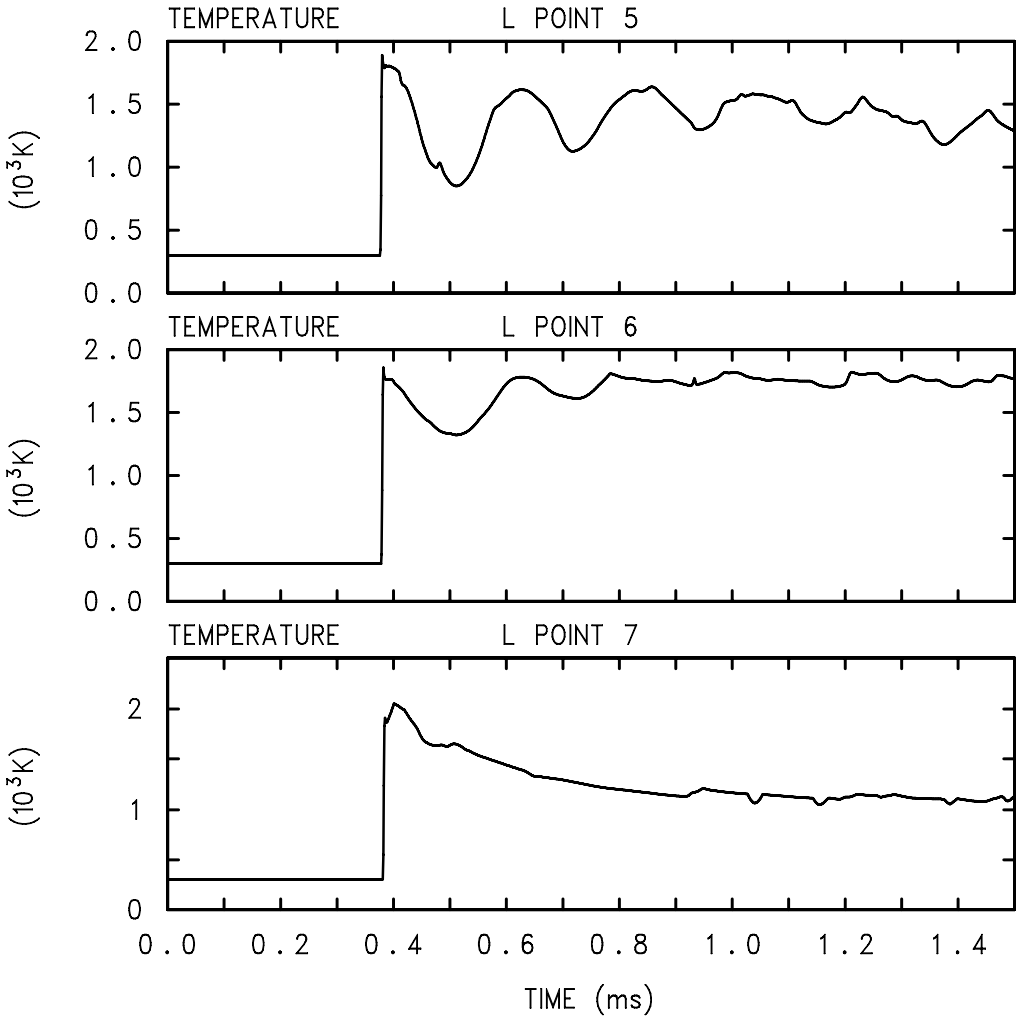

Fig. 65. Case 4 (detonation at lower region of the back-end tube)—gas mixture temperature profile near the bottom window.

Fig. 56. Figures 59 and 60 also show the pressure profiles when the detonation wave reaches to the bottom window.

Transient temperature profiles in the gas mixtures are shown in Figs. 61–65. It is seen in the figures that the gas mixture temperatures go up as high as about 2,700 K.

4. SUMMARY AND CONCLUSION

Various cases of different detonation locations in the front-end and back-end vacuum tube structures were studied. Initial conditions were assumed for a stoichiometric air/hydrogen mixture at 92 K and 0.1 MPa for the detonations in the front-end tube and 300 K and 0.1 MPa in the back-end tube, respectively. Case 1 assumes a point detonation initiated at x = 0 and y = 177.27 cm point. A point detonation initiated at the location closer to the bottom window (x = 0 and y = 57.27 cm) was assumed in case 2. Cases 3 and 4 also simulate a point detonation in the back-end beam tube at y = 128.1 cm and 75 cm at the centerline (x = 0), respectively.

The detonation wave and following pressure wave profiles are presented in Sect. 3. The peak pressures at various locations in each tube are summarized in Table 2.

Comparing the results from cases 1 and 2, note that case 1 has a slightly higher pressure near the side wall and the bottom window. However, near the hemispherical region, case 2 yields a little higher pressure because in case 1, the detonation starts in the hemispherical region, and thus immediate transfer of the energy to the surrounding water is expected. For the detonation in the bottom beam tube, the peak pressures from cases 3 and 4 are very close. For the safety implication of the peak pressures to evaluate structural integrity of the corresponding walls, it is recommended to use the maximum peak pressure at each location listed in Table 2.

Gas mixture temperatures are also calculated, and their transient profiles are introduced in Sect. 3. Generally, CTH predicts that the gas temperatures vary between ~2,000 K and ~3,000 K. For the safety implication of these temperatures, it is recommended to use the safety multiplication factor of 1.25 for the front vacuum tube and 1.45 for the bottom beam tube because CTH predicts the C-J temperatures lower than CET89.

Table 2. Summary of peak pressures predicted by CTH for various cases

	Front-vacuum tube		**Bottom-beam tube**	
	Case 1	**Case 2**	**Case 3**	**Case 4**
Detonation y-location at x = 0	177.27 cm	57.27 cm	128.1 cm	75 cm
Pressure at the top window, MPa	4.5 ~ 6 (Fig. 4)	8 ~ 15 (Fig. 28)	2.5 ~ 6 (Fig. 40)	2.5 ~ 4 (Fig. 55)
Pressure at the bottom window, MPa	11 ~ 25 (Fig. 8)	10 ~ 21 (Fig. 27)	2.5 ~ 3 (Fig. 41)	2.5 ~ 3.5 (Fig. 56)
Pressure at the side wall, MPa	~7 (Fig. 5)	5 ~ 7 (Fig. 26)	1.5 ~ 3 (Fig. 39)	1.5 ~ 2.5 (Fig. 54)
Water pressure near the hemispherical region, MPa	~4.5 (Fig. 18)	Not monitored	Not monitored	Not monitored

REFERENCES

1. S. H. Kim and et al., *Hydrogen Detonation Study for Cold Source Design of High Flux Isotope Reactor*, ORNL/TM-13605, April 1998.

2. S. Gordon and B. J. McBride, *CET89: Computer program for calculation of complex chemical equilibrium compositions, rocket performance, incident and reflected shocks, and Chapman-Jouguet detonations*, NASA SP-273, Lewis Research Center, NASA, March 1976.

3. J. M. McGlaun and S. L. Thompson, "CTH: a three-dimensional shock-wave physics code," *Int. J. of Impact Eng*., **10**, 251–360 (1990).

INTERNAL DISTRIBUTION

1–15. D. H. Cook
16. M. B. Farrar
17. G. F. Flanagan
18. J. D. Freels
19. S. R. Greene
20. R. E. Hale
21. C. R. Hyman III
22–26. S. H. Kim
27. D. J. Newland
28. C. V. Parks
29. K. A. Smith
30. H. R. Vogel
31. G. L. Yoder, Jr.
32. ORNL Laboratory Records